

DRAFT VERSION MAY 8, 2024  
 Typeset using L<sup>A</sup>T<sub>E</sub>X default style in AASTeX62

## Optical Spectroscopy of Type Ia Supernovae by the Carnegie Supernova Projects I & II

N. MORRELL,<sup>1</sup> M. M. PHILLIPS,<sup>1</sup> G. FOLATELLI,<sup>2,3</sup> M. D. STRITZINGER,<sup>4</sup> M. HAMUY,<sup>5</sup> N. B. SUNTZEFF,<sup>6</sup> E. Y. HSIAO,<sup>7</sup> F. TADDIA,<sup>4</sup> C. R. BURNS,<sup>8</sup> P. HOEFLICH,<sup>7</sup> C. ASHALL,<sup>9</sup> C. CONTRERAS,<sup>1</sup> L. GALBANY,<sup>10,11</sup> J. LU,<sup>7</sup> A. L. PIRO,<sup>8</sup> J. ANAIS,<sup>1</sup> E. BARON,<sup>12,13,14</sup> A. BURROW,<sup>14</sup> L. BUSTA,<sup>1</sup> A. CAMPILLAY,<sup>1,15</sup> S. CASTELLÓN,<sup>1</sup> C. CORCO,<sup>1,16</sup> T. DIAMOND,<sup>7,17</sup> W. L. FREEDMAN,<sup>18</sup> C. GONZALEZ,<sup>1</sup> K. KRISCIUNAS,<sup>6</sup> S. KUMAR,<sup>7</sup> S. E. PERSSON,<sup>8</sup> J. SERÓN,<sup>19</sup> M. SHAHBADEH,<sup>7</sup> S. TORRES,<sup>16</sup> S. A. UDDIN,<sup>20</sup> J. P. ANDERSON,<sup>21,22</sup> C. BALTAY,<sup>23</sup> C. GALL,<sup>4,24</sup> A. GOOBAR,<sup>25</sup> E. HADJIYSKA,<sup>23</sup> S. HOLMBO,<sup>4</sup> M. KASLIWAL,<sup>26</sup> C. LIDMAN,<sup>27</sup> G. H. MARION,<sup>28</sup> P. A. MAZZALI,<sup>29,30</sup> P. NUGENT,<sup>31,32</sup> S. PERLMUTTER,<sup>32,31</sup> G. PIGNATA,<sup>33</sup> D. RABINOWITZ,<sup>23</sup> M. ROTH,<sup>1,34</sup> S. D. RYDER,<sup>35,36</sup> B. J. SHAPPEE,<sup>37</sup> J. VINKÓ,<sup>38,39,40,28</sup> J. C. WHEELER,<sup>28</sup> T. DE JAEGER,<sup>41</sup> P. LIRA,<sup>42</sup> M. T. RUIZ,<sup>42</sup> J. A. RICH,<sup>8</sup> J. L. PRIETO,<sup>43</sup> F. DI MILLE,<sup>1</sup> D. OSIP,<sup>1</sup> G. BLANC,<sup>1</sup> AND P. PALUNAS<sup>1</sup>

<sup>1</sup> Carnegie Observatories, Las Campanas Observatory, Casilla 601, La Serena, Chile

<sup>2</sup> Instituto de Astrofísica de La Plata (IALP), CONICET, Paseo del Bosque S/N, 1900, Argentina

<sup>3</sup> Facultad de Ciencias Astronómicas y Geofísicas (FCAG), Universidad Nacional de La Plata (UNLP), Paseo del Bosque S/N, 1900, Argentina

<sup>4</sup> Department of Physics and Astronomy, Aarhus University, Ny Munkegade 120, DK-8000 Aarhus C, Denmark

<sup>5</sup> Fundación Chilena de Astronomía, Santiago, Chile

<sup>6</sup> George P. and Cynthia Woods Mitchell Institute for Fundamental Physics and Astronomy, Texas A&M University, Department of Physics and Astronomy, College Station, TX 77843, USA

<sup>7</sup> Department of Physics, Florida State University, 77 Chieftan Way, Tallahassee, FL 32306, USA

<sup>8</sup> Observatories of the Carnegie Institution for Science, 813 Santa Barbara St, Pasadena, CA 91101, USA

<sup>9</sup> Department of Physics, Virginia Polytechnic Institute and State University, 850 West Campus Drive, Blacksburg, VA 24061, USA

<sup>10</sup> Institute of Space Sciences (ICE, CSIC), Campus UAB, Carrer de Can Magrans, s/n, E-08193 Barcelona, Spain

<sup>11</sup> Institut d'Estudis Espacials de Catalunya (IEEC), E-08034 Barcelona, Spain

<sup>12</sup> Planetary Science Institute, 1700 East Fort Lowell Road, Suite 106, Tucson, AZ 85719-2395, USA

<sup>13</sup> Hamburger Sternwarte, Gojenbergsweg 112, D-21029 Hamburg, Germany

<sup>14</sup> Dept of Physics & Astronomy, University of Oklahoma, Norman, OK 73019, USA

<sup>15</sup> Departamento de Física, Universidad de La Serena, Cisternas 1200, La Serena, Chile

<sup>16</sup> SOAR Telescope, Casilla 603, La Serena, Chile

<sup>17</sup> Laboratory of Observational Cosmology, Code 665, NASA Goddard Space Flight Center, Greenbelt, MD 20771, USA

<sup>18</sup> Department of Astronomy & Astrophysics & Kavli Institute for Cosmological Physics, University of Chicago, 5640 South Ellis Avenue, Chicago, IL 60637, USA

<sup>19</sup> Cerro Tololo Inter-American Observatory/NSF's NOIRLab, Casilla 603, La Serena, Chile

<sup>20</sup> Center for Space Studies, American Public University System, 111 W. Congress Street, Charles Town, WV 25414, USA

<sup>21</sup> European Southern Observatory, Alonso de Córdova 3107, Casilla 19, Santiago, Chile

<sup>22</sup> Millennium Institute of Astrophysics MAS, Nuncio Monsenor Sotero Sanz 100, Off.104, Providencia, Santiago, Chile

<sup>23</sup> Department of Physics, Yale University, 217 Prospect Street, New Haven, CT 06511, USA

<sup>24</sup> DARK, Niels Bohr Institute, University of Copenhagen, Jagtvej 128, 2200 Copenhagen, Denmark

<sup>25</sup> The Oskar Klein Centre, Department of Physics, Stockholm University, SE-106 91 Stockholm, Sweden

<sup>26</sup> Caltech, 1200 East California Boulevard, MC 249-17, Pasadena, CA 91125, USA

<sup>27</sup> The Research School of Astronomy and Astrophysics, Australian National University, ACT 2601, Australia

<sup>28</sup> Department of Astronomy, University of Texas at Austin, 2515 Speedway Stop C1400, Austin, TX, 78712-1205, USA

<sup>29</sup> Astrophysics Research Institute, Liverpool John Moores University, IC2, Liverpool Science Park, 146 Brownlow Hill, Liverpool L3 5RF, UK

<sup>30</sup> Max-Planck-Institut für Astrophysik, Karl-Schwarzschild Str. 1, D-85748 Garching, Germany

<sup>31</sup> Physics Department, University of California, Berkeley, CA 94720, USA

<sup>32</sup> Lawrence Berkeley National Laboratory, Department of Physics, 1 Cyclotron Road, Berkeley, CA 94720, USA

<sup>33</sup> Instituto de Alta Investigación, Universidad de Tarapacá, Casilla 7D, Arica, Chile

<sup>34</sup>GMTO Corporation, Presidente Riesco 5335, Of. 501, Nueva Las Condes, Santiago

<sup>35</sup>School of Mathematical and Physical Sciences, Macquarie University, NSW 2109, Australia

<sup>36</sup>Astrophysics and Space Technologies Research Centre, Macquarie University, Sydney, NSW 2109, Australia

<sup>37</sup>Institute for Astronomy, University of Hawaii, 2680 Woodlawn Drive, Honolulu, HI 96822, USA

<sup>38</sup>Konkoly Observatory, CSFK, MTA Centre of Excellence, Konkoly Thege M. út 15-17, Budapest, 1121, Hungary

<sup>39</sup>ELTE Eötvös Loránd University, Institute of Physics and Astronomy, Pázmány Péter sétány 1/A, Budapest, 1117 Hungary

<sup>40</sup>Department of Experimental Physics, University of Szeged, Dóm tér 9, Szeged, 6720, Hungary

<sup>41</sup>LPNHE, CNRS/IN2P3 & Sorbonne Université, 4 place Jussieu, 75005 Paris, France

<sup>42</sup>Departamento de Astronomía, Universidad de Chile, Camino del Observatorio 1515, Santiago, Chile

<sup>43</sup>Instituto de Estudios Astrofísicos, Facultad de Ingeniería y Ciencias, Universidad Diego Portales, Avenida Ejército Libertador 441, Santiago, Chile

Submitted to The Astrophysical Journal

## ABSTRACT

We present the second and final release of optical spectroscopy of Type Ia Supernovae (SNe Ia) obtained during the first and second phases of the *Carnegie Supernova Project* (CSP-I and CSP-II). The newly released data consist of 148 spectra of 30 SNe Ia observed in the course of the CSP-I, and 234 spectra of 127 SNe Ia obtained during the CSP-II. We also present 216 optical spectra of 46 historical SNe Ia, including 53 spectra of 30 SNe Ia observed by the Calán/Tololo Supernova Survey. We combine these observations with previously published CSP data and publicly-available spectra to compile a large sample of measurements of spectroscopic parameters at maximum light, consisting of pseudo-equivalent widths and expansion velocities of selected features, for 232 CSP and historical SNe Ia (including more than 1000 spectra). Finally, we review some of the strongest correlations between spectroscopic and photometric properties of SNe Ia. Specifically, we define two samples: one consisting of SNe Ia discovered by targeted searches (most of them CSP-I objects) and the other composed of SNe Ia discovered by untargeted searches, which includes most of the CSP-II objects. The analysed correlations are similar for both samples. We find a larger incidence of SNe Ia belonging to the Cool (CL) and Broad Line (BL) Branch subtypes among the events discovered by targeted searches, Shallow Silicon (SS) SNe Ia are present with similar frequencies in both samples, while Core Normal (CN) SNe Ia are more frequent in untargeted searches.

*Keywords:* supernovae: general — techniques: spectroscopic

## 1. INTRODUCTION

The number of observational studies of Type Ia supernovae (SNe Ia) has continually increased as the result of their great importance to multiple fields of astrophysics. For example, SNe Ia are the primary source of iron-peak elements in the Universe, and their energy input plays an important role in the heating of interstellar matter in galaxies. They also provide important constraints on binary evolution in the Galaxy. But, probably their most outstanding property is that they are excellent extragalactic distance indicators, e.g. Zwicky et al. (1961), and thus powerful tools for the determination of the cosmological expansion rate as a function of look-back time (e.g. Burns et al. 2018; Freedman 2021; Khetan et al. 2021; Riess et al. 2022; Uddin et al. 2023).

The *Carnegie Supernova Project* began taking data in 2004 with the expressed goal of obtaining high-precision optical and near-infrared photometry of a large sample of SNe Ia acquired in well-understood photometric systems in order to characterize the ultimate precision of these events for determining distances (Hamuy et al. 2006). During its first phase (CSP-I), which operated for five years between 2004-2009, light curves were obtained for 123 nearby SNe Ia (Contreras et al. 2010; Stritzinger et al. 2011; Krisciunas et al. 2017). A large number of optical spectra were also acquired for these SNe Ia, 604 of which were published by Folatelli et al. (2013). During a second phase of the project (CSP-II), carried out between 2011-2015, optical and near-infrared photometry were obtained for 214 SNe Ia, 125 of which were located in the smooth Hubble flow at redshifts  $0.027 < z < 0.137$  (Phillips et al. 2019). A major goal of the CSP-II was to obtain near-infrared spectroscopy, and more than 650 such spectra were acquired of 157 SNe Ia

(Hsiao et al. 2019). A significant number of optical spectra were also obtained, many for classification purposes, while more extensive follow-up was performed for a limited number of events.

In this data release paper, we present 148 previously unpublished optical spectra of 30 SNe Ia observed during the course of the CSP-I and 234 previously unpublished spectra of 127 SNe Ia observed during the CSP-II. The CSP-I spectra presented here were not included in Folatelli et al. (2013) because at the time of publication of that paper, definitive photometry was not yet available for the corresponding objects and as a consequence, the analysis of spectroscopic and photometric properties could not be carried out in the same way as for the other SNe Ia. CSP optical spectra have already been published for SN 2010ae (Stritzinger et al. 2014), SN 2011iv (Gall et al. 2018), SN 2012Z (Stritzinger et al. 2015), SN 2012fr (Childress et al. 2013), iPTF13ebh (Hsiao et al. 2015), SN 2013gy (Holmbo et al. 2019), ASASSN-14lp (Shappee et al. 2016), LSQ14fm (Hsiao et al. 2020), ASASSN-15hy (Lu et al. 2021), SN 2015bp (Wyatt et al. 2021), SN 2007if, SN 2009dc, LSQ12gpw, SN 2013ao, CSS140501-170414+174838 and SN 2015M (Ashall et al. 2021), and SN 2015bo (Hoogendam et al. 2022). Also, a large number of CSP optical spectra of SNe Ia obtained near maximum light have been analysed by Burrow et al. (2020) using Gaussian mixture models. The approach in this paper differs from the latter in that we intend to derive spectroscopic parameters at the time of maximum light for the SNe Ia in our sample, and only those objects for which such parameters were obtained are considered in the discussion that follows.

In addition, we include in this paper a number of spectra of what we shall refer to as “historical” SNe Ia. These consist of:

- 53 optical spectra of 30 SNe Ia observed by the Calán/Tololo Supernova Survey (Hamuy et al. 1993).
- 163 optical spectra of an additional 16 SNe Ia obtained mostly by members of the Calán/Tololo team. Several of these spectra have been included in previous publications: SN 1986G (Phillips et al. 1987), SN 1989B (Wells et al. 1994), SN 1991T (Phillips et al. 1992), SN 1991bg (Leibundgut et al. 1993), SN 1992A (Kirshner et al. 1993), and SN 1992K (Hamuy et al. 1994), but are not yet publicly available on WISEREP (Yaron & Gal-Yam 2012). Some of the spectra were acquired during the execution of the Supernova Optical and Infrared Survey (SOIRS, PI M. Hamuy, 1999-2000) (Hamuy 2001; Hamuy et al. 2002a,b).

The primary goal of this paper is to make these 598 optical spectra available to the community. We combine them with the 604 CSP-I spectra published by Folatelli et al. (2013) and the previously-published CSP-I and CSP-II optical spectra mentioned above to re-examine some of the correlations between spectral and photometric properties presented by these authors. Results for the SNe Ia drawn from targeted searches are compared with those discovered in untargeted (“blind”) searches. Incorporated in this new analysis is the color stretch parameter  $s_{BV}$  (Burns et al. 2014), which is more effective at characterizing the fastest-declining SNe Ia than the widely-used  $\Delta m_{15}(B)$  parameter (Phillips 1993). Note that all the newly-presented data, including spectra of CSP I & II targets and the historical SNe Ia, will be released electronically via WISEREP.

The outline of this paper is as follows: in §2 the different spectroscopic data sets are detailed; in §3 measurements of expansion velocities and pseudo-equivalent widths are presented along with notes on a few specific SNe; in §4 we re-examine some of the spectroscopic and photometric correlations derived by Folatelli et al. (2013) using the measurements presented in this paper, augmented by those of the SNe Ia published by these authors; finally, in §5 a brief summary of the results is given.

## 2. DATA

Summaries of the new observations, classifications and photometric properties of the SNe Ia considered in this paper are presented in Table 1 (for CSP-I and CSP-II data) and Table 2 (for the historical SNe Ia). Photometric parameters for the CSP I & II targets are taken from Uddin et al. (accepted for publication in ApJ). For the historical SNe Ia, template light-curve fits were computed using SNooPy (Burns et al. 2011) to the available photometry of our objects retrieved from the references given in the final column of Table 2.

In successive columns of Tables 1 and 2 we list: the SN identification; the number of new spectra released in this work (three dots mean that no new spectra are presented); the phase range covered by them; the supernova classification obtained from running SNID (Blondin & Tonry 2007) on the earliest spectrum available to us; the Wang (Wang et al.

2009) subtype; the Branch (Branch et al. 2006) subtype; the heliocentric redshift<sup>1</sup> of the host as listed in Krisciunas et al. (2017) and Phillips et al. (2019) except for LSQ12hnr, discussed in Section 3.3; the time of maximum light; and the decline rate ( $\Delta m_{15}$ )<sup>2</sup> and color stretch ( $s_{BV}$ ) parameters from SNooPy fits (unless otherwise specified).

Journals of the spectroscopic observations, including details about the telescopes and instruments used, are presented in Tables 3 and 4 for the CSP and historical SNe Ia, respectively.

The optical spectra obtained by the CSP collaboration were reduced using standard IRAF<sup>3</sup> routines as described in Hamuy et al. (2006). Briefly, reductions included bias subtraction, flat fielding, wavelength calibration with arc lamp exposures obtained right before or after the SN observation, and flux calibration with spectra of spectrophotometric standard stars observed during the same night as the science targets. In the vast majority of the cases, the slit was oriented according to the parallactic angle. A few exceptions were made when the parallactic orientation would result in a bright host nucleus significantly contaminating the supernova spectrum. At least one telluric standard chosen from Bessell (1999) was also observed during each observing night with the same slit width as that used for the SN observation in order to correct for telluric absorption features. When a telluric standard spectrum was not obtained on the same night as the science observations, no telluric correction was attempted. Such spectra are labeled as not corrected for telluric absorption in Table 3.

The spectra obtained with the GMOS instrument on Gemini were reduced following standard procedures with the IRAF Gemini/GMOS package.

Optical spectra taken with the Nordic Optical Telescope (NOT) were obtained using ALFOSC (Andalucia Faint Object Spectrograph and Camera) with grism #4. Data reduction of NOT spectra was performed following standard procedures using a set of custom MatLab scripts written by F. Taddia. Flux calibration was performed using sensitivity functions derived from observations of standard star(s) obtained on the same night as the science observations.

As in Folatelli et al. (2013), in the last column of Table 3, we provide the root mean square (rms) of the differences between two or more synthetic magnitudes calculated from the spectra and observed magnitudes in the same filters interpolated to the exact time of the spectral observation from the CSP light curves, after removal of a constant flux term. This number provides a measure of the correctness of the *shape* of the flux-calibrated spectrum. In some cases we were not able to perform this comparison, either due to the restricted wavelength coverage of the spectrum, or because the photometric data did not cover the epoch of the spectrum. When the rms was larger than  $\sim 0.15$  mag for at least three bandpasses, we used a low-order polynomial function to correct the overall shape of the spectrum.

Most of the spectra of the historical SNe Ia were also calibrated using standard IRAF routines. Unfortunately, for some of these observations, details of the exposure time, airmass, and, in a few cases, the instrument used have been lost. No attempt has been made to quantify errors in the shapes of the spectra introduced in the flux calibration through comparison with available photometry.

### 3. MEASUREMENTS

#### 3.1. Expansion velocities and pseudo-equivalent widths

We measured expansion velocities and pseudo-equivalent widths (pW) of selected features as described in Folatelli et al. (2013). Following the definitions in Garavini et al. (2007) (see Figure 4 and Table 5 of Folatelli et al. 2013) we performed measurements of the following features: Ca II H&K (pW1), Si II  $\lambda 4130$  (pW2), Mg II  $\lambda 4481$  (pW3; blended with Fe II and dominated by Ti II in the Branch CL class), Fe II at  $\sim 4600$  Å (pW4, blended with S II), the S II “W” feature at  $\sim 5400$  Å (pW5), Si II  $\lambda 5972$  (pW6), Si II  $\lambda 6355$  (pW7), and the Ca II “IR triplet” (pW8).

All measurements were made by means of the IRAF *splot* task from the *onedspec* package. Line expansion velocities were derived from Gaussian fitting of the minimum of each absorption trough. The pW measurements were obtained by direct integration between two defined pseudo-continuum positions. Error estimates were computed with *splot* setting the number of samples for error computation (the *nerrsample* parameter) to 100, the *sigma0* parameter (uniform component of the uncertainty) to the rms flux measured in the nearby pseudo-continuum, and disregarding any Poissonian component of the uncertainty (i.e. setting the *invgain* parameter to zero). We adopted 1 Å as the minimum realistic uncertainty for pW measurements. For some critical features, such as Si II  $\lambda 5972$ , when unable to obtain a

<sup>1</sup> The redshift quoted here is not precisely the redshift as defined in cosmology, in that it can contain peculiar velocities due to galaxy infall. If an averaged peculiar velocity of 300 km s<sup>-1</sup> is assumed, it would add a 0.001 uncertainty in the redshift, as estimated from the spectroscopic velocity.

<sup>2</sup>  $\Delta m_{15}$  is approximately equivalent to  $\Delta m_{15}(B)$ , but is measured via SNooPy fits to all photometric filters available, rather than being a direct measurement of the *B*-band light-curve decline rate.

<sup>3</sup> IRAF was distributed by the National Optical Astronomy Observatory, which is operated by the Association of Universities for Research in Astronomy (AURA) under cooperative agreement with the National Science Foundation.

reliable measurement because the feature was very weak or not detected, we estimated upper limits of pW considering the signal-to-noise ratio in the spectral region where such a feature would be expected.

### 3.2. Spectroscopic parameters at maximum light

The measurements described above for our own spectra were analysed in combination with similar measurements of spectra of the targets in Table 1 that are publicly available through WISeREP, specifically when our observations were not sufficiently close to maximum light to compute the desired spectroscopic parameters. The procedure followed is the same described in Folatelli et al. (2013) and is summarized as follows:

- In cases where several spectra encompassing maximum light were available to us, we fit low-order polynomials to our pW and expansion velocity measurements and used those functions to interpolate the values at maximum.
- When two spectra were available in the interval  $-4$  to  $+4$  days from maximum, we interpolated values at maximum from them.
- If only data before or after maximum were available, but one spectrum was obtained within 1 day of maximum light, an extrapolation was allowed.
- In the most frequent cases where only one spectrum was available within the range  $-4$  to  $+4$  days from maximum, we applied the slopes given in Tables 4 and 7 of Folatelli et al. (2013) to estimate values at maximum light, combining the errors estimated for our measurements with those coming from the assumed slopes.

This procedure allowed determination of pWs and expansion velocities at maximum light for the selected features in 15 CSP I SNe Ia not included in our previous spectroscopic release (Folatelli et al. 2013), 113 SNe Ia observed by the CSP II, and 27 historical SNe Ia. All targets for which we were able to derive spectroscopic parameters at maximum light are included, regardless of their being considered as “normal” or “peculiar” SNe Ia. The values of the pWs at maximum light are presented in Table 5. Measurements of expansion velocities at maximum light can be found in Table 6. Note that the SNe are sorted by Branch type (Branch et al. 2006) in both tables.

### 3.3. Notes on particular targets

**LSQ12ca:** This SN Ia has the lowest value of  $\Delta m_{15}$  in the CSP-II sample ( $0.618 \pm 0.081$  mag.), although its  $s_{BV}$  ( $1.195 \pm 0.097$ ), while high, is comparable to that of other normal SNe Ia. From the spectrum available to us, obtained at phase 2.8 days past maximum, we derive normal values for its expansion velocities and pseudo-equivalent widths at maximum light. C II absorption is probably present on the red side of the Si II  $\lambda 6355$  line.

**LSQ12gpw:** There are three public spectra of this SN Ia from PESSTO<sup>4</sup>, available in WISeREP: the one obtained at phase -1.5 days and the other two at phase -0.5 days. There is also one CSP spectrum at phase +5.8 days. All these spectra show an absorption line, redward of Si II  $\lambda 6355$ , well separated from the Si II feature that, if identified as C II  $\lambda 6580$ , yields expansion velocities of approximately  $7,500 \text{ km s}^{-1}$ ,  $7,400 \text{ km s}^{-1}$  and  $6,200 \text{ km s}^{-1}$ , for phases -1.5, -0.5, and +5.8 days, respectively.

**LSQ12hno** shows expansion velocities somewhat lower than usual ( $\sim 8000\text{-}9000 \text{ km s}^{-1}$ ) in our two spectra obtained at 2.4 and 1.5 days before maximum light, respectively.

**LSQ12hnr:** Two spectra of LSQ12hnr are available in WISeREP, both obtained by PESSTO, at phases +0.8 and +10.8 days, respectively. The classification report by Le Guillou et al. (2012) gave a possible redshift of  $z = 0.135$  inferred from the SN Ia spectrum. No obvious host is detected in our follow-up images or in a deep VLT-MUSE observation of the SN Ia site. However, an apparent cluster of galaxies is observed whose brightest member lies about  $40''$  West of the SN Ia location. We determined redshifts for the three brightest galaxies in that cluster (from a total of at least four) obtaining a weighted average of  $z = 0.1243 \pm 0.0002$ , the value we therefore adopted for LSQ12hnr assuming this SN Ia occurred in a fainter member of the same cluster of galaxies.

**OGLE-2013-SN-015:** There is only one CSP spectrum of this SN Ia, which, albeit noisy, seems normal, and was obtained very close to maximum light (phase = +0.7 days). However, our photometric follow-up was poor for this target and consequently we decided not to consider this SN Ia in our analysis of SN properties at maximum light.

<sup>4</sup> Public ESO Spectroscopic Survey of Transient Objects, Smartt et al. (2015).

## OGLE-2013-SN-123

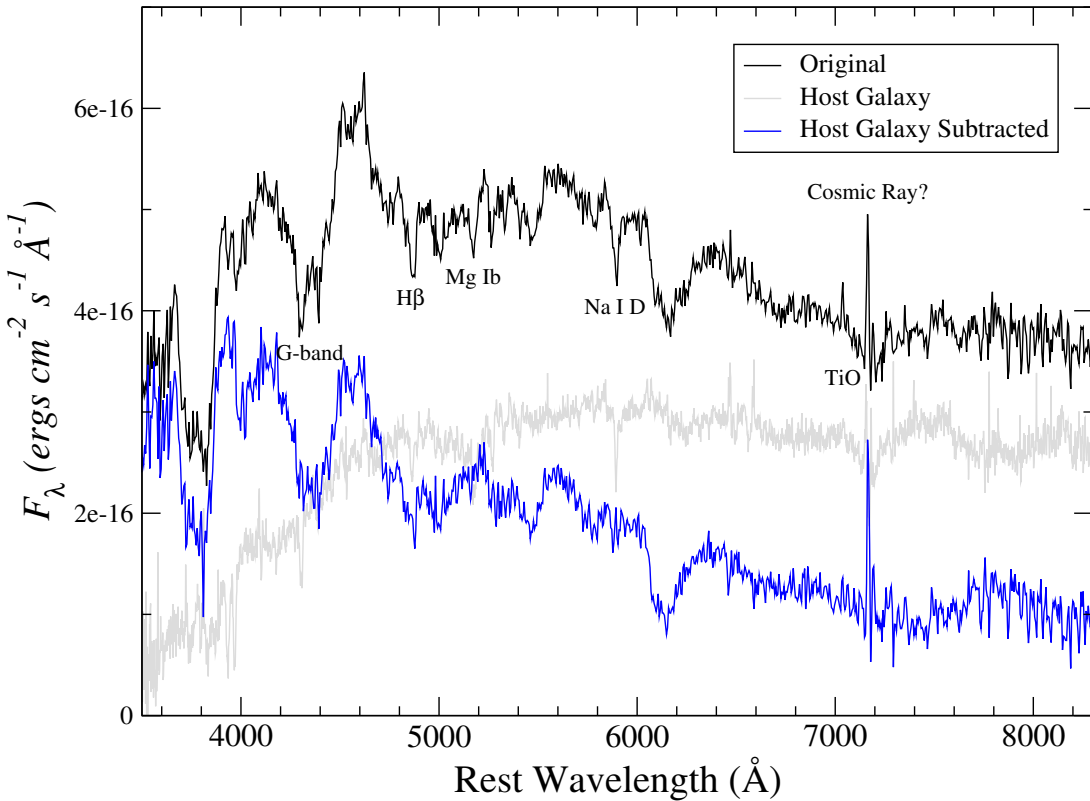


**Figure 1.** The spectrum of OGLE-2013-SN-123 after galaxy subtraction. The black spectrum is the original PESSTO observation, the gray spectrum is that of the host galaxy obtained by the CSP-II, and the blue spectrum is the difference between the two after scaling the host-galaxy spectrum to minimize the stellar features in the original PESSTO spectrum. Due to the differing wavelength resolution of the spectra, some residual subtraction features are evident (e.g., for the Na I D line). See text for further details.

**OGLE-2013-SN-123:** There is only one spectrum available from WISEREP, obtained by the PESSTO collaboration at maximum light, which shows clear evidence of host galaxy contamination and, therefore, the pWs measured from it are unreliable as well as the spectral type determined via SNID. However, we obtained a spectrum of the host galaxy with the WFCCD instrument on the Las Campanas 2.5 m du Pont telescope in 2019 to determine its redshift. By scaling the host spectrum and subtracting it from the SN Ia observation so as to make the obvious stellar Na I D blend at  $\sim 5892 \text{ \AA}$  absorption and the TiO feature at  $\sim 7150 \text{ \AA}$  disappear, the other stellar features such as Ca II H&K, the G-band at  $\sim 4300 \text{ \AA}$ , H $\beta$ , and Mg Ib  $\lambda 5175$  also mostly disappeared (see Figure 1). We therefore have used this host-galaxy subtracted spectrum to derive the spectroscopic properties at maximum light for this SN Ia.

**ASASSN-15eb:** The classification report by Childress et al. (2015) does not refer to any peculiarities, however SNID yields some matches with 91T-like SNe at maximum light. According to our light curve, this spectrum corresponds to phase +4.5 days. The pWs are indeed small, but this is clearly caused by strong host contamination. Also strong Galactic Na I D absorption is evident in that spectrum. The CSP spectrum published here, obtained at phase +11.0 days also exhibits significant host galaxy contamination as well as strong Na I D absorption from the Milky Way. Both spectra show absorption minima on the red side of Si II  $\lambda 6355$  which could be attributed to C II.

## 4. RESULTS

In this section, we combine the Si II expansion velocities and selected pW measurements from this paper with those derived by Folatelli et al. (2013) to take a second look at some of the plots and correlations discussed in that paper. In particular, our interest is to highlight agreements and differences between the properties of SNe Ia discovered in targeted versus untargeted searches.

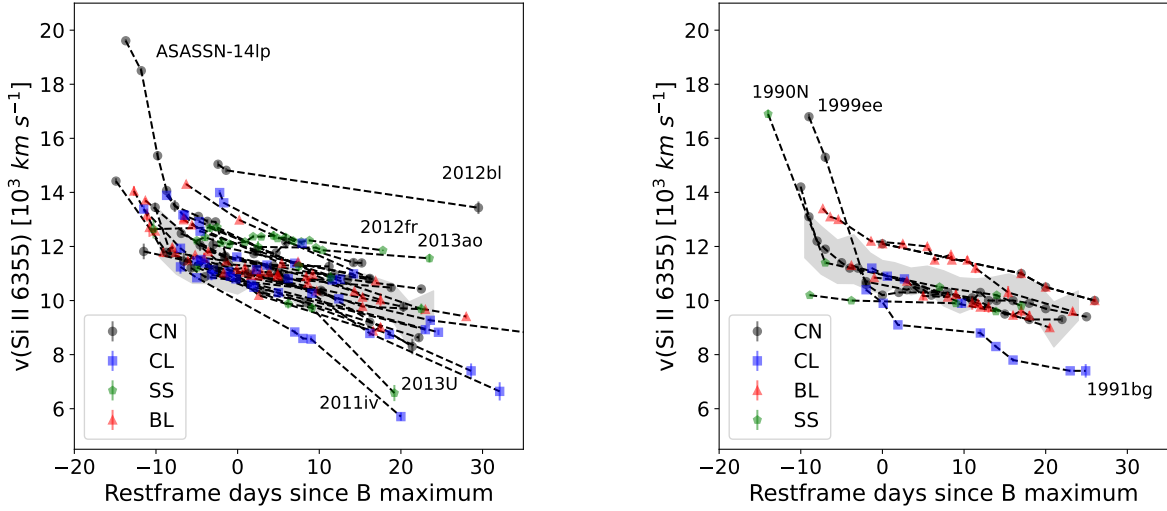


**Figure 2.** Temporal evolution of the expansion velocities of the Si II  $\lambda 6355$  line for samples of the CSP II targets (left) and the historical SNe Ia (right). The symbols reflect the corresponding Branch types: black circles for CN, green pentagons for SS, red triangles for BL and blue squares for CL. Error bars are plotted except when smaller than the symbols. Dashed lines connect data for each SN. In both panels, the shaded region represents the upper and lower  $1\sigma$  dispersion computed for all the Branch CN SNe with “normal” Wang classification subtypes in the whole CSP I & II sample.

#### 4.1. Temporal evolution of the expansion velocities of Si II $\lambda 6355$

For a limited number of CSP-II targets and historical SNe Ia, the available data span enough time to follow the evolution of the Si II  $\lambda 6355$  expansion velocity to at least 20 days past maximum light. These observations are presented in the left and right panels of Figure 2, respectively, with the different Branch types indicated by the colors and shapes of the symbols. In general, albeit with less data here, the behavior observed in this figure is very similar to that of Figure 9 of Folatelli et al. (2013). In both panels, the shaded region represents the upper and lower  $1\sigma$  dispersion of the Si II  $\lambda 6355$  expansion velocity evolution for the whole CSP I & II sample of Branch CN SNe with “normal” Wang classification subtypes (see Table 7 for details).

From Figure 2 (left panel), we can see that SN 2012bl shows high Si II  $\lambda 6355$  velocity which persists at 29 days past maximum light, although measurements of the minimum of Si II  $\lambda 6355$  after 20 days post maximum are questionable due to blending with other features. SN 2012fr (Childress et al. 2013; Contreras et al. 2018; Cain et al. 2018) is an example of “flat” velocity evolution, in which the expansion velocity of Si II  $\lambda 6355$  is almost constant over the period covered by our data ( $-5.0$  to  $+17.8$  days).

For all the SNe Ia presented in this paper with sufficient time coverage, the difference between the Si II  $\lambda 6355$  velocity at maximum light and at 20 days past maximum,  $\Delta v_{20}(\text{Si II})$ , was calculated using the same methodology described in §3.1.1 of Folatelli et al. (2013). These values are given in the last column of Table 6 and plotted in Figure 3 as a function of light-curve decline rate  $\Delta m_{15}$  and color-stretch  $s_{BV}$ , respectively, along with the CSP-I objects already presented in Folatelli et al. (2013). Figure 3 confirms the strong correlation<sup>5</sup> observed by Folatelli et al. (2013) between  $\Delta v_{20}(\text{Si II})$  and  $\Delta m_{15}$  for Branch SS, CN, and CL SNe, suggesting that these events form a single sequence. On the other hand, the lack of a correlation for the Branch BL events is consistent with previous hints that these objects may represent a distinct group of SNe Ia (e.g., see Wang et al. 2013; Burrow et al. 2020).

#### 4.2. Correlations involving spectroscopic parameters

In the analysis of spectroscopic parameters at maximum light, we consider separately the objects discovered by targeted and untargeted surveys. That is, SNe Ia in the CSP-I, CSP-II, and historical samples discovered by amateur astronomers or other targeted surveys (e.g., the Lick Observatory Supernova Survey, LOSS; or the Chilean Automatic

<sup>5</sup> All the correlations presented in this work have been computed via the *linmix* code (<https://github.com/jmeyers314/linmix>) based on Kelly (2007). In the corresponding figures we present the data along with best fit lines, intrinsic scatter lines, coefficients of determination ( $R^2$ ) and Pearson correlation coefficients ( $r$ ).

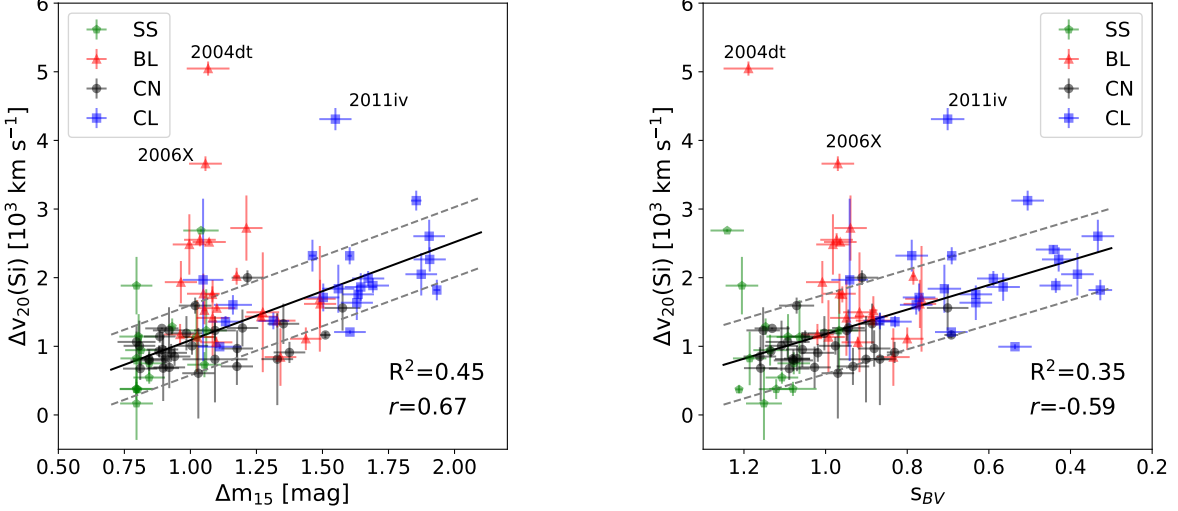


**Figure 3.** The left and right panels show the Si II  $\lambda 6355$  velocity decline rates as a function of the light curve decline rate  $\Delta m_{15}$  and color stretch  $s_{BV}$ , respectively, for all the SNe Ia with sufficient phase coverage in the combined sample which includes CSP I, CSP II and historical SNe Ia. The limited number of CSP II and historical targets for which this computation was possible causes the left panel of this figure to be very similar to Fig. 21 of Folatelli et al. (2013). As found in that work, the correlation is stronger when the BL SNe Ia are excluded from the fit. Shown in both figures are the best fit lines, intrinsic scatter lines (dotted grey), coefficients of determination ( $R^2$ ), and correlation coefficients ( $r$ ) excluding the BL events. The transitional SN Ia 2011iv is an obvious outlier.

Supernova Search, CHASE) will be considered as one sample, while all the targets drawn from untargeted surveys such as the La Silla Quest (LSQ), the Palomar Transient Factory (PTF, iPTF), the Sloan Digital Sky Survey (SDSS) or the Catalina Real Time Transient Survey (CRTS), ASAS-SN, among others, will be considered as a second sample. The Calán/Tololo SNe are a special case since the photographic plates were taken in an untargeted fashion, but were searched for stellar objects that appeared near galaxies. We therefore have grouped these SNe with the targeted events. Most of the CSP-I SNe Ia belong to the **targeted** group and most of the CSP-II SNe Ia belong to the untargeted one. However, there are a few exceptions. CSP-II SNe Ia for which we derived spectroscopic parameters at maximum light, and that are included in the first group of targeted survey discoveries are: PSN J13471211-2422171 and the SNe 2011iv, 2011jh, 2012E, 2012ah, 2012fr, 2012hd, 2012hr, 2012ht, 2013aa, 2013fz, 2013gy, 2013hn, 2014I, 2014Z, 2014ao, 2014at, 2014dn, 2014eg and 2015F. On the other hand, CSP-I targets for which we present spectroscopic parameters at maximum light that were discovered by untargeted searches are SNe 2007if, 2007ol, 2008bz and 2008fr.

#### 4.3. The Branch Diagram

Figure 4 displays the Branch et al. (2006) diagram for the targeted (left) and untargeted (right) samples of CSP and historical SNe Ia. In defining the boundaries between the four classes (CN = “core normal”, SS = “shallow silicon”, BL = “broad lined”, CL = “cool”), we follow the definitions adopted by Folatelli et al. (2013). The largest difference between these diagrams is for the BL SNe Ia, whose relative numbers are clearly different. To be precise, the BL SNe Ia represent  $31\% \pm 5\%$  of the targeted sample, but only  $13\% \pm 4\%$  of the untargeted events. This difference is explained by the fact that targeted searches are biased towards luminous galaxies, and high-velocity SNe Ia (approximately two-thirds of which belong to the BL class) are known to occur preferentially in luminous galaxies (Wang et al. 2013). Similarly to the BL events, CL SNe –those with relatively large values of pW6 (Si II 5972)– represent  $21\% \pm 4\%$  of the targeted, and  $15\% \pm 4\%$  of the untargeted samples, respectively. As for the CN SNe, they are more frequent in the untargeted sample, amounting to  $50\% \pm 9\%$  of the total, compared to  $33\% \pm 6\%$  of the targeted sample. The SS SNe, which correspond to the classical 1991T-like and 1999aa-like events, show a less significant difference, amounting to  $22\% \pm 5\%$  of the untargeted sample, while in the targeted sample they represent  $15\% \pm 4\%$ . These percentages are illustrated for the targeted and untargeted samples, respectively, in Figure 5. For further comparison, we show in

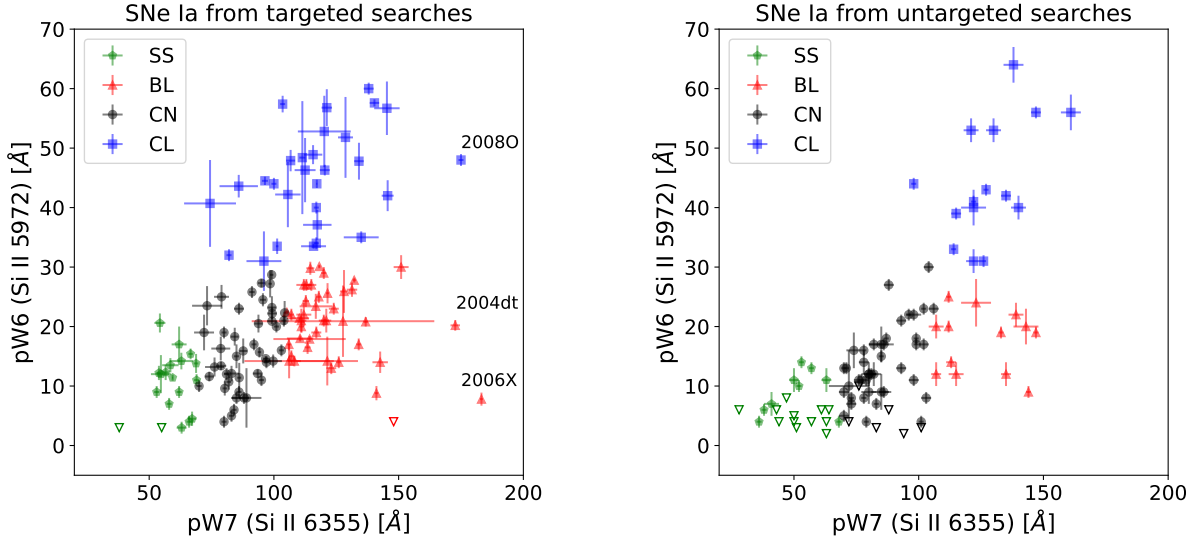


**Figure 4.** Branch diagrams for our two different samples. Left: Historical SNe Ia and CSP I+II SNe Ia discovered during targeted surveys (45 CN, 29 CL, 42 BL and 20 SS SNe Ia). Right: CSP I+II SNe Ia from untargeted surveys (48 CN, 15 CL, 13 BL and 21 SS SNe Ia). The meaning of the symbols is as follows: black dots represent CN SNe Ia; green pentagons represent SS SNe Ia; red triangles represent BL SNe Ia and blue squares represent CL SNe Ia. Open symbols represent upper limits.

Figure 6 histograms of our pW6 and pW7 measurements at maximum light for the untargeted and targeted samples, separately for each of the Branch types.

Another way to look at these numbers is to consider ratios. In particular, how do the ratios of the numbers of SS, CL and BL SNe Ia compare to the number of CN SNe Ia for the targeted and untargeted samples? In the case of the targeted SNe,  $N(\text{SS})/N(\text{CN})=0.44$ ,  $N(\text{CL})/N(\text{CN})=0.64$ , and  $N(\text{BL})/N(\text{CN})=0.93$ , while for the untargeted events we find  $N(\text{SS})/N(\text{CN})=0.44$ ,  $N(\text{CL})/N(\text{CN})=0.31$ , and  $N(\text{BL})/N(\text{CN})=0.27$ . These numbers imply that SS SNe Ia are equally common with respect to CN SNe in targeted vs. untargeted surveys. On the other hand, CL SNe Ia are twice as common and BL SNe are more than three times more common with respect to CN SNe Ia in targeted surveys compared to untargeted surveys. This likely reflects the fact that SS and CN SNe Ia occur in hosts over a large range of luminosity, whereas CL and BL SNe Ia prefer luminous hosts (e.g., see Neill et al. 2009; Wang et al. 2013; Pan 2020).

Note that Burrow et al. (2020) explored the Branch diagram through a cluster analysis instead of using pre-defined group boundaries as we have done in Figure 4. Comparing the Branch type classifications in Tables 1 and 2 for the 43 SNe Ia in common with the sample that Burrow et al. analyzed using a two-dimensional Gaussian mixture model (2D GMM), 60% are in agreement. Not surprisingly, the objects for which the classifications differ lie at or near the borders of the Branch groups.

Some studies have found correlations between SNe Ia ejecta velocities and their host properties (e.g. Pan et al. 2015; Pan 2020; Dettman et al. 2021). Considering that their results imply that high-velocity SNe Ia tend to prefer high-stellar-mass hosts, more frequent in targeted searches, we compared the Si II  $\lambda 6355$  expansion velocities at maximum light derived for our targeted and untargeted samples as a whole, as well as for the different Branch types within each sample. While the expansion velocities tend to be higher for BL SNe Ia, and somewhat lower for SS SNe Ia, the differences between the targeted and untargeted sample are insignificant considering the uncertainties. Figure 7 presents the average velocities at maximum light for Si II  $\lambda 6355$  as a function of the different Branch types, and for the whole targeted and untargeted samples, respectively.

#### 4.4. Correlations between pW values of different features at maximum light

In their study of SNe Ia from the CSP-I, Folatelli et al. (2013) searched for correlations between the different pW measurements at maximum light. In Figures 8 to 11, we reproduce the four strongest correlations that they found, plotting each separately for the targeted and untargeted samples. Folatelli et al. found that the correlations were tighter (Pearson correlation coefficients  $\rho > |0.75|$ ) if the high velocity and fast-declining ( $v(\text{Si II}(6355)) < 12,000 \text{ km s}^{-1}$  and

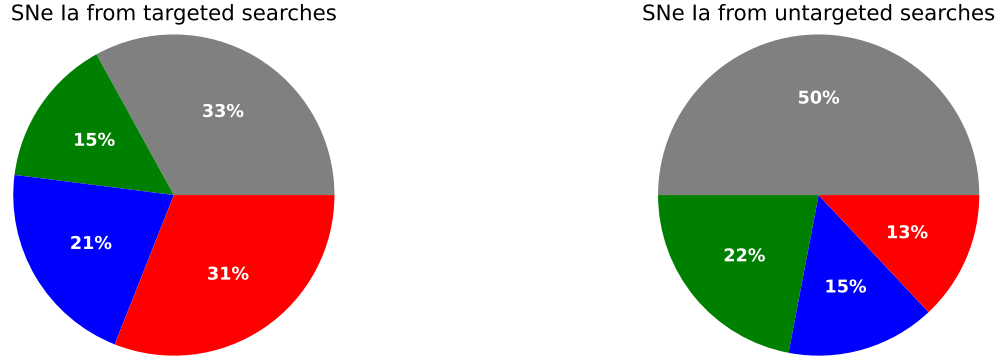


**Figure 5.** Pie charts showing the incidence of the different Branch types of SNe Ia (CN in grey, SS in green, CL in blue and BL in red) in our targeted and untargeted samples, respectively.

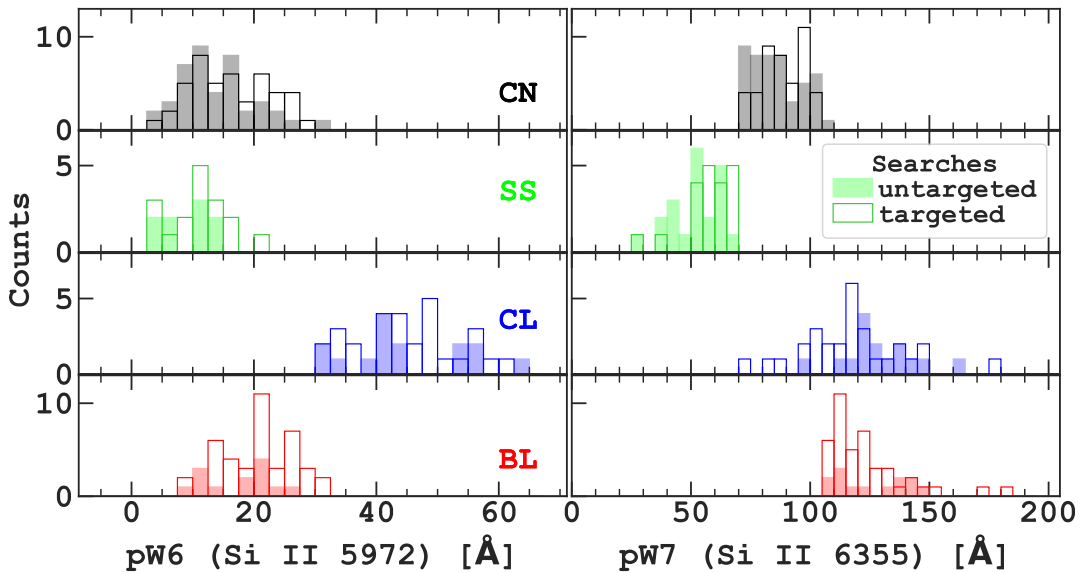


**Figure 6.** Histograms showing the distribution of the measured pW6 and pW7 separately for each Branch type. Colored and empty bars represent untargeted and targeted searches, respectively.

$\Delta m_{15}(B) < 1.7$  mag) events were excluded from the fits, but in this paper, we do not make this distinction. In each of the Figures 8 to 11, coefficients of determination ( $R^2$ ) and Pearson correlation coefficients ( $r$ ) are shown near the top left or bottom right corners of each panel.

As shown in the right panel of Figure 8, the strongest correlation for the untargeted sample is found between the pW values for Si II  $\lambda 4130$  versus Si II  $\lambda 5972$ . In this plot, the CL SN Ia LSQ14ip appears as an outlier in an otherwise strong positive correlation. However, the left panel of Figure 8 corresponding to the targeted sample shows a large dispersion in the measurements for the CL SNe Ia, with LSQ14ip lying within this dispersion. LSQ14ip is an extremely cool SN Ia, very similar to SN 1986G (Phillips et al. 1987), which showed strong Ti II absorption at maximum light. The Si II  $\lambda 4130$  line is blended with the Ti II absorption (e.g., see Ashall et al. 2016), making it difficult to measure an accurate pW value. This blending undoubtedly accounts for the large dispersion in the CL events observed in the targeted sample.

In Figure 9 we plot the pW values for the Si II  $\lambda 4130$  and Si II  $\lambda 6355$  absorptions. In this case, the correlation is tighter for the targeted sample. As might be expected, however, correlations between all three of the Si II lines are similarly strong for both the targeted and untargeted samples.

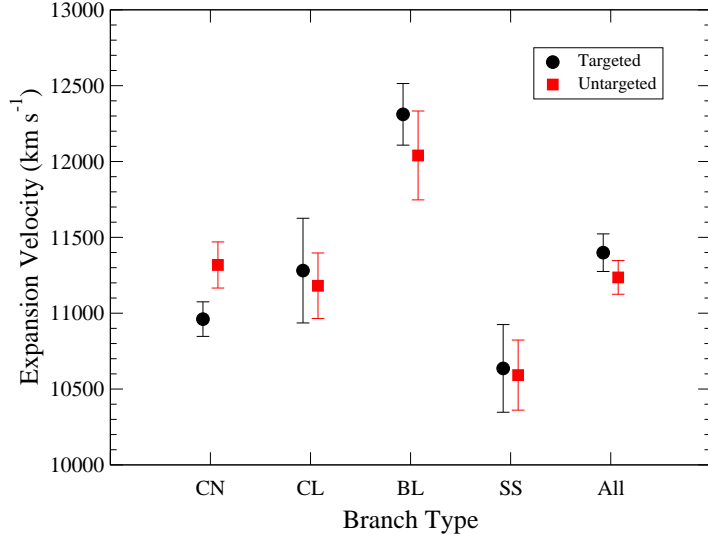


**Figure 7.** Average expansion velocities of the Si II  $\lambda 6355$  for each of the Branch types in the targeted and untargeted samples, and for each of the two samples together. The error bars represent the standard errors of the mean.

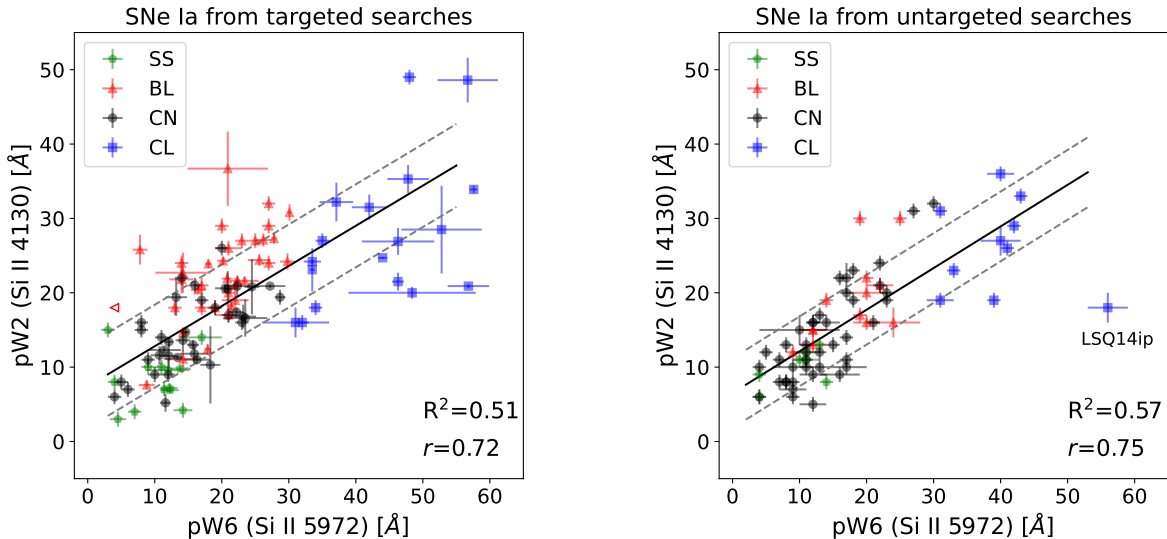


**Figure 8.** Correlation between pW values of Si II  $\lambda 4130$  and Si II  $\lambda 5972$  for our two different samples: historical SNe Ia and CSP SNe Ia from targeted searches (left) and CSP SNe Ia discovered by untargeted searches (right). The meaning of the symbols is as in Figure 4. The correlation strengths are similar for both samples as well as the slopes of the best-fit lines (**0.54±0.05** and **0.56±0.06** for the targeted and untargeted samples, respectively).

Figure 10 displays the pW values for the Ca II IR triplet plotted versus the pW4 (Fe II) measurements. The correlation is tighter for the SNe Ia discovered in untargeted searches. In Figure 11 the correlation between the pW8 (Ca II IR) and pW7 (Si II 6355) parameters is displayed. We see that the source of much of the dispersion, notably in the plot corresponding to the targeted searches, comes from the CL SNe Ia.

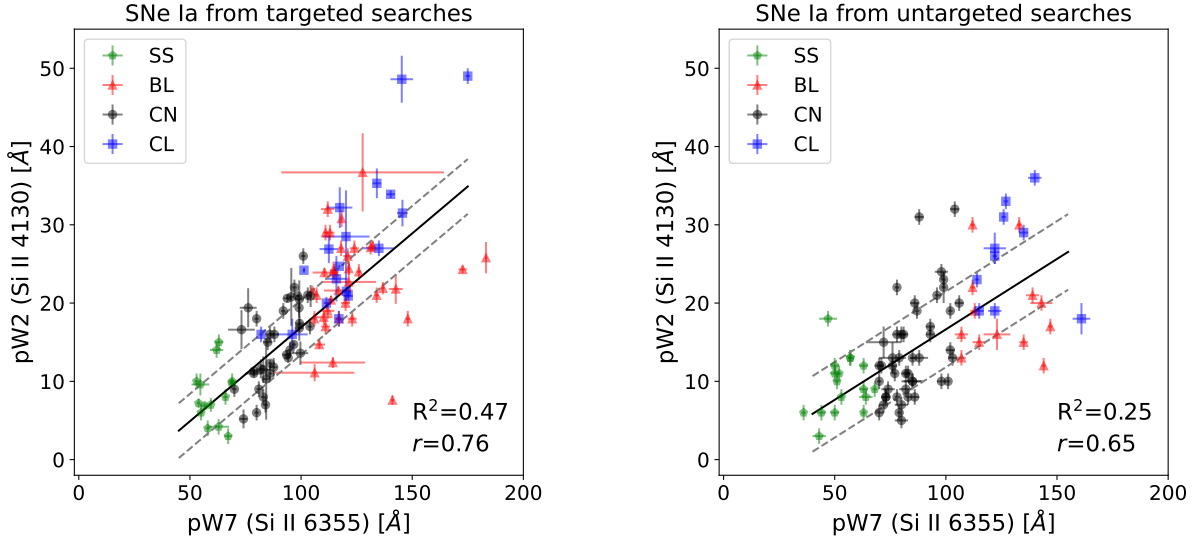


**Figure 9.** Correlation between pW values of Si II  $\lambda 4130$  and Si II  $\lambda 6355$  for our two different samples of SNe Ia discovered by targeted (left) and untargeted (right) searches. The meaning of the symbols is as in Figure 4. The correlation is stronger and has a smaller intrinsic scatter for the targeted sample. The best-fit lines have slopes of  $0.24 \pm 0.04$  and  $0.18 \pm 0.04$  for the targeted and untargeted samples, respectively.

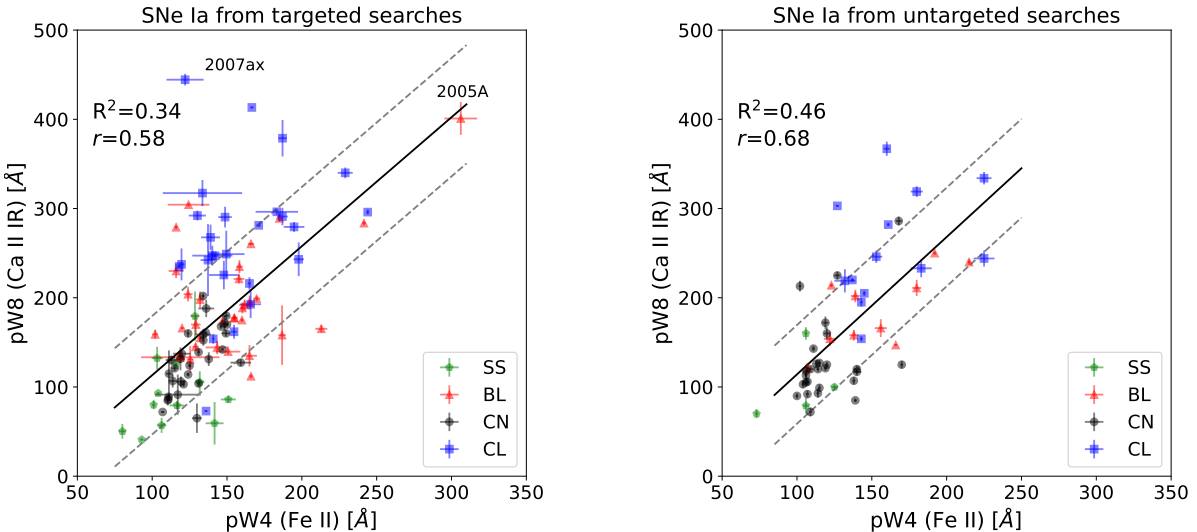


**Figure 10.** Correlation between pW values of the Ca II IR triplet and the Fe II feature at  $\sim 4600$  Å for our two different samples of SNe Ia discovered by targeted (left) and untargeted (right) searches. The meaning of the symbols is as in Figure 4. The correlation is a bit stronger for the untargeted sample, while the slopes are indistinguishable ( $1.51 \pm 0.21$  and  $1.54 \pm 0.24$  for the targeted and untargeted samples, respectively).

In order to provide a broader view of the possible correlations between the spectroscopic parameters under consideration, we present in Figure 12 correlation matrices for pairs of pW values and expansion velocities at maximum light for the objects in our targeted and untargeted samples, respectively.

#### 4.5. Correlations involving spectroscopic parameters at maximum light and photometric properties

We briefly review here the strongest correlations between pW values at maximum light and the light curve decline rate expressed by the typical  $\Delta m_{15}$  parameter, or the more recently defined color stretch parameter,  $s_{BV}$ . Figure 13

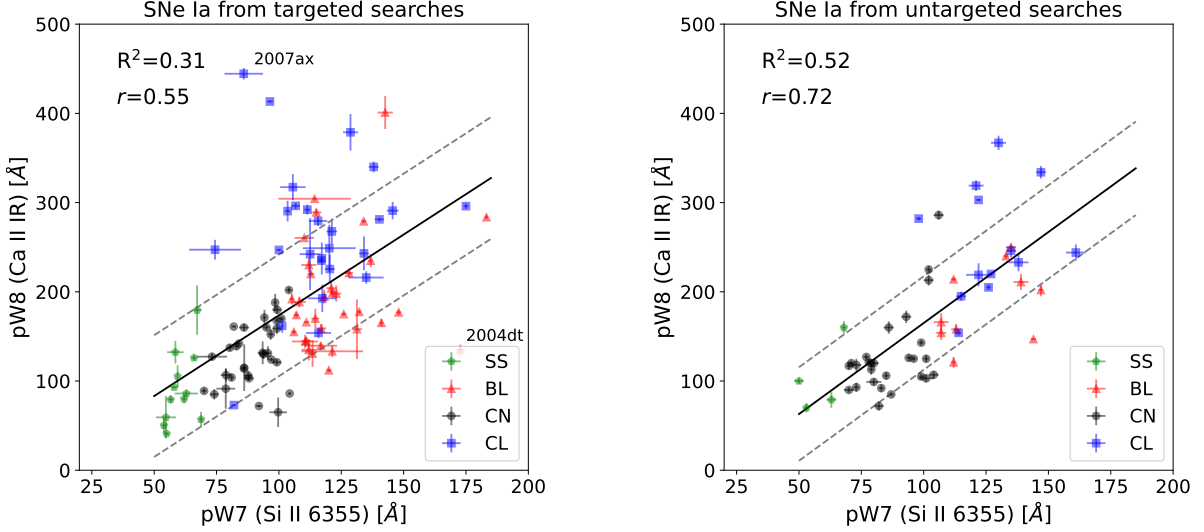


**Figure 11.** Correlation between pW values at maximum light of the Ca II IR triplet and Si II  $\lambda 6355$  for our two different samples of SNe Ia discovered by targeted (left) and untargeted (right) searches. The meaning of the symbols is as in Figure 4. The slopes of the best-fit lines are equivalent within the uncertainties:  $1.81 \pm 0.27$  and  $2.04 \pm 0.28$  for the targeted and untargeted samples, respectively.

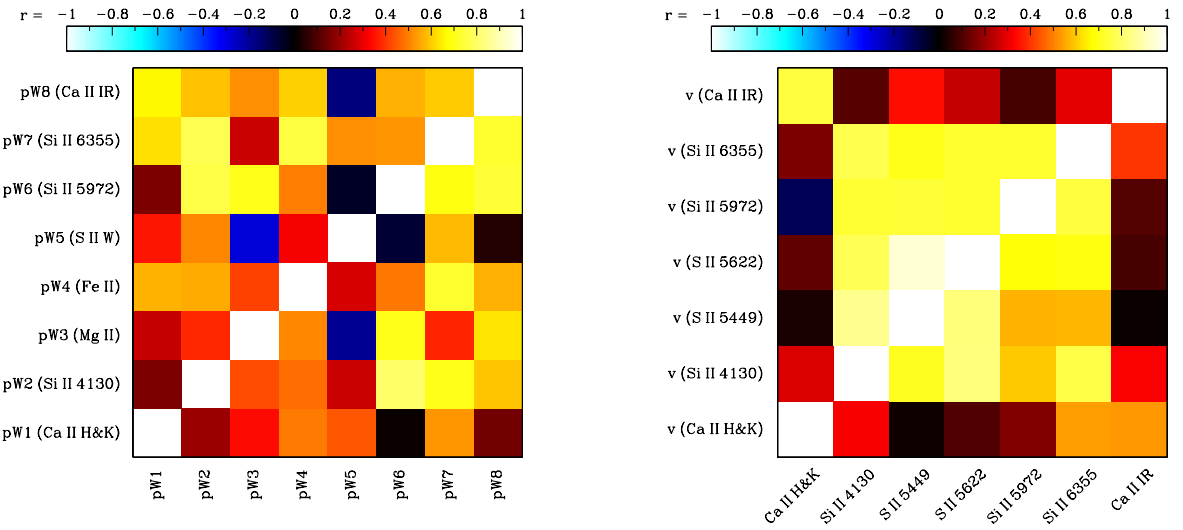


**Figure 12.** Correlation matrices for pairs of pseudo-equivalent widths (left) and expansion velocities (right) at maximum light for all the SNe Ia analysed in this paper. The upper left off-diagonal triangle of each matrix shows results for the targeted sample, while the lower right off-diagonal triangle represents the SNe Ia discovered in untargeted searches. As shown in the color scales on top of each panel, different colors correspond to different values of the Pearson coefficient ( $r$ ) with lighter colors indicating stronger correlation (or anti-correlation).

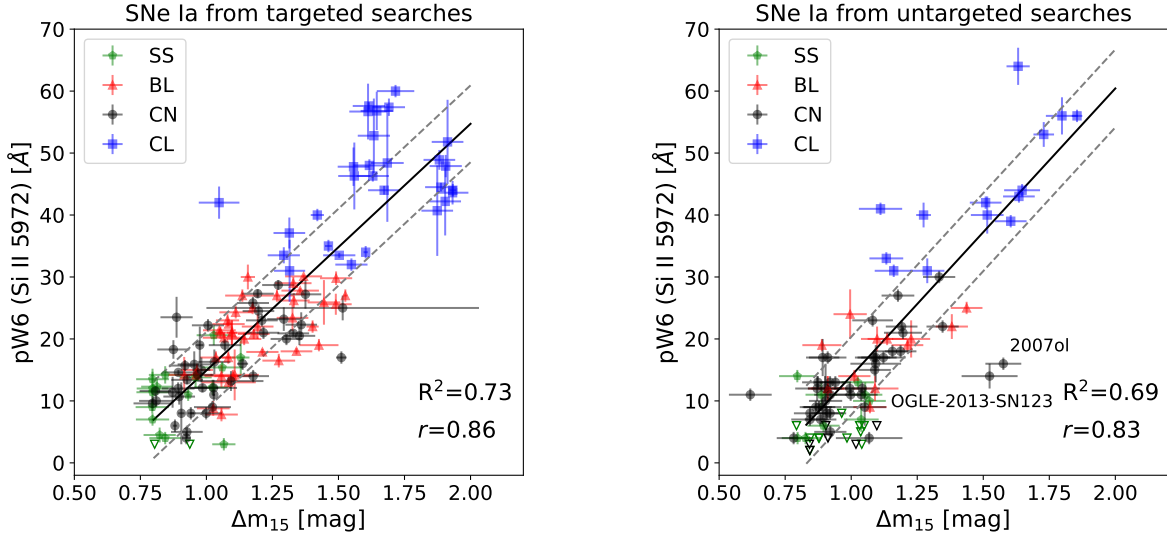


**Figure 13.** Pseudo equivalent width at maximum light of Si II  $\lambda 5972$  versus  $\Delta m_{15}$  for our two different samples of SNe Ia discovered by targeted (left) and untargeted (right) searches. The meaning of the symbols is as in Figure 4. The best-fit lines have slopes of  $39.8 \pm 2.2$  Å per mag, and  $46.4 \pm 3.5$  Å per mag, for the targeted and untargeted samples, respectively.

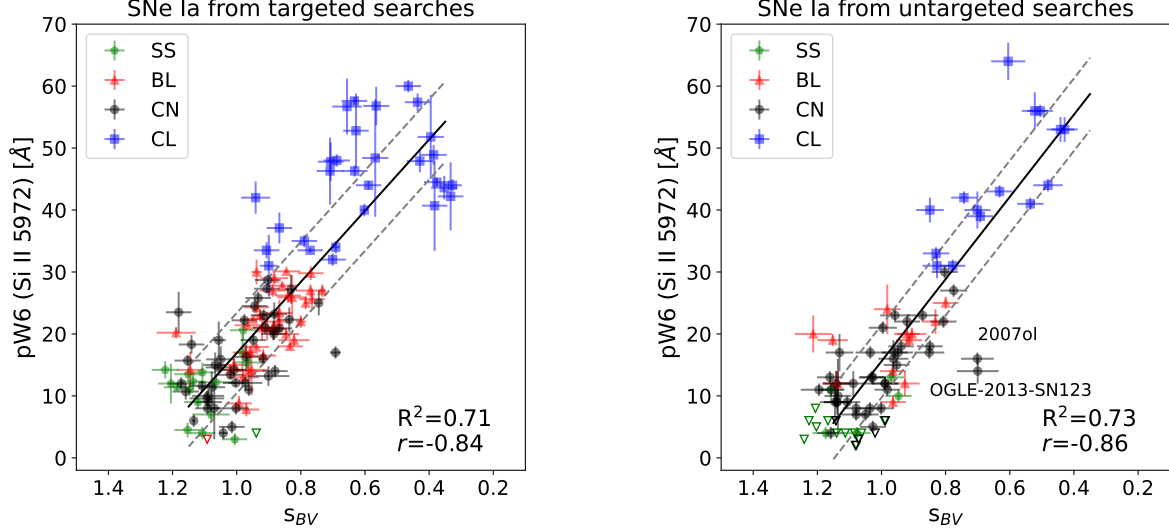
shows the correlations between pW6 (Si II 5972) and  $\Delta m_{15}$ . That these two parameters correlate strongly was first pointed out by Hachinger et al. (2006). The relations are similarly tight for both the targeted and untargeted samples. The most discrepant measurements in the untargeted sample correspond to the CNs SN 2007ol and SN OGLE-2013-SN-123. As explained in §3.3, the PESSTO spectrum of the latter suffered from considerable host galaxy contamination. While our attempt to correct for this problem was largely successful, the error in the pW6 (Si II 5972) measurement is likely underestimated due to uncertainties in the subtraction of the host galaxy spectrum. Accounting for this extra source of uncertainty would bring the error in pW6 up to  $\pm 7$  Å. On the other hand, the spectrum of SN 2007ol looks good and does not show indications of host galaxy contamination.

Figure 14 displays the relationship between pW6 (Si II 5972) and  $s_{BV}$ . We might have expected an improvement in the correlation since the  $s_{BV}$  parameter does a better job of discriminating between light curve shapes for fast-declining events. Nevertheless, the coefficients of determination and Pearson  $r$  coefficients are similar to those obtained using  $\Delta m_{15}$ .

Folatelli et al. (2013) found that pW2 (Si II 4130) also correlated strongly with the light curve decline rate. In Figures 15 and 16, this parameter is plotted against  $\Delta m_{15}$  and  $s_{BV}$ , respectively. Again, it is somewhat surprising to see that usage of  $s_{BV}$  does not significantly improve the tightness of the correlations. This could be related to the fact that  $s_{BV}$  seems not to work as well as  $\Delta m_{15}$  for SS SNe Ia (C. Burns, private communication).

## 5. SUMMARY

In this paper, we have presented 230 optical spectra of 130 SNe Ia observed during the course of the CSP-II campaign, which was carried out between 2011-2015. These data are complemented by an additional 148 optical spectra of 30 SNe Ia obtained during the CSP-I campaign (2004-2009) that were not included in the paper by Folatelli et al. (2013). Finally, we have appended to this paper an “historical” sample consisting of 53 spectra of 30 SNe Ia observed by the Calán/Tololo Supernova Survey between 1990-1993, along with 163 additional spectra of 16 SNe Ia obtained between 1986-2001, mostly by members of the Calán/Tololo team. A number of optical spectra of SNe Ia obtained in the course of the CSP campaigns already published in previous papers have also been considered in this work. Measurements of expansion velocities at maximum light, the Si II  $\lambda 6355$  velocity decline parameter,  $\Delta v_{20}(\text{Si II})$ , and pseudo-equivalent width features at maximum light in the system of Garavini et al. (2007) and Folatelli et al. (2013) have been provided for as many of these SNe Ia as possible. These data have been combined with measurements of the same parameters for the CSP-I SNe Ia published by Folatelli et al. (2013) to re-examine the Branch diagram and a few of the strongest correlations of parameters found for SNe Ia discovered in targeted versus untargeted searches. The most significant difference that we find is in the Branch diagram for targeted searches, which contains proportionately more CL and



**Figure 14.** Pseudo equivalent width at maximum light of Si II  $\lambda 5972$  versus color stretch for our two different samples of SNe Ia discovered by targeted (left) and untargeted (right) searches. The meaning of the symbols is as in Figure 4. The slopes of the best-fit lines are  $-57.4 \text{ \AA} \pm 3.2 \text{ \AA}$  and  $-66.4 \text{ \AA} \pm 4.4 \text{ \AA}$  for the targeted and untargeted samples, respectively. In this figure the abscissa has been inverted to facilitate comparison with Figure 13.

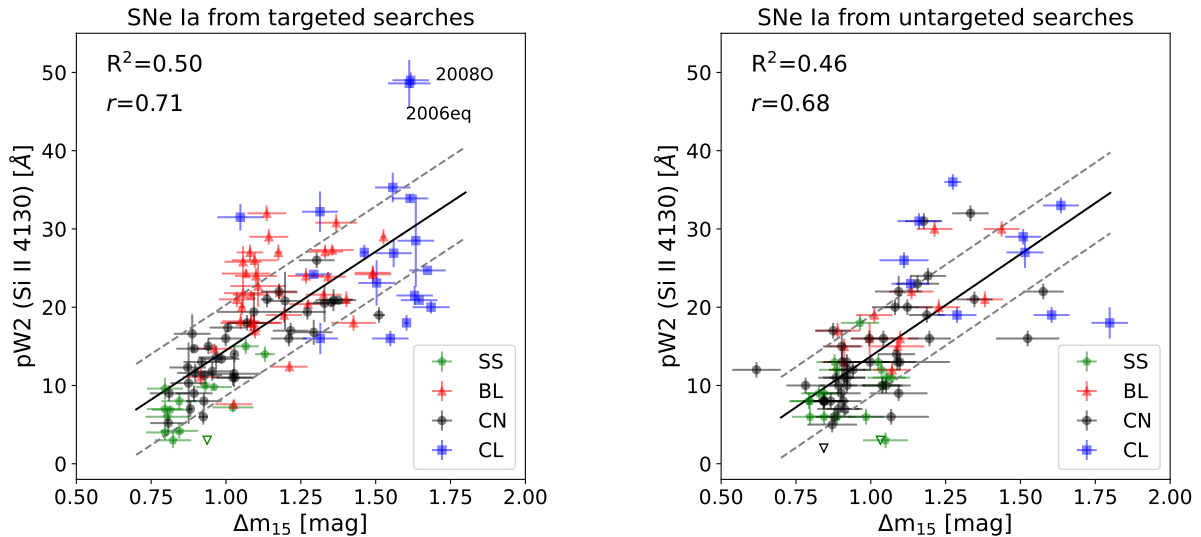


**Figure 15.** Pseudo equivalent width at maximum light of Si II  $\lambda 4130$  versus  $\Delta m_{15}$  for our two different samples of SNe Ia discovered by targeted (left) and untargeted (right) searches. The meaning of the symbols is as in Figure 4. The slopes of the best-fit lines are:  $25.2 \pm 2.6 \text{ \AA}$  per mag, and  $26.1 \pm 3.1 \text{ \AA}$  per mag, for the targeted and untargeted samples, respectively.

BL objects than is the case for untargeted searches. This difference is ascribed to the fact that targeted searches are dominated by SNe Ia discovered in luminous galaxies, and that CL and BL events are known to preferentially occur in such galaxies.

The work of the CSP has been supported by the National Science Foundation under grants AST0306969, AST0607438, AST1008343, AST1613426, AST1613455 and AST1613472. CSP-II also was supported in part by funding from the Danish Villum FONDEN (grant numbers 13261 and 28021) and the Independent Research Fund Denmark (IRFD) by a Sapere Aude II Fellowship awarded to M.D.S. Additional IRFD funding comes from Project

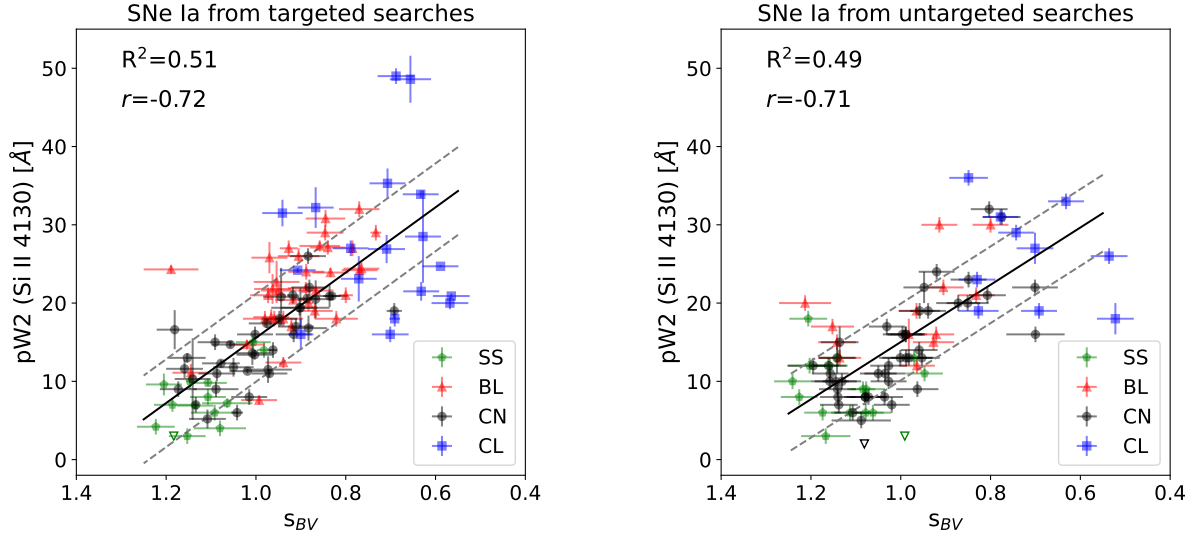


**Figure 16.** Pseudo equivalent width at maximum light of Si II  $\lambda$ 4130 versus color stretch for our two different samples of SNe Ia discovered by targeted (left) and untargeted (right) searches. The meaning of the symbols is as in Figure 4. The slopes of the best-fit lines are  $-41.7 \text{ \AA} \pm 4.1 \text{ \AA}$  and  $36.6 \text{ \AA} \pm 4.0 \text{ \AA}$  for the targeted and untargeted sample, respectively. Note that the abscissa ( $s_{BV}$ ) is inverted in this plot to facilitate comparison with Figure 15.

1 (8021-00170B) and Project 2 (10.46540/2032-00022B) grants. This paper includes data gathered with the 6.5 m Magellan Telescopes located at Las Campanas Observatory, the Gemini South, Cerro Pachón, Chile and Gemini North, Mauna Kea, Hawaii (Gemini Programs No. GS-2011B-Q-15-150-002 and GN-2013A-Q-68-82-002). Also based on observations collected at the European Organization for Astronomical Research in the Southern Hemisphere, Chile (ESO Programs 164.H-0376 and 0102.D-0095). C.G. is supported by a research grant (25501) by the Villum FONDEN. M.H. acknowledges support from FONDECYT-Chile through grants 92/0312 and 1060808; the National Science Foundation through grants GF-1002-96 and GF-1002-97; the Association of Universities for Research in Astronomy, Inc., under NSF Cooperative Agreement AST-8947990 and from Fundación Andes under project C-12984; the Hubble Fellowship grant HST-HF-01139.01-A (awarded by the Space Telescope Science Institute, which is operated by the Association of Universities for Research in Astronomy, Inc., for NASA, under contract NAS 5-26555); and the Carnegie Postdoctoral Fellowship. This work has been funded by ANID, Millennium Science Initiative, ICN12\_009. L.G. acknowledges financial support from the Spanish Ministerio de Ciencia e Innovación (MCIN), the Agencia Estatal de Investigación (AEI) 10.13039/501100011033, and the European Social Fund (ESF) “Investing in your future” under the 2019 Ramón y Cajal program RYC2019-027683-I and the PID2020-115253GA-I00 HOSTFLOWS project, from Centro Superior de Investigaciones Científicas (CSIC) under the PIE project 20215AT016, and the program Unidad de Excelencia María de Maeztu CEX2020-001058-M. C.A., acknowledges support by NASA grants JWST-GO-02114, JWST-GO-02122 and JWST-GO-04436.024-A; and JPL grant SS03-17-23. The research of J.C.W. and J.V. is supported by NSF AST-1813825. J.V. is also supported by OTKA grant K-142534 of the National Research, Development and Innovation Office, Hungary. The authors want to thank an anonymous referee for their kind report and useful suggestions.

**Facilities:** Magellan:Baade (IMACS imaging spectrograph), Magellan:Clay (LDSS3, MagE, MIKE), du Pont (WFCCD, B&C spectrograph, MODSPEC), ESO:3.6m (EFOSC-2), NTT (EMMI), ESO:1.52m (B&C spectrograph), ESO: VLT (MUSE), NOT (ALFOSC), Gemini-South (GMOS), Gemini:Gillett (GMOS), CTIO:1.0m (B&C spectrograph), CTIO:1.5m (R-C spectrograph), Blanco (R-C spectrograph), UH:2.2m, KPNO:2.1m (Gold camera), MMT (Red channel), Shane (Cassegrain spectrograph), Nickel (Cassegrain spectrograph), FLWO:1.5m (Z Machine), La Silla-QUEST, CRTS, PTF, iPTF, OGLE, ASAS-SN, PS1, KISS, ISSP, MASTER, SMT, Calán/Tololo Supernova Survey.

## REFERENCES

- Ashall, C., Mazzali, P. A., Pian, E., & James, P. A. 2016, MNRAS, 463, 1891, doi: [10.1093/mnras/stw2114](https://doi.org/10.1093/mnras/stw2114)
- Ashall, C., Lu, J., Hsiao, E. Y., et al. 2021, ApJ, 922, 205, doi: [10.3847/1538-4357/ac19ac](https://doi.org/10.3847/1538-4357/ac19ac)
- Bessell, M. S. 1999, PASP, 111, 1426, doi: [10.1086/316454](https://doi.org/10.1086/316454)
- Blondin, S., & Tonry, J. L. 2007, ApJ, 666, 1024, doi: [10.1086/520494](https://doi.org/10.1086/520494)
- Branch, D., Dang, L. C., Hall, N., et al. 2006, PASP, 118, 560, doi: [10.1086/502778](https://doi.org/10.1086/502778)
- Burns, C. R., Stritzinger, M., Phillips, M. M., et al. 2011, AJ, 141, 19, doi: [10.1088/0004-6256/141/1/19](https://doi.org/10.1088/0004-6256/141/1/19)
- . 2014, ApJ, 789, 32, doi: [10.1088/0004-637X/789/1/32](https://doi.org/10.1088/0004-637X/789/1/32)
- Burns, C. R., Parent, E., Phillips, M. M., et al. 2018, ApJ, 869, 56, doi: [10.3847/1538-4357/aae51c](https://doi.org/10.3847/1538-4357/aae51c)
- Burrow, A., Baron, E., Ashall, C., et al. 2020, ApJ, 901, 154, doi: [10.3847/1538-4357/abafa2](https://doi.org/10.3847/1538-4357/abafa2)
- Cain, C., Baron, E., Phillips, M. M., et al. 2018, ApJ, 869, 162, doi: [10.3847/1538-4357/aaef34](https://doi.org/10.3847/1538-4357/aaef34)
- Childress, M., Scalzo, R., Yuan, F., et al. 2015, The Astronomer's Telegram, 7180, 1
- Childress, M., Aldering, G., Antilogus, P., et al. 2013, ApJ, 770, 107, doi: [10.1088/0004-637X/770/2/107](https://doi.org/10.1088/0004-637X/770/2/107)
- Contreras, C., Hamuy, M., Phillips, M. M., et al. 2010, AJ, 139, 519, doi: [10.1088/0004-6256/139/2/519](https://doi.org/10.1088/0004-6256/139/2/519)
- Contreras, C., Phillips, M. M., Burns, C. R., et al. 2018, ApJ, 859, 24, doi: [10.3847/1538-4357/aabaf8](https://doi.org/10.3847/1538-4357/aabaf8)
- Dettman, K. G., Jha, S. W., Dai, M., et al. 2021, ApJ, 923, 267, doi: [10.3847/1538-4357/ac2ee5](https://doi.org/10.3847/1538-4357/ac2ee5)
- Folatelli, G., Morrell, N., Phillips, M. M., et al. 2013, ApJ, 773, 53, doi: [10.1088/0004-637X/773/1/53](https://doi.org/10.1088/0004-637X/773/1/53)
- Freedman, W. L. 2021, ApJ, 919, 16, doi: [10.3847/1538-4357/ac0e95](https://doi.org/10.3847/1538-4357/ac0e95)
- Gall, C., Stritzinger, M. D., Ashall, C., et al. 2018, A&A, 611, A58, doi: [10.1051/0004-6361/201730886](https://doi.org/10.1051/0004-6361/201730886)
- Garavini, G., Folatelli, G., Nobili, S., et al. 2007, A&A, 470, 411, doi: [10.1051/0004-6361:20065400](https://doi.org/10.1051/0004-6361:20065400)
- Hachinger, S., Mazzali, P. A., & Benetti, S. 2006, MNRAS, 370, 299, doi: [10.1111/j.1365-2966.2006.10468.x](https://doi.org/10.1111/j.1365-2966.2006.10468.x)
- Hamuy, M., Maza, J., Phillips, M. M., et al. 1993, AJ, 106, 2392, doi: [10.1086/116811](https://doi.org/10.1086/116811)
- Hamuy, M., Phillips, M. M., Maza, J., et al. 1994, AJ, 108, 2226, doi: [10.1086/117235](https://doi.org/10.1086/117235)
- Hamuy, M., Phillips, M. M., Suntzeff, N. B., et al. 1996, AJ, 112, 2408, doi: [10.1086/118192](https://doi.org/10.1086/118192)
- Hamuy, M., Maza, J., Pinto, P. A., et al. 2002a, AJ, 124, 417, doi: [10.1086/340968](https://doi.org/10.1086/340968)
- . 2002b, AJ, 124, 2339, doi: [10.1086/344839](https://doi.org/10.1086/344839)
- Hamuy, M., Folatelli, G., Morrell, N. I., et al. 2006, PASP, 118, 2, doi: [10.1086/500228](https://doi.org/10.1086/500228)
- Hamuy, M. A. 2001, PhD thesis, University of Arizona
- Holmbo, S., Stritzinger, M. D., Shappee, B. J., et al. 2019, A&A, 627, A174, doi: [10.1051/0004-6361/201834389](https://doi.org/10.1051/0004-6361/201834389)
- Hoogendam, W. B., Ashall, C., Galbany, L., et al. 2022, ApJ, 928, 103, doi: [10.3847/1538-4357/ac54aa](https://doi.org/10.3847/1538-4357/ac54aa)
- Hsiao, E. Y., Burns, C. R., Contreras, C., et al. 2015, A&A, 578, A9, doi: [10.1051/0004-6361/201425297](https://doi.org/10.1051/0004-6361/201425297)
- Hsiao, E. Y., Phillips, M. M., Marion, G. H., et al. 2019, PASP, 131, 014002, doi: [10.1088/1538-3873/aae961](https://doi.org/10.1088/1538-3873/aae961)
- Hsiao, E. Y., Hoeflich, P., Ashall, C., et al. 2020, ApJ, 900, 140, doi: [10.3847/1538-4357/abaf4c](https://doi.org/10.3847/1538-4357/abaf4c)
- Kelly, B. C. 2007, ApJ, 665, 1489, doi: [10.1086/519947](https://doi.org/10.1086/519947)
- Khetan, N., Izzo, L., Branchesi, M., et al. 2021, A&A, 647, A72, doi: [10.1051/0004-6361/202039196](https://doi.org/10.1051/0004-6361/202039196)
- Kirshner, R. P., Jeffery, D. J., Leibundgut, B., et al. 1993, ApJ, 415, 589, doi: [10.1086/173188](https://doi.org/10.1086/173188)
- Krisciunas, K., Suntzeff, N. B., Phillips, M. M., et al. 2004a, AJ, 128, 3034, doi: [10.1086/425629](https://doi.org/10.1086/425629)
- Krisciunas, K., Phillips, M. M., Suntzeff, N. B., et al. 2004b, AJ, 127, 1664, doi: [10.1086/381911](https://doi.org/10.1086/381911)
- Krisciunas, K., Contreras, C., Burns, C. R., et al. 2017, AJ, 154, 211, doi: [10.3847/1538-3881/aa8df0](https://doi.org/10.3847/1538-3881/aa8df0)
- Le Guillou, L., Baumont, S., Sullivan, M., et al. 2012, The Astronomer's Telegram, 4673, 1
- Leibundgut, B., Kirshner, R. P., Phillips, M. M., et al. 1993, AJ, 105, 301, doi: [10.1086/116427](https://doi.org/10.1086/116427)
- Lennarz, D., Altmann, D., & Wiebusch, C. 2012, A&A, 538, A120, doi: [10.1051/0004-6361/201117666](https://doi.org/10.1051/0004-6361/201117666)
- Lira, P., Suntzeff, N. B., Phillips, M. M., et al. 1998, AJ, 115, 234, doi: [10.1086/300175](https://doi.org/10.1086/300175)
- Lu, J., Ashall, C., Hsiao, E. Y., et al. 2021, ApJ, 920, 107, doi: [10.3847/1538-4357/ac1606](https://doi.org/10.3847/1538-4357/ac1606)
- Marion, G. H., Brown, P. J., Vinkó, J., et al. 2016, ApJ, 820, 92, doi: [10.3847/0004-637X/820/2/92](https://doi.org/10.3847/0004-637X/820/2/92)
- Neill, J. D., Sullivan, M., Howell, D. A., et al. 2009, ApJ, 707, 1449, doi: [10.1088/0004-637X/707/2/1449](https://doi.org/10.1088/0004-637X/707/2/1449)
- Pan, Y.-C. 2020, ApJL, 895, L5, doi: [10.3847/2041-8213/ab8e47](https://doi.org/10.3847/2041-8213/ab8e47)
- Pan, Y. C., Sullivan, M., Maguire, K., et al. 2015, MNRAS, 446, 354, doi: [10.1093/mnras/stu2121](https://doi.org/10.1093/mnras/stu2121)
- Phillips, M. M. 1993, ApJL, 413, L105, doi: [10.1086/186970](https://doi.org/10.1086/186970)
- Phillips, M. M., Wells, L. A., Suntzeff, N. B., et al. 1992, AJ, 103, 1632, doi: [10.1086/116177](https://doi.org/10.1086/116177)
- Phillips, M. M., Phillips, A. C., Heathcote, S. R., et al. 1987, PASP, 99, 592, doi: [10.1086/132020](https://doi.org/10.1086/132020)
- Phillips, M. M., Contreras, C., Hsiao, E. Y., et al. 2019, PASP, 131, 014001, doi: [10.1088/1538-3873/aae8bd](https://doi.org/10.1088/1538-3873/aae8bd)

- Prieto, J. L., Garnavich, P. M., Phillips, M. M., et al. 2007, arXiv e-prints, arXiv:0706.4088.  
<https://arxiv.org/abs/0706.4088>
- Riess, A. G., Yuan, W., Macri, L. M., et al. 2022, ApJL, 934, L7, doi: [10.3847/2041-8213/ac5c5b](https://doi.org/10.3847/2041-8213/ac5c5b)
- Scalzo, R. A., Aldering, G., Antilogus, P., et al. 2010, ApJ, 713, 1073, doi: [10.1088/0004-637X/713/2/1073](https://doi.org/10.1088/0004-637X/713/2/1073)
- Shappee, B. J., Piro, A. L., Holoi, T. W. S., et al. 2016, ApJ, 826, 144, doi: [10.3847/0004-637X/826/2/144](https://doi.org/10.3847/0004-637X/826/2/144)
- Singh, M., Misra, K., Sahu, D. K., et al. 2018, MNRAS, 474, 2551, doi: [10.1093/mnras/stx2916](https://doi.org/10.1093/mnras/stx2916)
- Smartt, S. J., Valenti, S., Fraser, M., et al. 2015, A&A, 579, A40, doi: [10.1051/0004-6361/201425237](https://doi.org/10.1051/0004-6361/201425237)
- Stritzinger, M. D., Phillips, M. M., Boldt, L. N., et al. 2011, AJ, 142, 156, doi: [10.1088/0004-6256/142/5/156](https://doi.org/10.1088/0004-6256/142/5/156)
- Stritzinger, M. D., Hsiao, E., Valenti, S., et al. 2014, A&A, 561, A146, doi: [10.1051/0004-6361/201322889](https://doi.org/10.1051/0004-6361/201322889)
- Stritzinger, M. D., Valenti, S., Hoeflich, P., et al. 2015, A&A, 573, A2, doi: [10.1051/0004-6361/201424168](https://doi.org/10.1051/0004-6361/201424168)
- Strolger, L. G., Smith, R. C., Suntzeff, N. B., et al. 2002, AJ, 124, 2905, doi: [10.1086/343058](https://doi.org/10.1086/343058)
- Uddin, S. A., Burns, C. R., Phillips, M. M., et al. 2023, arXiv e-prints, arXiv:2308.01875, doi: [10.48550/arXiv.2308.01875](https://doi.org/10.48550/arXiv.2308.01875)
- Wang, X., Wang, L., Filippenko, A. V., Zhang, T., & Zhao, X. 2013, Science, 340, 170, doi: [10.1126/science.1231502](https://doi.org/10.1126/science.1231502)
- Wang, X., Filippenko, A. V., Ganeshalingam, M., et al. 2009, ApJL, 699, L139, doi: [10.1088/0004-637X/699/2/L139](https://doi.org/10.1088/0004-637X/699/2/L139)
- Wells, L. A., Phillips, M. M., Suntzeff, B., et al. 1994, AJ, 108, 2233, doi: [10.1086/117236](https://doi.org/10.1086/117236)
- Wyatt, S. D., Sand, D. J., Hsiao, E. Y., et al. 2021, ApJ, 914, 57, doi: [10.3847/1538-4357/abf7c3](https://doi.org/10.3847/1538-4357/abf7c3)
- Yaron, O., & Gal-Yam, A. 2012, PASP, 124, 668, doi: [10.1086/666656](https://doi.org/10.1086/666656)
- Zwicky, F., Humason, M. L., Gomes, A. M., & Gates, H. S. 1961, PASP, 73, 351, doi: [10.1086/127709](https://doi.org/10.1086/127709)

**Table 1.** Summary of observations, spectroscopic and photometric properties of CSP SNe Ia considered in this work

SN	N	Phase range [d]	SNID	Wang	Branch	$z_{He\text{I}o}$	t(max) [MJD]	$\Delta m_{15}$ [mag]	$s_{BV}$
(1)	(2)	(3)	(4)	(5)	(6)	(7)	(8)	(9)	(10)
<b>CSP I</b>									
2005gj	18	38.0, 341.4	Ia-CSM	...	...	0.0616	53657.30(1.28) <sup>a</sup>	...	...
2007if <sup>b</sup>	...	6.5, 30.5	Ia-pec (SC)	Normal	SS	0.0742	54348.4 <sup>c</sup>	...	...
2007jd	5	14.4, 44.3	Normal	HV	BL	0.0726	54361.9(1.0)	1.304(0.065)	0.891(0.054)
2007ol	7	-3.5, 20.1	Normal	Normal	CN	0.0559	54412.9(0.2)	1.576(0.068)	0.701(0.051)
2007so	5	22.5, 41.0	Normal	...	...	0.0297	54428.0(0.5)	1.196(0.067)	0.925(0.041)
2007st	6	6.7, 35.9	Normal	...	...	0.0212	54454.4(0.7)	1.428(0.081)	0.863(0.046)
2008O	3	0.5, 28.4	Normal	HV	CL	0.0389	54491.8(0.6)	1.617(0.061)	0.688(0.041)
2008ae	4	0.6, 28.7	Ia-pec	...	...	0.0300	54508.63(0.60) <sup>d</sup>	1.648(0.078)	...
2008bd	4	7.6, 13.5	91bg-like	91bg	...	0.0301	54531.2(0.5)	1.785(0.072)	0.660(0.055)
2008bi	6	9.8, 47.2	91bgi-like	91bg	...	0.0134	54543.3 (0.9)	1.977 (0.073)	0.512 (0.046)
2008bt	2	9.7, 23.4	91bg-like	91bg	...	0.0154	54572.3(0.1)	1.815(0.061)	0.498(0.041)
2008bz	5	2.1, 27.5	Normal	Normal	CN	0.0603	54578.9(0.3)	1.093(0.079)	0.948(0.046)
2008cc	5	9.2, 42.8	Normal	...	...	0.0104	54573.0(0.2)	1.402(0.069)	0.813(0.044)
2008cd	1	12.3	Normal	...	...	0.0074	54578.9(1.1)	1.071(0.169)	1.080(0.149)
2008cf	5	2.6, 20.7	Normal	Normal	SS	0.0460	54594.7(0.7)	0.804(0.073)	1.092(0.053)
2008ff	6	19.4, 88.2	Normal	...	...	0.0193	54704.2(0.2)	0.880(0.061)	1.083 (0.041)
2008fl	8	3.1, 45.3	Normal	Normal	BL	0.0199	54720.8 (0.6)	1.329(0.069)	0.883(0.043)
2008fr	2	4.6, 25.5	Normal	Normal	CN	0.0397	54732.7(0.2)	0.911(0.071)	1.035 (0.046)
2008fu	2	4.6, 25.5	Normal	Normal	...	0.0520	54732.6(0.4)	1.402(0.074)	0.822 (0.047)
2008fw	7	5.6, 88.8	91T-like	91T	SS	0.0085	54731.8(0.2)	0.844(0.070)	1.117(0.046)
2008gg	7	4.7, 69.7	Normal	HV	BL	0.0320	54749.2(0.6)	0.876(0.072)	1.054(0.047)
2008go	3	0.6, 7.5	Normal	HV	BL	0.0623	54766.1(0.2)	1.093(0.089)	0.939(0.044)
2008ha	2	7.1, 11.1	Ia-pec	...	...	0.0046	54781.89(0.37) <sup>d</sup>	1.969(0.049)	...
2008hj	7	-7.1, 26.5	Normal	HV	BL	0.0379	54801.5(0.5)	0.964(0.061)	1.008(0.040)
2009I	4	-3.7, 18.7	Normal	Normal	CN	0.0262	54851.9(0.1)	0.810(0.065)	1.089(0.050)
2009P	7	1.8, 49.5	Normal	HV	SS	0.0251	54868.4(0.3)	0.796(0.063)	1.080(0.058)
2009U <sup>e</sup>	1	13: <sup>e</sup>	91bg-like	91bg	...	0.0165	...	...	...
2009al	6	12.3, 57.3	Normal	...	...	0.0221	54893.4(0.8)	0.674(0.063)	0.920(0.042)
2009cz	4	-5.0, 8.6	Normal	Normal	CN	0.0211	54943.1(0.1)	0.893(0.062)	1.173(0.041)
2009dc <sup>b</sup>	...	-8.4, 34.5	SC	Normal	SS	0.0214	54946.87(0.49) <sup>d</sup>	0.785(0.042)	...
2009ds	5	-9.7, 20.7	Normal	HV	SS	0.0193	54961.0(0.5)	0.795(0.063)	1.121(0.043)
2009le	1	-4.6	Normal	HV	CN	0.0178	55165.9(0.1)	1.023(0.070)	1.087(0.041)
2010ae	...	17.8, 22.6:	Ia-pec	...	...	0.0037	...	...	...
<b>CSP II</b>									
ASASSN-14ad	1	7.3	Normal	...	...	0.0264	56692.70(0.50)	0.918(0.060)	1.013(0.040)
ASASSN-14hp	1	-2.3	Normal	Normal	SS	0.0389	56929.53(0.06)	0.844(0.061)	1.084(0.027)
ASASSN-14hr	1	-5.1	Normal	Normal	CN	0.0336	56932.64(0.06)	1.333(0.061)	0.803(0.041)
ASASSN-14hu	1	-6.7	Normal	Normal	CN	0.0216	56935.24(0.04)	0.884(0.060)	1.050(0.041)
ASASSN-14jc	...	...	Normal	HV	BL	0.0113	56955.60(0.57)	1.213(0.060)	0.914(0.040)
ASASSN-14kd	1	3.4	91T-like	Normal	SS	0.026	56982.30(0.51)	0.797(0.060)	1.174(0.041)
ASASSN-14kq	1	-2.2	Normal	Normal	CN	0.0336	56990.41(0.06)	0.921(0.061)	1.157(0.041)
ASASSN-14lo	2	11.2, 54.4	Normal	...	...	0.0199	57001.70(0.60)	1.041(0.072)	0.950(0.044)
ASASSN-14lp	13	-1.1, 207.6	Normal	Normal	CN	0.0051	57015.29(0.03)	0.920(0.060)	1.027(0.040)
ASASSN-14lt	...	...	Normal	Normal	SS	0.0320	57006.86(0.15)	1.069(0.062)	0.947(0.041)
ASASSN-14me	1	-1.7	Normal	Normal	SS	0.0178	57019.83(0.50)	0.844(0.060)	1.078(0.040)
ASASSN-14mf	1	5.1	Normal	...	...	0.0311	57012.82(0.17)	1.009(0.062)	0.982(0.040)
ASASSN-14mw	1	18.5	Normal	...	...	0.0274	57029.06(0.04)	0.875(0.060)	1.063(0.041)

*Table 1 continued on next page*

**Table 1** (*continued*)

SN	N	Phase range [d]	SNID	Wang	Branch	$z_{Heli}$	t(max) [MJD]	$\Delta m_{15}$ [mag]	$s_{BV}$
(1)	(2)	(3)	(4)	(5)	(6)	(7)	(8)	(9)	(10)
ASASSN-14my	5	-3.5, 27.0	Normal	Normal	BL	0.0205	57030.75(0.05)	1.098(0.061)	0.921(0.040)
ASASSN-15aj	2	-1.3, 21.6	Normal	Normal	CL	0.0109	57035.46(0.07)	1.133(0.064)	0.830(0.041)
ASASSN-15al	2	5.7, 14.7	Normal	HV	CN	0.0338	57032.98(0.22)	0.844(0.071)	1.079(0.048)
ASASSN-15as	1	11.4	Normal	Normal	SS	0.0286	57036.52(0.26)	0.827(0.060)	1.077(0.042)
ASASSN-15ba	2	3.9, 11.8	Normal	HV	BL	0.0231	57044.34(0.57)	1.012(0.061)	0.965(0.040)
ASASSN-15be	1	-1.4	Normal	Normal	CN	0.0219	57049.54(0.06)	0.866(0.061)	1.140(0.040)
ASASSN-15bm	2	1.1, 3.1	Normal	Normal	CN	0.0208	57054.21(0.04)	0.995(0.061)	0.989(0.040)
ASASSN-15cb	2	6.9, 9.9	Normal	Normal	CN	0.0400	57048.04(0.76)	0.871(0.083)	1.088(0.066)
ASASSN-15cd	1	11.0	Normal	Normal	CN	0.0344	57052.79(0.09)	0.920(0.061)	1.001(0.040)
ASASSN-15da	2	2.0, 12.7	Normal	HV	CN	0.0487	57065.79(0.76)	1.122(0.084)	0.851(0.047)
ASASSN-15db	4	-0.4, 3.5	Normal	Normal	CN	0.0110	57075.84(0.12)	1.089(0.061)	0.953(0.040)
ASASSN-15dd	1	2.0	Normal	Normal	CN	0.0244	57076.27(0.16)	1.156(0.072)	0.849(0.040)
ASASSN-15eb	1	10.8	91T-like?	...	...	0.0165	57081.98(0.19)	1.112(0.090)	0.820(0.044)
ASASSN-15fr	1	0.2	Normal	Normal	BL	0.0334	57108.75(0.60)	1.136(0.074)	0.905(0.045)
ASASSN-15ga	2	5.2, 20.2	91bg-like	91bg	...	0.0066	57115.88(0.63)	2.132(0.041) <sup>d</sup>	0.500(0.051)
ASASSN-15go	...	...	Normal	HV	CN	0.0189	57124.12(0.07)	0.842(0.060)	1.072(0.041)
ASASSN-15gr	1	9.4	Normal	Normal	CN	0.0243	57126.42(0.14)	0.874(0.060)	1.031(0.040)
ASASSN-15hf	2	-7.1, -1.0	Normal	Normal	CN	0.0062	57137.22(0.05)	1.187(0.060)	0.939(0.040)
ASASSN-15hg	1	19.8	...	...	...	0.0298	57132.59(0.61)	1.160(0.072)	0.824(0.045)
ASASSN-15hy <sup>b</sup>	...	-10.1, 70.9	Normal	...	...	0.0250	57151.57(0.19) <sup>d</sup>	1.054(0.075)	...
CSS130315:114144-171348	...	...	Normal	HV	CN	0.0500	56356.91(1.35)	1.068(0.126)	1.089(0.055)
CSS131031:095508+064831	...	...	Normal	Normal	CN	0.0776	56607.00(0.58)	0.892(0.063)	1.131(0.043)
CSS140501-170414+174839 <sup>b</sup>	...	...	Ia-pec	HV	CN	0.0798	56788.48(0.33)	1.093(0.096)	0.963(0.047)
CSS140914-010107-101840	1	4.9	Normal	Normal	CN	0.03	56926.05(0.18)	1.086(0.062)	0.959(0.041)
iPTF13duj	1	1.5	Normal	HV	CN?	0.0170	56601.30(0.16)	0.782(0.064)	1.158(0.042)
iPTF13dym	1	-4.6	Normal?	...	...	0.0422	56609.83(0.65)	1.977(0.061)	0.517(0.047)
iPTF13dyt	1	-4.7	Normal	...	...	0.110	56610.45(0.50)	1.497(0.109)	...
iPTF13ebh	...	...	Normal	Normal	CL	0.0133	56623.29(0.03)	1.635(0.060)	0.632(0.040)
iPTF14w	1	-4.5	Normal	Normal	CL	0.0189	56669.93(0.03)	1.509(0.060)	0.743(0.040)
iPTF14aje	1	0.6	Normal	Normal	CN	0.0276	56758.70(0.080)	1.589(0.061)	0.685(0.040)
iPTF14gnl	1	0.3	Normal	...	CN	0.0537	56956.78(0.13)	0.912(0.061)	1.020(0.040)
iPTF15wb <sup>e</sup>	1	8. <sup>e</sup>	Normal	...	...	0.0304	...	...	...
KISS15m	3	-5.9, 7.7	91bg-like	91bg	CL	0.0243	57144.15(0.10)	1.729(0.039) <sup>d</sup>	0.429(0.041)
LSQ11bk	2	-1.0, 13.3	Normal	HV	CN	0.0403	55912.30(0.20)	1.018(0.062)	1.071(0.043)
LSQ11ot	5	-5.3, -1.4	Normal	Normal	CN	0.0273	55927.65(0.05)	0.998(0.061)	0.982(0.040)
LSQ12agq	1	2.9	Normal	HV	BL	0.0642	55985.03(0.66)	0.889(0.074)	1.152(0.048)
LSQ12aor	1	-3.9	Normal	Normal	CL	0.0934	55992.42(0.60)	1.288(0.065)	0.827(0.045)
LSQ12bld	1	-7.5	Normal	...	...	0.0837	56025.42(0.06)	1.081(0.065)	0.892(0.041)
LSQ12blp	1	3.3	Normal	Normal	CN	0.0743	56024.44(0.11)	1.038(0.062)	0.947(0.041)
LSQ12btn	1	15.1	Normal	HV	BL	0.0542	56032.08(0.19)	1.381(0.061)	0.832(0.041)
LSQ12ca	1	2.8	Normal	Normal	CN	0.0988	55950.91(0.80)	0.618(0.081)	1.195(0.057)
LSQ12cdl	...	...	Normal	Normal	CN	0.1080	56045.32(0.81)	1.097(0.167)	0.988(0.060)
LSQ12fuk	2	17.4, 18.3	Normal	...	...	0.0206	56233.53(0.56)	0.975(0.061)	1.003(0.040)
LSQ12fd	3	3.7, 5.6	Normal	Normal	CN	0.0312	56246.40(0.04)	0.940(0.060)	1.161(0.040)
LSQ12gdj	3	-3.5, -1.6	Normal	Normal	SS	0.0303	56253.62(0.07)	0.895(0.061)	1.167(0.041)
LSQ12gpw <sup>b</sup>	...	5.8	91T-like	91T	SS	0.0506	56268.83(0.71) <sup>d</sup>	0.796(0.069)	...
LSQ12gxj	2	2.5, 6.6	Normal	Normal	CN	0.0353	56275.32(0.06)	0.878(0.062)	1.107(0.041)
LSQ12gyc	...	...	Normal	Normal	CN	0.0932	56265.87(0.21)	1.051(0.082)	1.145(0.047)
LSQ12hno	2	-2.4, -1.5	Normal	Normal	CN	0.0473	56284.72(0.17)	1.042(0.066)	0.989(0.043)
LSQ12hnr	...	...	Normal	HV	SS	0.1243*	56283.48(0.82)	1.049(0.075)	1.167(0.055)
LSQ12hnx <sup>e</sup>	1	3. <sup>f</sup>	Normal	...	...	0.1564	...	...	...
LSQ12hvj	1	-2.3	Normal	Normal	SS	0.0713	56290.97(0.13)	0.964(0.064)	1.206(0.042)

Table 1 continued on next page

**Table 1** (*continued*)

SN	N	Phase range [d]	SNID	Wang	Branch	$z_{He\text{I}\alpha}$	t(max) [MJD]	$\Delta m_{15}$ [mag]	$s_{BV}$
(1)	(2)	(3)	(4)	(5)	(6)	(7)	(8)	(9)	(10)
LSQ12hzj	1	-3.1	Normal	Normal	SS	0.0334	56301.51(0.08)	1.025(0.061)	0.970(0.040)
LSQ12hzs	1	-5.7	Normal	...	...	0.0721	56299.12(0.10)	0.989(0.063)	1.145(0.042)
LSQ13ry	2	-8.8, -6.3	Normal	...	...	0.0299	56395.46(0.03)	1.296(0.060)	0.880(0.040)
LSQ13cwp	1	-6.7	Normal	...	...	0.0665	56612.33(0.14)	1.082(0.068)	0.940(0.043)
LSQ13dcy	...	...	Normal	HV	BL	0.083	56624.49(0.38)	1.227(0.072)	1.213(0.058)
LSQ13dsm	1	-5.9	Normal	...	...	0.0424	56670.06(0.04)	1.230(0.060)	0.908(0.040)
LSQ14ip	1	-3.2	91bg-like	HV	CL	0.0613	56688.41(0.10)	1.798(0.061)	0.522(0.041)
LSQ14jp	1	-7.5	Normal	...	...	0.0454	56693.05(0.52)	1.155(0.064)	0.677(0.041)
LSQ14xi	...	...	Normal/91T	Normal	CN	0.0508	56720.29(0.08)	0.904(0.062)	1.142(0.041)
LSQ14act	...	...	Normal	Normal	CL	0.0591	56726.81(0.09)	1.515(0.062)	0.701(0.041)
LSQ14asu	1	-1.9	Normal	Normal	CN	0.0684	56756.08(0.10)	1.177(0.062)	0.775(0.042)
LSQ14auy	1	3.1	Normal	Normal	CN	0.0825	56761.74(0.14)	0.903(0.063)	1.136(0.042)
LSQ14azy	2	1.4, 1.4	Normal	HV	BL	0.0458	56762.65(0.66)	0.911(0.075)	1.136(0.048)
LSQ14bbv	1	10.5	Normal	...	...	0.0588	56772.16(0.14)	0.928(0.062)	1.039(0.041)
LSQ14fmgb	...	...	Ia-pec	Normal	SS	0.0661	56938.53(0.34)	0.796(0.031)	...
LSQ14fms	1	-3.7	Normal	HV	CL	0.0780	56931.22(0.61)	1.274(0.028)	0.849(0.043)
LSQ14gfb	...	...	Normal/91bg	Normal	CL	0.0527	56987.78(0.75)	1.632(0.044)	0.605(0.053)
LSQ14gfn	1	-9.3	Normal	...	...	0.1217	56998.68(0.34)	1.069(0.072)	0.991(0.046)
LSQ14gov	1	1.1	Normal	Normal	CN	0.0896	57027.76(0.08)	0.979(0.061)	1.141(0.041)
LSQ15bv	1	12.9	Normal	...	...	0.0689	57043.32(0.82)	1.164(0.061)	0.955(0.041)
LSQ15aae	2	-3.6, 19.4	Normal	Normal	SS	0.0516	57116.02(0.08)	0.793(0.061)	1.226(0.041)
LSQ15agh	2	-3.6, 12.4	91T-like	Normal	SS	0.0603	57139.85(0.09)	0.879(0.061)	1.140(0.041)
LSQ15aja	1	3.2	Normal	Normal	CN	0.0700	57147.77(0.05)	0.921(0.061)	1.027(0.041)
LSQ15alq	4	-11.0, 20.4	Normal	Normal	CN	0.0471	57154.54(0.06)	1.191(0.060)	0.920(0.040)
MASTERJ093953.18+165516.4	...	...	Normal	Normal	SS	0.048	56329.58(0.23)	0.877(0.072)	1.145(0.047)
OGLE-2012-SN-040	1	24.7	...	...	...	0.0147	56258.18(0.96)	1.970(0.073)	0.484(0.047)
OGLE-2013-SN-015	1	0.7	Normal	Normal	CN	0.0890	56340.32(1.10)	0.679(0.219)	0.768(0.246)
OGLE-2013-SN-118	...	...	Normal	Normal	CN	0.0750	56623.91(0.23)	0.892(0.071)	1.138(0.042)
OGLE-2013-SN-123	...	...	Normal/91T	Normal	CN	0.0614	56622.38(0.91)	1.524(0.106)	0.700(0.065)
OGLE-2014-SN-021	...	...	Normal	Normal	BL	0.0422	56714.33(0.63)	0.996(0.063)	0.982(0.041)
OGLE-2014-SN-107	...	...	91T-like	Normal	SS	0.0664	56954.35(0.71)	1.038(0.066)	1.215(0.053)
PS1-14ra	2	3.5, 11.2	Normal	Normal	CL	0.0281	56724.54(0.08)	1.161(0.072)	0.778(0.040)
PS1-14xw	2	-1.2, 3.6	Normal	Normal	CN	0.0245	56785.47(0.08)	0.908(0.061)	1.036(0.041)
PS15sv	3	-1.3, 92.5	91T-like	Normal	SS	0.0333	57113.54(0.09)	0.984(0.061)	1.113(0.042)
PSN J13471211-2422171	2	-2.2, 7.7	Normal	HV	BL	0.0199	57070.43(0.13)	1.136(0.065)	0.720(0.040)
PTF11phk	1	-3: <sup>e</sup>	Normal	...	...	0.073	...	...	...
PTF11qnr	1	-0.7	Normal	Normal	CN	0.0162	55903.58(0.04)	1.346(0.061)	0.807(0.041)
SMTJ03253351-5344190	...	...	Normal	Normal	BL	0.059	56637.02(0.15)	0.911(0.063)	1.142(0.042)
2011hb	3	-7.4, 20.7	Normal	...	...	0.0289	55871.75(0.04)	0.978(0.060)	1.157(0.041)
2011hk	3	1.7, 28.1	91bg-like	91bg	CL	0.0176	55864.58(0.55)	...	0.442(0.043)
2011iv	...	...	Normal	Normal	CL	0.0065	55906.08(0.05)	1.549(0.061)	0.701(0.041)
2011iy	3	51.9, 204.0	Normal	...	...	0.0043	55893.24(0.23)	1.007(0.061)	1.033(0.040)
2011jh	6	-8.7, 116.1	Normal	HV	CL	0.0078	55931.06(0.02)	1.462(0.013) <sup>d</sup>	0.789(0.040)
2012E	4	0.1, 6.0	Normal	Normal	BL	0.0203	55949.91(0.08)	1.143(0.065)	0.846(0.041)
2012G	1	-1.5	Normal	Normal	SS	0.0258	55948.85(0.05)	0.887(0.060)	1.158(0.040)
2012Z	...	...	Ia-pec	...	...	0.0071	55968.89(0.26)	1.092(0.068)	...
2012ah	2	3.9, 12.7	Normal	Normal	BL	0.0124	55975.16(0.71)	1.096(0.076)	0.905(0.046)
2012aq	1	6.2	Normal	HV	CN	0.052	55981.86(0.20)	1.196(0.072)	0.996(0.044)
2012ar	2	14.5, 54.5	Normal	...	...	0.0283	55991.31(0.53)	1.439(0.060)	0.809(0.040)
2012bl	3	-2.4, 29.0	Normal	HV	CN	0.0187	56018.76(0.55)	0.843(0.061)	1.081(0.043)
2012bo	2	13.7, 25.5	Normal	...	...	0.0254	56021.04(0.50)	0.931(0.061)	1.160(0.041)
2012cg <sup>f</sup>	2	16.6, 68.6	Normal	...	...	0.0015	56081.3(0.5) <sup>g</sup>	...	...

Table 1 continued on next page

**Table 1** (*continued*)

SN	N	Phase range [d]	SNID	Wang	Branch	$z_{He\text{I}o}$	t(max) [MJD]	$\Delta m_{15}$ [mag]	$s_{BV}$
(1)	(2)	(3)	(4)	(5)	(6)	(7)	(8)	(9)	(10)
2012fr	...	...	Normal	HV	SS	0.0055	56243.32(0.02)	0.844(0.060)	1.107(0.040)
2012gm	1	5.1	Normal	...	...	0.0148	56261.65(0.02)	1.037(0.061)	0.987(0.040)
2012hd	2	17.3, 32.2	Normal	Normal	BL	0.0120	56265.53(0.04)	1.267(0.051)	0.888(0.040)
2012hl	1	2.8	Normal	HV	BL	0.0332	56272.00(0.24)	1.090(0.089)	0.927(0.046)
2012hr	6	-6.6, 51.9	Normal	HV	BL	0.0076	56288.91(0.02)	1.036(0.060)	0.973(0.040)
2012ht	6	-7.6, 84.0	Normal	Normal	BL	0.0036	56295.75(0.03)	1.194(0.060)	0.869(0.040)
2012id	1	10.9	Normal	...	...	0.0157	56287.03(0.94)	1.446(0.083)	0.824(0.052)
2012ij	4	-3.1, 38.3	91bg-like	91bg	CL	0.0110	56302.54(0.05)	1.111(0.082)	0.536(0.041)
2013E	4	-10.0, 32.7	Normal	...	...	0.0094	56308.22(0.49)	0.888(0.060)	1.131(0.040)
2013H	3	-10.5, 31.0	Normal	...	...	0.0155	56309.92(0.49)	0.899(0.060)	1.048(0.040)
2013U	1	6.0	91T-like	...	...	0.0345	56335.05(0.59)	0.796(0.061)	1.239(0.041)
2013Y	1	0.6	Normal	Normal	CN	0.0766	56333.52(0.31)	1.081(0.077)	0.872(0.049)
2013aa	2	-2.0, 43.7	Normal	Normal	CN	0.0040	56343.42(0.04)	0.999(0.060)	1.002(0.040)
2013ad	1	0.8	Normal	Normal	SS	0.0363	56348.05(0.13)	1.032(0.065)	0.991(0.042)
2013aj	3	9.7, 27.7	Normal	Normal	BL	0.0091	56361.37(0.04)	1.437(0.060)	0.800(0.040)
2013ao <sup>b</sup>	...	10.0, 44.4	Normal	HV	SS	0.0435	56360.67(0.39)	1.053(0.065)	...
2013as	1	5.8	Normal	...	...	0.0685	56365.80(0.67)	0.968(0.074)	1.010(0.046)
2013ba	1	-7.0	Normal	...	...	0.080	56396.75(0.61)	1.044(0.070)	0.985(0.043)
2013bc	...	...	91bg-like	91bg	CL	0.0225	56384.42(0.58)	1.647(0.068)	0.481(0.046)
2013bz	2	17.0, 29.8	Normal	...	...	0.0192	56409.65(0.07)	0.812(0.061)	1.152(0.041)
2013cs	4	-6.8, 16.9	Normal	HV	BL	0.0093	56436.83(0.05)	1.071(0.063)	0.964(0.040)
2013ct	1	95.5	Normal	...	...	0.0038	56411.31(0.38)	0.796(0.064)	1.002(0.040)
2013fy	1	4.9	Normal	...	...	0.0309	56600.03(0.54)	0.930(0.062)	1.174(0.041)
2013fz	...	...	Normal	Normal	CN	0.0206	56601.67(0.52)	0.926(0.060)	1.015(0.040)
2013gr	4	11.1, 264.5	Ia-pec	...	...	0.0074	56606.85(0.44)	...	...
2013gy	...	...	Normal	Normal	CN	0.0140	56648.75(0.04)	1.216(0.060)	0.911(0.040)
2013hh	2	8.3, 32.0	91T-like?	Normal	SS	0.0130	56638.82(0.58)	1.036(0.063)	1.203(0.049)
2013hn	...	...	Normal	HV	BL	0.0151	56642.94(0.69)	1.426(0.074)	0.821(0.048)
2014D	1	3.8	Normal	Normal	CN	0.0082	56665.27(0.70)	...	0.958(0.046)
2014I	3	1.0, 43.7	Normal	Normal	CN	0.0300	56683.86(0.04)	1.210(0.060)	0.916(0.040)
2014Z	...	...	Normal	HV	BL	0.0213	56721.92(0.70)	1.084(0.103)	0.980(0.049)
2014ao	1	15.9	Normal	Normal	CN	0.0141	56767.84(0.08)	1.177(0.060)	0.881(0.040)
2014at	1	9.9	Normal	Normal	CN	0.0322	56774.05(0.05)	1.070(0.061)	0.948(0.040)
2014dk	1	-0.1	Normal	Normal	CN	0.034	56931.15(0.07)	0.844(0.061)	1.079(0.042)
2014dl	1	-7.8	91T-like	91T	SS	0.0330	56935.02(0.06)	1.052(0.066)	1.227(0.042)
2014dn	1	2.9	91bg-like	91bg	CL	0.0222	56925.34(0.53)	1.716(0.071)	0.465(0.040)
2014dt	1	126.7	Ia-pec	...	...	0.0052	56949.84 <sup>h</sup>	...	...
2014du	1	7.1	Normal	...	...	0.0325	56968.63(0.10)	1.188(0.061)	0.815(0.041)
2014eg	1	-2.1	91T-like	91T	SS	0.0186	56991.23(0.07)	0.937(0.061)	1.183(0.041)
2014ek	1	13.4	Ia-pec	...	...	0.0231	56959.29(0.61)	1.630(0.065)	...
2015F	1	29.1	Normal	Normal	CN	0.0049	57106.85(0.03)	1.303(0.060)	0.884(0.040)
2015H	2	18.2, 23.9	02cx-like	...	...	0.0125	57054.00(0.46)	1.532(0.066)	...
2015M <sup>b</sup>	...	-10.1, 22.0	Normal?	HV	SS	0.0231	57168.45(0.52)	1.040(0.067)	1.241(0.041)
2015bo	...	2.3, 31.6	Normal	Normal	CL	0.0162	57076.02(0.11)	1.855(0.020) <sup>d</sup>	0.505(0.040)
2015bp	...	-4.5, 135.7	Normal	Normal	CL	0.0041	57112.67(0.04)	1.604(0.060)	0.692(0.040)

Table 1 continued on next page

**Table 1** (*continued*)

SN (1)	N (2)	Phase range [d] (3)	SNID (4)	Wang (5)	Branch (6)	$z_{Heli}$ (7)	t(max) [MJD] (8)	$\Delta m_{15}$ [mag] (9)	$s_{BV}$ (10)
-----------	----------	------------------------	-------------	-------------	---------------	-------------------	---------------------	------------------------------	------------------

<sup>a</sup> t(max) derived from *g*-band light curve (Prieto et al. 2007)

<sup>b</sup> 03fg-like (Ashall et al. 2021)

<sup>c</sup> t(max) from (Scalzo et al. 2010)

<sup>d</sup> t(max),  $\Delta m_{15}$  and  $s_{BV}$  are derived from the observed light curves instead of **SNooPy** fits.

<sup>e</sup> Observed during the course of the CSP, but not included in the final sample.

<sup>f</sup> Phase estimated using SNID.

<sup>g</sup> t(max) from (Marion et al. 2016)

<sup>h</sup> t(max) from (Singh et al. 2018)

NOTE—The meaning of the columns is as follows: 1: SN designation. 2: Number of spectra released in this work. Three dots mean that we are not presenting new spectroscopic observations of the target, but, based on previously published spectra, we include it in the discussion of SN properties at maximum light. 3: Phases (expressed in days) of the first and last spectra. 4: SNID classification. 5: Wang subtype. 6: Branch subtype. 7: Heliocentric redshift of the host. (\*) The adopted redshift for LSQ12hnr is discussed in Section 3.3 8: MJD of B maximum light from **SNooPy** fit when available. 9:  $\Delta m_{15}$  (in magnitudes) from the **SNooPy** fit when available. 10: Color stretch  $s_{BV}$  from **SNooPy** fit when available. For data in columns 8, 9, and 10, errors are given in parentheses.

**Table 2.** Summary of observations, spectroscopic and photometric properties of historical SNe Ia

SN	N	Phase range [d]	SNID	Wang	Branch	$z_{He\text{I}}$	t(max) [MJD]	$\Delta m_{15}$ [mag]	$s_{BV}$	Photometry
(1)	(2)	(3)	(4)	(5)	(6)	(7)	(8)	(9)	(10)	(11)
1981B	...	...	Normal	HV	BL	0.0060	44671.5	1.10(0.07)	...	
1986G	17	-6.1, 55.8	91bg	91bg	CL	0.0018	46561.192(0.077)	1.420(0.025)	0.602(0.012)	1
1989B	59	-8.2, 345.3	Normal	Normal	BL	0.0024	47565.377(0.180)	1.053(0.011)	0.883(0.010)	2
1990N	7	-14.0, 37.6	Normal	Normal	SS	0.0033	48082.208(0.040)	0.931(0.009)	1.147(0.008)	3
1990O	6	-7.4, 19.6	Normal	Normal	CN	0.0303	48075.945(0.171)	0.905(0.012)	1.107(0.032)	4
1990T <sup>a</sup>	4	14.5, 34.7	Normal	...	...	0.0404	48083.068(0.210)	1.066(0.008)	0.985(0.017)	4
1990Y <sup>a</sup>	1	19	Normal	...	...	0.0360	48114.129(0.612)	1.035(0.023)	1.099(0.067)	4
1990af <sup>a</sup>	2	-3.6, -3.6	91bg	91bg	CN	0.0506	48195.867(0.120)	1.516(0.021)	0.744(0.009)	4
1991S <sup>a</sup>	1	18.5	Normal	...	...	0.0546	48346.883(0.361)	0.918(0.017)	1.096(0.061)	4
1991T	20	-8.9, 338.8	91T	91T	SS	0.0070	48374.999(0.128)	0.801(0.015)	1.212(0.009)	3
1991U <sup>a</sup>	2	11.5, 11.9	Normal	...	...	0.0317	48354.353(0.392)	1.027(0.012)	1.018(0.028)	4
1991ag <sup>a</sup>	2	5.6, 6.7	Normal	...	...	0.0141	48413.528(0.328)	0.744(0.011)	1.117(0.021)	4
1991bg	11	0.1, 112.4	91bg	91bg	CL	0.00354	48603.401(0.645)	1.933(0.013)	0.327(0.029)	5
1992A	21	-7.3, 283.9	Normal	HV	CN	0.006261	48640.557(0.036)	1.175(0.013)	0.785(0.005)	6
1992J <sup>a</sup>	2	12.1, 12.8	91T/Normal	...	...	0.0446	48673.776(0.630)	0.336(0.021)	0.769(0.033)	4
1992K <sup>a</sup>	2	12.2, 40.7	91bg	...	...	0.0103	48674.91	1.93	...	4
1992P <sup>a</sup>	2	-0.6, 4.2	Normal	Normal	CN	0.0252	48718.945(0.306)	0.981(0.034)	1.067(0.037)	4
1992ae <sup>a</sup>	1	3.5	Normal	Normal	SS	0.0752	48803.590(0.578)	1.130(0.033)	0.982(0.016)	4
1992ag <sup>a</sup>	2	0.0, 25.3	Normal	Normal	SS	0.0249	48806.100(0.647)	1.066(0.044)	1.006(0.039)	4
1992al	2	-5.6, 3.1	Normal	Normal	CN	0.0146	48838.021(0.047)	1.028(0.005)	0.962(0.009)	4
1992aq <sup>a</sup>	1	2.4	Normal	Normal	CL/CN	0.1018	48833.628(0.752)	1.315(0.059)	0.900(0.028)	4
1992au <sup>a</sup>	1	59.3	Normal	...	...	0.0614	48833.238(1.041)	1.041(0.453)	0.726(0.058)	4
1992bc <sup>a</sup>	3	-10.7, 36.4	Normal	...	...	0.0202	48912.047(0.076)	0.844(0.012)	1.135(0.024)	4
1992bg <sup>a</sup>	1	7.3	Normal	...	...	0.0352	48914.683(0.342)	1.075(0.021)	0.978(0.012)	4
1992bh <sup>a</sup>	1	2.5	Normal	Normal	CN	0.0450	48919.598(0.221)	0.941(0.012)	1.091(0.039)	4
1992bk <sup>a</sup>	2	7.6, 8.6	Normal	...	...	0.0581	48939.054(0.650)	1.434(0.042)	0.801(0.021)	4
1992bl <sup>a</sup>	1	0.9	Normal	Normal	BL/CN	0.0437	48947.121(0.447)	1.402(0.023)	0.800(0.016)	4
1992bo <sup>a</sup>	1	0.8	Normal	Normal	BL	0.0189	48986.256(0.055)	1.526(0.008)	0.733(0.012)	4
1992bp <sup>a</sup>	1	6.8	Normal	...	...	0.0793	48979.832(0.353)	1.160(0.034)	0.882(0.020)	4
1992br <sup>a</sup>	1	0.1	91T/Normal	Normal	CN	0.0882	48987.000(0.785)	1.860(0.140)	0.592(0.069)	4
1992bs <sup>a</sup>	1	3.3	Normal	Normal	CN/SS	0.0637	48983.708(0.348)	0.975(0.014)	1.056(0.022)	4
1993B <sup>a</sup>	1	12.4	Normal	...	...	0.0696	49002.010(0.623)	1.011(0.037)	1.189(0.046)	4
1993H <sup>a</sup>	4	-1.3, 9.7	Normal	Normal	CL	0.0239	49068.533(0.183)	1.603(0.008)	0.691(0.012)	4
1993O <sup>a</sup>	2	-5.7, 0.0	Normal	Normal	CN	0.051	49134.065(0.139)	1.137(0.021)	0.918(0.013)	4
1993af <sup>a</sup>	1	185: <sup>b</sup>	Ia-pec	...	...	0.0034	49305.5	...	...	4
1993ag <sup>a</sup>	1	2.2	Normal	HV	BL	0.049	49315.984(0.297)	1.157(0.027)	0.938(0.016)	4
1993ah <sup>a</sup>	1	15.9	Normal	...	...	0.0286	49301.708(1.494)	1.307(0.049)	0.853(0.033)	4
1994D	5	-6, 15	Normal	Normal	CN	0.0015	49432.535(0.080)	1.511(0.020)	0.692(0.017)	6
1999aw	5	-0.6, 61.1	Normal	...	...	0.0380	51253.709(0.331)	0.800(0.024)	1.319(0.020)	7
1999cs	2	6, 10	Normal	...	...	0.0620	51291.0	...	...	8
1999ee	...	...	Normal	Normal	CN	0.0114	51469.123(0.035)	0.881(0.008)	1.134(0.006)	9
1999ei	1	15.2	Normal	...	...	0.0315	51451.527(0.226)	0.891(0.008)	1.136(0.010)	6
1999ek	4	-5.6, 1.2	Normal	Normal	BL	0.0177	51482.061(0.083)	1.097(0.019)	0.921(0.008)	10
2000bh	2	6.5, 29.5	Normal	...	...	0.0233	51636.550(0.656)	1.085(0.048)	0.964(0.022)	11
2000ca	3	0.1, 29.1	91T/Normal	Normal	CN	0.0243	51665.869(0.177)	0.924(0.016)	1.042(0.013)	11
2001ba	3	-3.8, 20.5	Normal	Normal	BL/CN	0.0294	52033.965(0.168)	1.083(0.024)	0.959(0.010)	11
2001bt	1	-8.6	Normal	...	...	0.0149	52064.135(0.137)	1.191(0.010)	0.875(0.009)	10
2001cn	2	2.2, 10.1	Normal	HV	BL	0.0156	52072.032(0.646)	1.080(0.044)	0.927(0.020)	10

Table 2 continued on next page

**Table 2** (*continued*)

SN	N	Phase range [d]	SNID	Wang	Branch	$z_{He\text{lio}}$	t(max) [MJD]	$\Delta m_{15}$ [mag]	$s_{BV}$	Photometry
(1)	(2)	(3)	(4)	(5)	(6)	(7)	(8)	(9)	(10)	(11)

<sup>a</sup> Calán/Tololo Supernova Survey.

<sup>b</sup> Phase estimated using SNID.

NOTE—The meaning of the columns is as in Table 1. SNooPy fits are available for all SN other than 1993af and 1999cs. Photometry references are:  
(1) Phillips et al. (1987); (2) Wells et al. (1994); (3) Lira et al. (1998); (4) Hamuy et al. (1996); (5) Leibundgut et al. (1993) (6) Suntzeff, N. B. (unpublished); (7) Strolger et al. (2002); (8) Lennarz et al. (2012); (9) Hamuy et al. (2002a); (10) Krisciunas et al. (2004a); (11) Krisciunas et al. (2004b).

**Table 3.** CSP Optical Spectra of SNe Ia considered in this work

Date [UT]	MJD	Phase [d]	Tel.	Inst.	$\lambda$ range [\AA]	Res. [\AA]	exp. [s]	airmass	rms
(1)	(2)	(3)	(4)	(5)	(6)	(7)	(8)	(9)	(10)
<b>CSP I</b>									
SN 2005gj									
2005-11-24.2 <sup>a</sup>	53698.2	38.0	DUP	MS	3780-7290	7.0	3x900	1.15	0.163
2005-11-25.2	53699.2	39.0	DUP	MS	3780-7290	7.0	3x900	1.15	0.054
2005-12-18.2	53722.2	60.7	NTT	EM	3400-5300	6.0	3x300	1.45	0.053
2005-12-18.2	53722.2	60.7	NTT	EM	4000-10200	9.0	3x300	1.61	...
2005-12-18.2	53722.2	60.7	NTT	EM	5800-10200	9.0	3x300	1.80	...
2005-12-20.2	53724.2	62.5	DUP	WF	3800-9235	8.0	3x900	1.21	0.034
2005-12-21.1	53725.1	63.4	DUP	WF	3800-9235	8.0	3x900	1.25	0.049
2005-12-22.2	53726.2	64.4	DUP	WF	3800-9235	8.0	3x1200	1.32	0.040
2005-12-23.2	53727.2	65.3	DUP	WF	3800-9235	8.0	3x1200	1.38	0.039
2005-12-24.2	53728.2	66.3	DUP	WF	3800-9235	8.0	3x1200	1.41	0.038
2006-01-16.1	53751.1	87.9	NTT	EM	3400-5300	6.0	3x300	1.30	0.040
2006-01-16.1	53751.1	87.9	NTT	EM	4000-10200	9.0	3x300	1.39	...
2006-01-16.1	53751.1	87.9	NTT	EM	5800-10200	9.0	3x300	1.49	...
2006-01-24.1	53759.1	95.4	CLA	LD	3788-6134	2.0	900	1.57	0.038
2006-01-24.1	53759.1	95.5	CLA	LD	5778-10000	4.0	900	1.87	...
2006-03-05.0	53799.0	133.0	DUP	WF	3800-9235	8.0	1200	1.78	...
2006-09-27.2	54005.2	327.3	DUP	WF	3800-9235	8.0	3x1800	1.24	...
2006-10-12.2	54020.2	341.4	DUP	WF	3800-9235	8.0	3x1800	1.14	...
SN 2007if									
2007-09-12.4	54355.4	6.5	DUP	BC	3500-9700	8.0	900	1.70	...
2007-09-18.3	54361.3	12.0	DUP	BC	3500-9700	8.0	3x1200	1.63	0.056
2007-09-22.3 <sup>a</sup>	54365.3	15.8	CLA	LD	3720-6000	3.0	2x1200	1.69	0.188
2007-09-22.4 <sup>a</sup>	54365.4	15.8	CLA	LD	5780-9900	6.0	2x1200	1.70	...
2007-10-04.2	54377.2	26.8	3P6	EF	3300-6075	20	3x900	1.43	0.077
2007-10-04.2	54377.2	26.8	3P6	EF	5220-9260	30	3x900	1.43	...
2007-10-08.2	54381.2	30.5	BAA	IM	4000-9500	4.0	3x900	1.42	0.124
SN 2007jd									
2007-10-04.2	54377.2	14.3	3P6	EF	3300-6075	20	3x1200	1.24	0.097
2007-10-04.3	54377.3	14.4	3P6	EF	5220-9260	30	3x1200	1.16	...
2007-10-08.3	54381.3	18.1	BAA	IM	4000-9500	4.0	2x1200	1.16	0.097
2007-11-05.3	54409.3	44.2	3P6	EF	3300-6075	20	1200	1.46	...
2007-11-05.3	54409.3	44.2	3P6	EF	5220-9260	30	1200	1.93	...
SN 2007ol									
2007-11-05.2 <sup>a</sup>	54409.2	-3.5	3P6	EF	3300-6075	20	3x1200	1.17	0.359
2007-11-05.2	54409.2	-3.5	3P6	EF	5220-9260	30	3x1200	1.30	...
2007-11-11.3	54415.3	2.3	DUP	WF	3800-9235	8.0	3x900	1.62	0.063
2007-11-17.2	54421.2	7.9	BAA	IM	4000-10200	4.0	3x600	1.28	0.070

Table 3 continued on next page

**Table 3** (*continued*)

Date [UT]	MJD	Phase [d]	Tel.	Inst.	$\lambda$ range [\AA]	Res. [\AA]	exp. [s]	airmass	rms
(1)	(2)	(3)	(4)	(5)	(6)	(7)	(8)	(9)	(10)
2007-11-19.2	54423.2	8.8	NTT	EM	4100-10000	9.0	3x900	1.37	...
2007-11-30.1	54434.1	20.1	3P6	EF	3300-6075	20	3x1200	1.15	...
2007-11-30.1	54434.1	20.1	3P6	EF	5220-9260	30	3x1200	1.23	...
SN 2007so									
2007-12-17.1	54451.1	22.4	BAA	IM	4100-10200	4.0	3x600	1.35	0.060
2007-12-18.1	54452.1	23.4	NTT	EM	4000-10000	9.0	3x600	1.37	0.020
2008-01-03.0	54468.0	38.8	3P6	EF	3300-6075	20	3x900	1.36	0.055
2008-01-03.1	54468.1	38.9	3P6	EF	5220-9260	30	3x900	1.42	...
2008-01-05.1	54470.1	40.9	DUP	BC	4160-10000	8.0	3x1200	1.68	0.070
SN 2007st									
2007-12-28.2	54462.2	7.6	BAA	IM	3800-9454	6.0	600	1.87	0.079
2008-01-04.1	54469.1	14.4	3P6	EF	3300-6075	20	3x500	1.14	0.064
2008-01-04.1	54469.1	14.4	3P6	EF	5220-9260	30	3x500	1.19	...
2008-01-10.0	54475.0	20.2	DUP	WF	3800-9235	8.0	3x600	1.36	0.131
2008-01-27.0	54492.0	36.8	3P6	EF	3300-6975	20	3x600	1.24	0.132
2008-01-27.1	54492.1	36.9	3P6	EF	5220-9260	30	3x600	1.33	...
SN 2008O									
2008-01-27.2	54492.2	0.5	3P6	EF	3300-6075	20	3x900	1.08	0.010
2008-01-27.2	54492.2	0.4	3P6	EF	5220-9260	30	3x900	1.14	...
2008-02-25.2 <sup>a</sup>	54521.2	28.3	CLA	LD	3620-9426	7.0	900	1.21	0.185
SN 2008ae									
2008-02-13.3	54509.3	0.6	NTT	EM	4000-10170	9.0	3x900	1.49	0.080
2008-02-25.3	54521.3	12.3	CLA	LD	3620-9426	7.0	1800	1.55	0.044
2008-03-13.1	54538.1	28.7	3P6	EF	3300-6030	20.0	3x1200	1.30	...
2008-03-13.2	54538.2	28.7	3P6	EF	5220-9260	30.0	3x1200	1.41	...
SN 2008bd									
2008-03-14.1	54539.1	7.7	3P6	EF	3300-6030	20.0	3x600	1.20	...
2008-03-14.1	54539.1	7.7	3P6	EF	5220-9260	30.0	3x600	1.11	...
2008-03-19.1	54544.1	12.5	CLA	MA	3228-9470	0.5	1200	1.04	0.072
2008-03-20.1	54545.1	13.5	CLA	LD	3630-9430	7.0	3x900	1.07	0.074
SN 2008bi									
2008-03-28.1	54553.1	9.7	NTT	EM	3500-5300	6.0	3x300	1.27	0.044
2008-03-28.1	54553.1	9.7	NTT	EM	4000-10200	9.0	3x300	1.35	...
2008-03-31.1	54556.1	12.6	DUP	WF	3800-9235	8.0	3x400	1.18	0.095
2008-04-07.1	54563.1	19.5	DUP	WF	3800-9235	8.0	3x600	1.22	0.119
2008-04-13.1	54569.1	25.5	DUP	WF	3800-9235	8.0	3x900	1.26	0.061
2008-05-05.0	54591.0	47.2	DUP	WF	3800-9235	8.0	3x900	1.20	...
SN 2008bt									
2008-04-26.1	54582.1	9.7	CLA	LD	3750-9400	7.0	3x600	1.10	0.048
2008-05-11.0	54596.0	23.3	DUP	WF	3800-9235	8.0	3x600	1.05	0.034

Table 3 continued on next page

**Table 3** (*continued*)

Date [UT]	MJD	Phase [d]	Tel.	Inst.	$\lambda$ range [\AA]	Res. [\AA]	exp. [s]	airmass	rms
(1)	(2)	(3)	(4)	(5)	(6)	(7)	(8)	(9)	(10)
SN 2008bz									
2008-04-25.2	54581.2	2.2	BAA	IM	4000-10300	6.0	3x600	1.51	0.068
2008-04-26.2	54582.2	3.1	CLA	LD	3626-9433	7.0	3x900	1.40	0.045
2008-05-05.1	54591.1	11.5	DUP	WF	3800-9235	8.0	3x900	1.31	0.031
2008-05-11.1	54597.1	17.2	DUP	WF	3800-9235	8.0	3x900	1.32	0.020
2008-05-22.1	54608.1	27.5	BAA	IM	4450-9300	6.0	3x600	1.38	0.151
SN 2008cc									
2008-04-26.3	54582.3	9.2	CLA	LD	3626-9433	7.0	3x600	1.55	0.019
2008-04-26.4	54582.4	9.3	BAA	IM	3900-10370	6.0	3x600	1.39	0.071
2008-05-16.4	54602.4	29.1	BAA	IM	4200-10500	5.0	600	1.28	0.071
2008-05-22.3	54608.3	35.0	BAA	IM	4250-10500	6.0	3x600	1.32	0.053
2008-05-30.3	54616.3	42.8	DUP	BC	3480-9673	8.0	3x900	1.33	0.044
SN 2008cd									
2008-05-05.2	54591.2	12.2	DUP	WF	3800-9235	8.0	600	1.27	0.314
SN 2008cf									
2008-05-11.2	54597.2	2.4	DUP	WF	3800-9235	8.0	3x600	1.07	0.026
2008-05-12.2	54598.2	3.3	DUP	WF	3800-9235	8.0	3x900	1.012	0.035
2008-05-15.2	54601.2	6.2	BAA	IM	4200-10500	6.0	3x600	1.05	0.099
2008-05-22.2 <sup>a</sup>	54608.2	12.9	BAA	IM	4430-9300	6.0	3x600	1.19	0.160
2008-05-30.2	54616.2	20.6	DUP	BC	3480-9200	8.0	3x900	1.09	0.059
SN 2008ff									
2008-09-15.0	54724.0	19.4	BAA	IM	4030-10725	6.0	3x500	1.04	0.064
2008-09-22.0	54731.0	26.3	DUP	WF	3800-9235	8.0	3x800	1.04	0.022
2008-09-29.0	54738.0	33.2	DUP	WF	3800-9235	8.0	3x600	1.04	0.038
2008-10-20.1	54759.1	53.8	DUP	WF	3800-9235	8.0	3x900	1.30	0.046
2008-10-28.1	54767.1	61.7	DUP	WF	3800-9235	8.0	3x900	1.29	0.030
2008-11-24.1	54794.1	88.2	DUP	WF	3800-9235	8.0	3x1200	1.78	0.033
SN 2008fl									
2008-09-15.0	54724.0	3.1	BAA	IM	4030-10725	6.0	3x400	1.02	0.085
2008-09-17.0	54726.0	5.1	CLA	LD	3650-9450	7.0	3x400	1.01	0.011
2008-09-21.2	54730.2	9.2	DUP	WF	3800-9235	8.0	3x500	1.38	0.034
2008-09-29.0	54738.0	16.9	DUP	WF	3800-9235	8.0	3x600	1.01	0.020
2008-10-15.0	54754.0	32.6	NTT	EF	3300-5990	27.0	3x600	1.06	0.055
2008-10-15.0	54754.0	32.6	NTT	EF	5240-9210	39.0	3x900	1.16	...
2008-10-20.0	54759.0	37.5	DUP	WF	3800-9235	8.0	3x600	1.12	0.036
2008-10-28.0	54767.0	45.3	DUP	WF	3800-9235	8.0	3x600	1.25	0.054
SN 2008fr									
2008-09-28.3	54737.3	4.4	DUP	WF	3800-9235	8.0	3x900	1.46	0.030
2008-10-28.1	54767.1	33.1	DUP	WF	3800-9235	8.0	3x900	1.42	0.059
SN 2008fu									

Table 3 continued on next page

**Table 3** (*continued*)

Date [UT]	MJD	Phase [d]	Tel.	Inst.	$\lambda$ range [\AA]	Res. [\AA]	exp. [s]	airmass	rms
(1)	(2)	(3)	(4)	(5)	(6)	(7)	(8)	(9)	(10)
2008-09-28.3 <sup>a</sup>	54737.3	4.5	DUP	WF	3800-9235	8.0	3x900	1.01	0.284
2008-10-20.3	54759.3	25.4	DUP	WF	3800-9235	8.0	900	1.08	0.073
SN 2008fw									
2008-09-28.4	54737.4	5.6	DUP	WF	3800-9235	8.0	250	2.21	...
2008-10-20.4	54759.4	27.4	DUP	WF	3800-9235	8.0	400	1.84	0.030
2008-10-28.3	54767.3	35.2	DUP	WF	3800-9235	8.0	3x699	1.68	0.048
2008-11-19.3	54789.3	57.0	NTT	EF	3300-6994	27.0	3x600	1.46	0.062
2008-11-19.3	54789.3	57.0	NTT	EF	5240-9210	39.0	3x600	1.29	...
2008-11-23.4	54793.4	61.1	DUP	WF	3800-9235	8.0	600	1.21	0.043
2008-12-21.3	54821.3	88.7	DUP	WF	3800-9235	8.0	3x800	1.19	0.109
SN 2008gg									
2008-10-15.1	54754.1	4.7	NTT	EF	3351-6020	27.0	3x600	1.15	0.015
2008-10-15.1	54754.1	4.8	NTT	EF	5240 9210	39.0	3x300	1.09	...
2008-10-20.1	54759.1	9.6	DUP	WF	3800-9235	8.0	3x600	1.05	0.019
2008-10-27.2	54766.2	16.5	DUP	WF	3800-9235	8.0	3x600	1.06	0.022
2008-11-02.2	54772.2	22.3	BAA	IM	4100-10700	6.0	3x600	1.06	0.027
2008-11-24.2	54794.2	43.6	DUP	WF	3800-9235	8.0	3x900	1.22	0.038
2008-12-21.1	54821.1	69.7	DUP	WF	3800-9235	8.0	3x1200	1.15	0.034
SN 2008go									
2008-10-27.0	54766.0	-0.1	DUP	WF	3800-9235	8.0	3x1200	1.02	0.005
2008-11-02.0	54772.0	5.6	BAA	IM	4100-10700	6.0	3x900	1.03	0.019
2008-11-04.0	54774.0	7.4	CLA	LD	3640-9400	7.0	3x1000	1.02	0.018
SN 2008ha									
2008-11-23.0	54789.0	7.1	NTT	EF	3310-6000	27.0	3x900	1.49	0.038
2008-11-23.0	54793.0	11.1	DUP	WF	3800-9235	8.0	3x1200	1.51	0.063
SN 2008hj									
2008-11-24.1	54794.1	-7.1	DUP	WF	3800-9235	8.0	3x800	1.36	...
2008-11-25.1	54795.1	-6.2	DUP	WF	3800-9235	8.0	3x800	1.09	0.015
2008-12-08.1	54808.1	6.3	BAA	IM	4000-10300	7.0	900	1.21	0.066
2008-12-15.1	54815.1	13.1	CLA	LD	3630-9425	7.0	600	1.32	0.015
2008-12-22.0	54822.0	19.8	DUP	WF	3800-9235	8.0	3x1200	1.26	0.028
2008-12-27.1	53827.1	24.6	DUP	WF	3800-9235	8.0	3x900	1.53	0.099
2008-12-29.1	54829.1	26.5	DUP	WF	3800-9235	8.0	3x900	1.42	0.030
SN 2009I									
2009-01-17.1	54848.1	-3.7	CLA	LD	3630-9430	6.0	700	1.22	0.069
2009-01-22.1	54853.1	1.1	CLA	LD	3650-9400	7.0	600	1.34	0.056
2009-02-09.0	54871.0	18.7	NTT	EF	3300-6004	27.0	3x600	1.52	...
2009-02-09.1	54871.1	18.7	NTT	EF	5240-9210	39.0	600	1.79	...
SN 2009P									
2009-02-08.2	54870.2	1.8	CLA	LD	3716-9437	6.0	3x500	1.24	0.027

Table 3 continued on next page

**Table 3** (*continued*)

Date [UT]	MJD	Phase [d]	Tel.	Inst.	$\lambda$ range [\AA]	Res. [\AA]	exp. [s]	airmass	rms
(1)	(2)	(3)	(4)	(5)	(6)	(7)	(8)	(9)	(10)
2009-02-09.2	54871.2	2.7	CLA	LD	3716-9347	6.0	3x500	1.32	0.024
2009-02-14.3	54876.3	7.7	BAA	IM	4060-10120	6.0	3x500	1.12	0.030
2009-02-16.4 <sup>a</sup>	54878.4	9.7	BAA	IM	4060-10129	6.0	500	1.38	0.178
2009-02-24.2	54886.2	17.4	DUP	WF	3800-9235	8.0	3x500	1.11	0.126
2009-03-16.2 <sup>a</sup>	54906.2	32.5	BAA	IM	4050-10100	8.0	3x900	1.12	0.231
2009-03-22.2	54919.2	49.5	DUP	WF	3800-9235	8.0	3x600	1.12	0.197
SN 2009U									
2009-02-08.3	54870.3	13.0 <sup>b</sup>	CLA	LD	3716-9437	6.0	3x400	1.06	
SN 2009al									
2009-03-16.1	54906.1	12.4	NTT	EF	5240-9210	39.0	3x600	1.29	0.036
2009-03-16.2	54906.2	12.5	NTT	EF	3300-6004	27.0	3x600	1.26	...
2009-03-29.1	54919.1	25.1	DUP	WF	3800-9235	8.0	3x700	1.26	0.037
2009-04-18.1	54939.1	44.7	DUP	BC	3450-9650	8.0	3x900	1.31	0.022
2009-04-23.2	54944.2	49.7	DUP	BC	3370-9640	8.0	3x900	1.68	0.095
2009-05-01.1	54952.1	57.4	CLA	LD	3720-9440	6.0	800	1.46	...
SN 2009cz									
2009-04-17.0	54938.0	-5.0	CLA	LD	3720-9430	6.0	800	1.92	0.036
2009-04-22.0	54943.0	-0.1	DUP	BC	3370-9550	8.0	3x900	1.92	0.014
2009-04-23.0	54943.0	-0.2	DUP	BC	3370-9550	8.0	3x900	1.93	0.095
2009-05-01.0	54952.0	8.6	CLA	LD	3720-9440	6.0	3x500	1.93	...
SN 2009dc									
2009-04-17.3	54938.3	-8.4	CLA	LD	3720-9430	6.0	600	1.78	...
2009-04-18.3	54939.3	-7.4	DUP	BC	3450-9650	8.0	3x900	1.73	...
2009-04-22.3	54943.3	-3.5	DUP	BC	3360-9560	8.0	3x1000	1.72	0.009
2009-04-23.3	54944.3	-2.5	DUP	BC	3370-9565	8.0	3x900	1.77	0.016
2009-04-30.3	54951.3	4.3	CLA	LD	3730-9410	6.0	3x500	1.73	0.020
2009-05-01.3	54952.3	5.3	CLA	LD	3730-9410	6.0	3x500	1.88	0.080
2009-05-14.2	54965.2	17.9	BAA	IM	4000-10100	7.0	3x500	1.75	0.041
2009-05-23.2	54974.2	26.8	DUP	BC	3360-9560	8.0	3x700	1.73	0.103
2009-05-31.2	54982.2	34.5	DUP	BC	3400-9570	8.0	3x700	1.74	...
SN 2009ds									
2009-04-30.2	54951.2	-9.7	CLA	LD	3730-9410	6.0	3x400	1.21	...
2009-05-01.1	54952.1	-8.7	CLA	LD	3730-9410	6.0	400	1.14	0.067
2009-05-14.1	54965.1	4.0	BAA	IM	4000-10100	7.0	3x400	1.07	0.054
2009-05-23.1	54974.1	12.8	DUP	BC	3360-9560	8.0	3x600	1.13	0.072
2009-05-31.1	54982.1	20.7	DUP	BC	3400-9570	8.0	3x600	1.40	...
SN 2009le									
2009-11-26.2	55161.2	-4.6	CLA	LD	3650-9440	6.0	3x300	1.45	0.016
SN 2010ae									
2010-03-15.2	55270.2	...	DUP	WF	3700-9250	8.0	3x600	1.80	...

Table 3 continued on next page

**Table 3** (*continued*)

Date [UT]	MJD	Phase [d]	Tel.	Inst.	$\lambda$ range [\AA]	Res. [\AA]	exp. [s]	airmass	rms
(1)	(2)	(3)	(4)	(5)	(6)	(7)	(8)	(9)	(10)
2010-03-20.2	55275.2	...	DUP	WF	3700-9250	8.0	900	1.48	...
<b>CSP II</b>									
ASASSN-14ad									
2014-02-12.2 <sup>c</sup>	56700.2	7.3	NOT	AL	3500-9100	17.0	1500	1.03	0.030
ASASSN-14hp									
2014-09-27.1	56927.1	-2.3	DUP	WF	3700-9200	8.0	800	1.37	0.023
ASASSN-14hr									
2014-09-27.4 <sup>a</sup>	56927.4	-5.1	DUP	WF	3680-9200	8.0	900	1.24	0.154
ASASSN-14hu									
014-09-28.4	56928.4	-6.7	DUP	WF	3640-9200	8.0	600	1.40	0.017
ASASSN-14kd									
2014-11-24.8 <sup>a,c</sup>	56985.8	3.4	NOT	AL	3400-9100	17.0	...	1.09	0.011
ASASSN-14kq									
2014-11-27.1	56988.1	-2.2	DUP	WF	3630-9200	8.0	2x600	1.32	0.039
ASASSN-14lo									
2014-12-22.1 <sup>a</sup>	57013.1	11.2	NOT	AL	3750-9000	17.0	2400	1.78	0.105
2015-02-04.2 <sup>a</sup>	57057.2	54.4	NOT	AL	3800-9100	17.0	2400	1.02	0.355
ASASSN-14lp									
2014-12-23.2 <sup>a,c</sup>	57014.2	-1.1	NOT	AL	3300-9100	17.0	3x900	1.43	0.355
2014-12-28.3 <sup>c</sup>	57019.3	4.0	DUP	WF	3640-9200	8.0	3x90	1.51	0.033
2014-12-29.4 <sup>c</sup>	57020.4	5.0	DUP	WF	3640-9200	8.0	60	1.42	0.021
2015-01-05.2 <sup>c</sup>	57027.2	11.9	NOT	AL	3300-9100	17.0	3x720	1.27	0.030
2015-01-09.4	57031.4	16.0	CLA	MA	3170-9400	1.0	200	1.23	0.070
2015-01-25.3	57047.3	31.8	DUP	WF	3600-9165	8.0	3x400	1.37	0.038
2015-02-02.3	57055.3	39.8	DUP	WF	3600-9165	8.0	300	1.20	0.025
2015-02-04.3	57057.3	41.8	DUP	WF	3600-9165	8.0	400	1.15	0.021
2015-02-05.3	57058.3	42.8	DUP	WF	3600-9165	8.0	300	1.15	0.032
2015-02-06.3	57059.3	43.8	DUP	WF	3600-9165	8.0	300	1.14	0.025
2015-02-24.3	57077.3	61.7	DUP	WF	3600-9165	8.0	300	1.19	0.030
2015-04-24.2 <sup>a,c</sup>	57136.2	120.3	DUP	WF	3640-9200	8.0	400	1.30	0.336
2015-07-21.0	57224.0	207.6	DUP	WF	3640-9160	8.0	3x1000	1.36	...
ASASSN-14me									
2014-12-27.1 <sup>c</sup>	57018.1	-1.7	DUP	WF	3640-9200	8.0	600	1.27	0.098
ASASSN-14mf									
2014-12-27.1 <sup>c</sup>	57018.1	5.1	DUP	WF	3640-9200	8.0	900	1.29	0.048
ASASSN-14mw									

Table 3 continued on next page

**Table 3** (*continued*)

Date [UT]	MJD	Phase [d]	Tel.	Inst.	$\lambda$ range [\AA]	Res. [\AA]	exp. [s]	airmass	rms
(1)	(2)	(3)	(4)	(5)	(6)	(7)	(8)	(9)	(10)
2015-01-26.1	57048.1	18.5	DUP	WF	3700-9140	8.0	600	1.65	0.023
ASASSN-14my									
2015-01-05.2 <sup>c</sup>	57027.2	-3.5	NOT	AL	3300-9100	17.0	1800	1.37	0.066
2015-01-17.2 <sup>c</sup>	57039.2	8.3	NOT	AL	3400-9075	17.0	1800	1.27	0.031
2015-01-26.3	57048.3	17.2	DUP	WF	3610-9165	8.0	800	1.12	0.032
2015-02-03.3	57056.3	25.0	DUP	WF	3630-9160	8.0	600	1.06	0.034
2015-02-05.3	57058.3	27.0	DUP	WF	3630-9160	8.0	1200	1.06	0.041
ASASSN-15aj									
2015-01-12.2 <sup>c</sup>	57034.2	-1.3	CLA	MI	3350-9400		3x900	1.84	...
2015-02-04.3	57057.3	21.6	DUP	WF	3630-9160	8.0	1200	1.02	0.024
ASASSN-15al									
2015-01-16.9 <sup>a,c</sup>	57038.9	5.7	NOT	AL	3500-9140	17.0	2400	1.64	0.043
2015-01-26.2	57048.2	14.7	DUP	WF	3630-9160	8.0	900	1.60	0.028
ASASSN-15as									
2015-01-26.3	57048.3	11.4	DUP	WF	3630-9160	8.0	800	1.23	0.007
ASASSN-15ba									
2015-01-26.4	57048.4	3.9	DUP	WF	3630-9160	8.0	600	1.37	0.018
2015-02-03.4	57056.4	11.8	DUP	WF	3630-9160	8.0	500	1.31	0.021
ASASSN-15be									
2015-01-26.1	57048.1	-1.4	DUP	WF	3630-9160	8.0	600	1.37	0.021
ASASSN-15bm									
2015-02-02.4 <sup>a</sup>	57055.4	1.1	DUP	WF	3630-9160	8.0	600	1.22	0.210
2015-02-04.4	57057.4	3.1	DUP	WF	3630-9160	8.0	900	1.25	0.070
ASASSN-15cb									
2015-02-02.2 <sup>c</sup>	57055.2	6.9	NOT	AL	3420-9140	17.0	1800	1.15	0.115
2015-02-05.4 <sup>a</sup>	57058.4	9.9	DUP	WF	3630-9160	8.0	1200	1.20	0.329
ASASSN-15cd									
2015-02-11.1 <sup>a,c</sup>	57064.1	11.0	NOT	AL	3450-9140	17.0	1800	1.11	0.369
ASASSN-15da									
2015-02-14.9 <sup>a,c</sup>	57067.9	2.0	NOT	AL	3600-9100	17.0	1800	1.71	0.202
2015-02-26.1	57079.1	12.7	DUP	WF	3630-9160	8.0	900	1.33	0.463
ASASSN-15db									
2015-02-22.4	57075.4	-0.4	DUP	WF	3630-9160	8.0	200	1.47	0.061
2015-02-23.2 <sup>c</sup>	57076.2	0.4	NOT	AL	3500-9100	17.0	1200	1.09	0.141
2015-02-25.4	57078.4	2.5	DUP	WF	3600-9160	8.0	3x300	1.55	0.023
2015-02-26.4	57079.4	3.5	DUP	WF	3600-9160	8.0	300	1.48	0.087
ASASSN-15dd									

Table 3 continued on next page

**Table 3** (*continued*)

Date [UT]	MJD	Phase [d]	Tel.	Inst.	$\lambda$ range [Å]	Res. [Å]	exp. [s]	airmass	rms
(1)	(2)	(3)	(4)	(5)	(6)	(7)	(8)	(9)	(10)
2015-02-25.4	57078.4	2.0	DUP	WF	3600-9160	8.0	700	1.64	0.050
ASASSN-15eb									
2015-03-11.0 <sup>a</sup>	57093.0	10.8	NOT	AL	3770-9100	17.0	1800	1.62	0.470
ASASSN-15fr									
2015-03-27.0 <sup>c</sup>	57109.0	0.2	NOT	AL	3500-9100	17.0	1800	1.34	...
ASASSN-15ga									
2015-04-09.1 <sup>c</sup>	57121.1	5.2	NOT	AL	3500-9100	17.0	1800	1.11	0.066
2015-04-24.3 <sup>c</sup>	57136.3	20.2	DUP	WF	3630-9200	8.0	600	1.88	0.164
ASASSN-15gr									
2015-04-24.0	57136.0	9.4	DUP	WF	3630-9200	8.0	600	1.40	0.030
ASASSN-15hf									
2015-04-18.1	57130.1	-7.1	DUP	BC	3650-6815	3.7	2x1800	1.02	0.079
2015-04-24.2 <sup>a</sup>	57136.2	-1.0	DUP	WF	3640-9200	8.0	300	1.25	0.155
ASASSN-15hg									
2015-05-10.9 <sup>a,c</sup>	57152.9	19.8	NOT	AL	3600-9100	17.0	2400	1.27	0.319
ASASSN-15hy									
2015-04-29.2 <sup>c</sup>	57141.2	-10.1	NOT	AL	3400-9100	17.0	1800	1.47	0.094
2015-06-17.1 <sup>a,c</sup>	57190.1	37.6	NOT	AL	3500-9100	17.0	1800	1.25	0.308
2015-07-21.2 <sup>a</sup>	57224.2	70.9	DUP	WF	3630-9160	8.0	3x1000	1.17	0.193
CSS140914-010107-101840									
2014-10-01.0 <sup>c</sup>	56931.0	4.9	NOT	AL	3500-9100	17.0	2100	1.31	0.046
iPTF13duj									
2013-11-06.9 <sup>c</sup>	56602.9	1.5	NOT	AL	3300-9100	17.0	2400	1.07	0.03
iPTF13dym									
2013-11-09.1 <sup>a,c</sup>	56605.1	-4.6	DUP	WF	3640-9170	8.0	1000	1.42	0.221
iPTF13dyt									
2013-11-09.3 <sup>c</sup>	56605.3	-4.7	DUP	WF	3640-9170	8.0	3x700	1.18	0.349
iPTF13ebh									
2013-11-15.2	56611.8	-11.5	WHT	ISIS	5000-9400	...	500	1.55	0.018
2013-11-16.2	56612.8	-10.5	HCT	HFOSC	3700-9000	...	2700	1.06	0.062
2013-11-20.7	56616.2	-7.1	ARC	DIS	3400-9800	...	300	1.01	0.069
2013-11-22.3	56618.3	5.0	FTN	FLOYDS	3200-10800	...	...	...	0.041
2013-11-23.1	56619.6	-4.2	NOT	AL	3400-9000	17.0	...	...	0.074
2013-11-24.3	56620.3	-3.0	FTN	FLOYDS	3200-10800	...	...	...	0.063
2013-11-26.4	56622.4	-0.9	P200	DBSP	3400-10500	...	600	1.55	0.030
2013-11-29.5	56625.5	2.2	Keck	DEIMOS	4880-10100	...	...	...	...

Table 3 continued on next page

**Table 3** (*continued*)

Date [UT]	MJD	Phase [d]	Tel.	Inst.	$\lambda$ range [\AA]	Res. [\AA]	exp. [s]	airmass	rms
(1)	(2)	(3)	(4)	(5)	(6)	(7)	(8)	(9)	(10)
2013-12-02.3	56628.3	5.0	Keck	LRIS	3200-10200	...	...	...	0.045
2013-12-20.9	56646.9	23.6	NOT	AL	3500-9100	17.0	...	...	0.016
2013-12-31.0 <sup>a,c</sup>	56657.0	33.7	BAA	IM	3800-9700	3.0	900	2.19	0.214
iPTF14w									
2014-01-08.3	56665.3	-4.5	DUP	WF	3630-9160	8.0	600	1.36	0.005
iPTF14aje									
2014-04-06.3	56753.3	0.6	DUP	WF	3630-9160	8.0	1010	1.16	...
iPTF14gnl									
2014-10-27.1 <sup>a,c</sup>	56957.1	0.3	NOT	AL	3600-9100	17.0	2400	1.83	0.169
iPTF15wb									
2015-04-03.0 <sup>c</sup>	57116.0	8 <sup>b</sup>	NOT	AL	3480-9000	17.0	1800	1.28	
KISS15m									
2015-04-26.1 <sup>c</sup>	57138.1	-5.9	NOT	AL	3850-9100	17.0	2400	1.39	0.077
2015-04-30.0 <sup>c</sup>	57143.0	-1.1	NOT	AL	3500-9100	17.0	1800	1.02	0.118
2015-05-10.1 <sup>a,c</sup>	57152.1	7.7	NOT	AL	3600-9110	17.0	2400	1.33	0.310
LSQ11bk									
2011-12-16.3 <sup>c</sup>	55911.3	-1.0	BAA	IM	4100-10050	6.0	2x900	1.48	0.081
2011-12-31.3	55926.2	13.3	DUP	WF	3640-9200	8.0	3x1000	1.22	0.059
LSQ11ot									
2011-12-27.2 <sup>c</sup>	55922.2	-5.3	DUP	WF	3640-9200	8.0	3x1200	1.38	0.040
2011-12-27.9 <sup>c</sup>	55922.9	-4.7	NOT	AL	3500-9100	17.0	2400	1.16	0.059
2011-12-28.1 <sup>c</sup>	55923.1	-4.4	DUP	WF	3640-9200	8.0	3x1000	1.24	0.048
2011-12-29.3 <sup>c</sup>	55924.3	-3.3	DUP	WF	3640-9200	8.0	3x1000	1.73	0.042
2011-12-31.2 <sup>c</sup>	55926.2	-1.4	DUP	WF	3640-9200	8.0	3x1000	1.58	0.056
LSQ12agq									
2012-03-02.2	55988.2	2.9	CLA	LD	3700-9400	7.0	900	1.08	...
LSQ12aor									
2012-03-02.2	55988.2	-3.9	CLA	LD	3700-9400	7.0	3x900	1.04	...
LSQ12bld									
2012-03-31.3	56017.3	-7.5	DUP	WF	3640-9200	8.0	3x1600	1.25	0.062
LSQ12blp									
2012-04-11.0 <sup>c</sup>	56028.0	3.3	NOT	AF	3500-9100	17.0	2700	1.37	0.052
LSQ12btn									
2012-05-01.0	56048.0	15.1	DUP	WF	3640-9200	8.0	3x1000	1.06	0.055
LSQ12ca									
2012-01-28.0 <sup>a,c</sup>	55954.0	2.8	GES	GM	3600-9200	...	2x450	1.04	0.063

Table 3 continued on next page

**Table 3** (*continued*)

Date [UT]	MJD	Phase [d]	Tel.	Inst.	$\lambda$ range [\AA]	Res. [\AA]	exp. [s]	airmass	rms
(1)	(2)	(3)	(4)	(5)	(6)	(7)	(8)	(9)	(10)
LSQ12fuk									
2012-11-20.3	56251.3	17.4	DUP	WF	3640-9600	8.0	600	1.03	0.033
2012-11-21.2	56252.2	18.3	DUP	WF	3640-9600	8.0	3x600	1.06	0.029
LSQ12fxd									
2012-11-19.2	56250.2	3.7	DUP	WF	3600-9600	8.0	3x600	1.02	0.018
2012-11-20.3	56251.3	4.8	DUP	WF	3600-9600	8.0	600	1.16	0.022
2012-11-21.2	56252.2	5.6	DUP	WF	3600-9600	8.0	3x600	1.02	0.014
LSQ12gdj									
2012-11-19.0	56250.0	-3.5	DUP	WF	3600-9600	8.0	3x600	1.01	0.021
2012-11-20.0	56251.0	-2.5	DUP	WF	3600-9600	8.0	600	1.00	0.023
2012-11-21.0	56252.0	-1.6	DUP	WF	3600-9600	8.0	600	1.00	0.028
LSQ12gpw									
2012-12-13.9 <sup>c</sup>	56274.9	5.8	NOT	AL	3500-9100	17.0	2400	1.34	0.041
LSQ12gxj									
2012-12-16.9 <sup>c</sup>	56277.9	2.5	NOT	AL	3500-9100	17.0	2400	1.22	0.017
2012-12-21.1	56282.1	6.6	DUP	WF	3800-9600	8.0	1200	1.33	0.076
LSQ12hno									
2012-12-21.2	56282.2	-2.4	DUP	WF	3770-9600	8.0	1200	1.46	...
2012-12-22.1	56283.1	-1.5	DUP	WF	3700-9600	8.0	1000	1.17	0.046
LSQ12hnx									
2012-12-22.1	56283.1	3 <sup>b</sup>	DUP	WF	3700-9600	8.0	1200	1.06	
LSQ12hvj									
2012-12-27.0 <sup>c</sup>	56288.0	-2.3	NOT	AL	3500-9100	17.0	2400	1.96	0.085
LSQ12hzj									
2013-01-06.3 <sup>a</sup>	56298.3	-3.1	DUP	WF	3600-9600	8.0	2x600	1.09	0.123
LSQ12hzs									
2012-12-30.0 <sup>c</sup>	56293.0	-5.7	NOT	AL	3500-9100	17.0	2400	1.80	0.074
LSQ13ry									
2013-04-04.4 <sup>c</sup>	56386.4	-8.8	GEN	GM	3500-9650		2x450	1.24	...
2013-04-06.9 <sup>c</sup>	56388.9	-6.3	NOT	AL	3340-9120	17.0	1800	1.11	0.022
LSQ13cwp									
2013-11-09.2	56605.2	-6.7	DUP	WF	3600-9160	8.0	3x1500	1.12	0.013
LSQ13dsm									
2014-01-06.9 <sup>c</sup>	56663.9	-5.9	NOT	AL	3500-9120	17.0	2400	1.74	0.081
LSQ14ip									

Table 3 continued on next page

**Table 3** (*continued*)

Date [UT]	MJD	Phase [d]	Tel.	Inst.	$\lambda$ range [\AA]	Res. [\AA]	exp. [s]	airmass	rms
(1)	(2)	(3)	(4)	(5)	(6)	(7)	(8)	(9)	(10)
2014-01-28.0 <sup>a,c</sup>	56685.0	-3.2	NOT	AL	3500-9120	17.0	2400	1.19	0.186
LSQ14jp									
2014-01-28.2	56685.2	-7.5	NOT	AL	3500-9100	17.0	2400	1.46	0.090
LSQ14asu									
2014-04-07.1 <sup>a</sup>	56754.1	-1.9	DUP	WF	3640-9200	8.0	3x900	1.04	0.234
LSQ14aauy									
2014-04-18.1	56765.1	3.1	NOT	AL	3500-9100	17.0	2400	1.20	0.020
LSQ14azy									
2014-04-17.1 <sup>c</sup>	56764.1	1.4	NTT	EF	3500-6030	12.6	600	1.33	...
2014-04-17.1 <sup>c</sup>	56764.1	1.4	NTT	EF	5200-9250	16.6	600	1.36	...
LSQ14bbv									
2014-05-06.3	56783.3	10.5	DUP	WF	3800-9200	8.0	700	1.25	0.113
LSQ14fmg									
2014-09-24.9	56924.9	-13.6	NOT	AL	3500-9100	17.0	2400	1.04	0.056
2014-09-30.1	56930.1	-8.4	NOT	AL	3500-9100	17.0	2400	1.39	0.043
2014-10-13.0 <sup>a</sup>	56943.1	4.5	NOT	AL	3700-9100	17.0	2400	1.37	0.093
LSQ14fms									
2014-09-27.2	56927.2	-3.7	DUP	WF	3650-9200	8.0	1200	1.12	0.080
LSQ14gfn									
2014-11-27.2	56988.2	-9.3	DUP	WF	3920-9200	8.0	2x1800	1.26	...
LSQ14gov									
2015-01-06.9 <sup>a,c</sup>	57028.9	1.1	NOT	AL	3500-9100	17.0	2400	1.40	0.090
LSQ15bv									
2015-02-04.1 <sup>c</sup>	57057.1	12.9	NOT	AL	3900-9100	17.0	1800	1.45	0.142
LSQ15aae									
2015-03-31.2 <sup>a,c</sup>	57112.2	-3.6	NOT	AL	3500-9100	17.0	2400	1.12	0.258
2015-04-24.4	57136.4	19.4	DUP	WF	3700-9200	8.0	1200	1.54	0.025
LSQ15agh									
2015-04-24.1	57136.1	-3.6	DUP	WF	3650-9200	8.0	3x1000	1.65	0.036
2015-05-11.0 <sup>a</sup>	57153.0	12.4	NOT	AL	3500-9100	17.0	2100	1.29	0.306
LSQ15aja									
2015-05-09.2 <sup>a,c</sup>	57151.2	3.2	NOT	AL	3600-9100	17.0	2400	1.12	0.229
LSQ15alq									
2015-05-01.0 <sup>a,c</sup>	57143.0	-11.0	NOT	AL	3800-9100	17.0	2400	1.73	0.179
2015-05-10.0 <sup>a,c</sup>	57152.0	-2.4	NOT	AL	3500-9100	17.0	1500	1.78	0.292

Table 3 continued on next page

**Table 3** (*continued*)

Date [UT]	MJD	Phase [d]	Tel.	Inst.	$\lambda$ range [\AA]	Res. [\AA]	exp. [s]	airmass	rms
(1)	(2)	(3)	(4)	(5)	(6)	(7)	(8)	(9)	(10)
2015-05-22.9 <sup>a,c</sup>	57164.9	9.9	NOT	AL	3700-9100	17.0	1800	1.76	0.310
2015-06-02.9 <sup>a,c</sup>	57175.9	20.4	NOT	AL	3800-9100	17.0	2400	1.73	0.342
OGLE-2012-SN-040									
2012-12-22.3	56283.3	24.7	DUP	WF	3700-9500	8.0	500	1.35	0.128
OGLE-2013-SN-015									
2013-02-18.1	56341.1	0.7	DUP	BC	3340-9400	8.0	1800	1.74	...
PS1-14ra									
2014-03-12.2 <sup>c</sup>	56728.2	3.5	NOT	AL	3500-9120	17.0	1800	1.09	0.023
2014-03-20.1 <sup>c</sup>	56736.1	11.2	NOT	AL	3500-9120	17.0	1800	1.19	0.038
PS1-14xw									
2014-05-07.3	56784.3	-1.2	DUP	WF	3640-9200	8.0	1000	1.18	0.026
2014-05-12.1 <sup>c</sup>	56789.1	3.6	NOT	AL	3500-9100	17.0	1500	1.12	0.035
PS15sv									
2015-03-31.1 <sup>a,c</sup>	57112.1	-1.3	NOT	AL	3500-9100	17.0	1200	1.21	0.195
2015-04-24.4	57136.4	22.1	DUP	WF	3640-9200	8.0	1000	1.29	0.040
2015-07-06.2	57209.2	92.5	DUP	WF	3800-9100	8.0	1581	1.27	...
PSN J13471211-2422171									
2015-02-15.2 <sup>a,c</sup>	57068.2	-2.2	NOT	AL	3500-9120	17.0	1800	1.76	0.387
2015-02-25.3	57078.3	7.7	DUP	WF	3620-9200	8.0	600	1.02	0.052
PTF11phk									
2011-11-01.1 <sup>c</sup>	55866.1	-3 <sup>b</sup>	DUP	WF	3700-9200	8.0	300	1.95	...
PTF11qnr									
2011-12-07.9 <sup>c</sup>	55902.9	-0.7	NOT	AL	3500-9100	17.0	2400	1.29	0.024
SN 2011hb									
2011-10-30.1	55864.1	-7.4	DUP	WF	3640-9200	8.0	3x600	1.33	...
2011-11-18.0	55883.0	11.0	DUP	WF	3640-9200	8.0	900	1.29	0.013
2011-11-28.0	55893.0	20.7	DUP	WF	3640-9200	8.0	3x600	1.35	0.037
SN 2011hk									
2011-11-01.3 <sup>c</sup>	55866.3	1.7	DUP	WF	3700-9180	8.0	3x1200	1.39	0.020
2011-11-18.1	55883.1	18.2	DUP	WF	3800-9200	8.0	3x900	1.08	0.066
2011-11-28.2	55893.2	28.1	DUP	WF	3800-9200	8.0	900	1.20	0.056
SN 2011iv									
2011-12-04.0	55899.0	-7.1	DUP	BC	3900-5800	2.0	2x900	1.30	...
2011-12-04.1	55899.1	-7.0	GES	GM	3800-9300	...	300	1.01	...
2011-12-05.1	55900.1	-6.0	DUP	BC	3648-5276	2.0	3x900	1.08	...
2011-12-06.1	55901.1	-5.0	DUP	BC	5230-6860	2.0	4x900	1.08	...
2011-12-18.0 <sup>c</sup>	55913.0	7.0	WHT	ISIS	3350-9050	...	...	...	...

Table 3 continued on next page

**Table 3** (*continued*)

Date [UT]	MJD	Phase [d]	Tel.	Inst.	$\lambda$ range [\AA]	Res. [\AA]	exp. [s]	airmass	rms
(1)	(2)	(3)	(4)	(5)	(6)	(7)	(8)	(9)	(10)
2011-12-19.0 <sup>c</sup>	55914.0	8.0	WHT	ISIS	3350-9040	...	...	...	...
2011-12-20.0 <sup>c</sup>	55915.0	9.0	WHT	ISIS	3300-9030	...	...	...	...
2011-12-21.0 <sup>c</sup>	55916.0	10.0	WHT	ISIS	3300-9030	...	...	...	...
2011-12-27.0 <sup>c</sup>	55922.0	16.0	NOT	AL	3400-9140	...	...	...	0.088
2011-12-31.1	55926.1	20.1	DUP	WF	3630-9200	8.0	3x400	1.07	0.018
2012-01-19.0	55945.0	38.9	DUP	WF	3630-9200	8.0	300	1.02	0.034
2012-03-02.1	55988.1	82.0	CLA	LD	3700-9400	8.0	400	1.72	0.044
2012-05-01.0	56048.0	141.9	DUP	WF	3800-9100	8.0	2x300	2.56	...
2012-08-10.4	56149.4	243.3	DUP	WF	3700-9200	8.0	3x1000	1.12	...
2012-09-11.3	56181.3	275.2	DUP	WF	3640-9200	8.0	3x1200	1.03	...
SN 2011iy									
2012-01-19.3	55945.3	51.9	DUP	WF	3630-9200	8.0	100	1.16	0.031
2012-04-30.2	56047.2	153.3	DUP	WF	3630-9200	8.0	900	1.11	0.012
2012-06-20.1	56098.1	204.0	DUP	WF	3630-9200	8.0	3x1500	1.28	...
SN 2011jh									
2011-12-27.3 <sup>c</sup>	55922.3	-8.7	DUP	WF	3630-9200	8.0	3x800	1.67	0.056
2011-12-29.3 <sup>c</sup>	55924.3	-6.7	DUP	WF	3630-9200	8.0	3x900	1.61	0.027
2011-12-31.3 <sup>c</sup>	55926.3	-4.7	DUP	WF	3635-9200	8.0	3x900	1.65	0.104
2012-01-11.2 <sup>c</sup>	55937.2	6.1	NOT	AL	3500-9100	17.0	1800	1.48	0.033
2012-01-19.3	55945.3	14.1	DUP	WF	3640-9200	8.0	400	1.22	0.027
2012-05-01.1	56048.1	116.1	DUP	WF	3650-9200	8.0	3x800	1.06	0.133
SN 2012E									
2012-01-24.0 <sup>c</sup>	55950.0	0.1	GES	GM	3600-6425		600	1.54	0.077
2012-01-24.1 <sup>c</sup>	55950.1	0.1	GES	GM	5400-9650		600	1.61	...
2012-01-30.0 <sup>c</sup>	55956.0	6.0	GES	GM	3600-6425		1100	1.56	0.072
2012-01-30.0 <sup>c</sup>	55956.0	6.0	GES	GM	5400-9650		1100	1.68	...
SN 2012G									
2012-01-21.3 <sup>c</sup>	55947.3	-1.5	CLA	LD	3700-9430	0.6	500	2.22	...
SN 2012Z									
2012-02-12.8	55969.8	1.0	NOT	AL	3100-9100	17	...	...	0.041
2012-02-18.9	55975.9	7.0	NOT	AL	3100-9199	17	1800	1.78	0.011
2012-02-22.1	55979.1	10.2	CLA	LD	3500-9400	7	...	...	0.028
2012-02-25.8	55982.9	14.0	NOT	AL	3200-9100	17	...	...	0.022
2012-03-02.1	55988.1	19.2	CLA	LD	3700-9400	8	300	1.92	0.032
2012-09-12.3	56182.3	213.4	DUP	WF	3640-9200	8	3x1200	1.06	...
SN 2012ah									
2012-02-22.1 <sup>c</sup>	55979.1	3.9	CLA	LD	3700-9430	0.6	600	2.48	...
2012-03-02.0	55988.0	12.7	CLA	LD	3700-9430	7.0	300	2.33	0.026
SN 2012aq									
2012-03-02.3	55988.3	6.2	CLA	LD	3700-9430	7.0	3x600	1.62	0.026

Table 3 continued on next page

**Table 3** (*continued*)

Date [UT]	MJD	Phase [d]	Tel.	Inst.	$\lambda$ range [\AA]	Res. [\AA]	exp. [s]	airmass	rms
(1)	(2)	(3)	(4)	(5)	(6)	(7)	(8)	(9)	(10)
SN 2012ar									
2012-03-20.2 <sup>c</sup>	56006.2	14.5	NOT	AL	3600-9150	17.0	1800	1.42	0.139
2012-05-02.4	56047.4	54.5	DUP	WF	3700-9200	8.0	4x1200	1.22	0.085
SN 2012bl									
2012-03-30.3	56016.3	-2.4	DUP	WF	3640-9200	8.0	3x700	1.66	0.014
2012-03-31.4	56017.4	-1.3	DUP	WF	3640-9200	8.0	3x700	1.27	0.046
2012-05-01.3	56048.3	29.0	DUP	WF	3640-9200	8.0	3x900	1.60	0.054
SN 2012bo									
2012-04-18.1 <sup>a,c</sup>	56035.1	13.7	NOT	AL	3600-9100	17.0	1800	1.46	0.229
2012-04-30.2	56047.2	25.5	DUP	WF	3640-9200	8.0	900	1.07	0.030
SN 2012cg									
2012-06-20.0	56098.0	16.6	DUP	WF	3640-9200	8.0	3x900	1.27	...
2016-08-11.0	56150.0	68.6	DUP	WF	3640-9200	8.0	3x300	2.23	...
SN 2012fr									
2012-11-07.3	56238.3	-5.0	DUP	WF	3500-9600	8.0	60	1.08	0.022
2012-11-08.3	56239.3	-4.0	DUP	WF	3500-9600	8.0	60	1.07	0.075
2012-11-10.3	56241.3	-2.0	DUP	WF	3500-9600	8.0	80	1.07	0.046
2012-11-11.3	56242.3	-1.0	DUP	WF	3500-9600	8.0	90	1.07	0.065
2012-11-13.2	56244.2	0.9	DUP	WF	3600-9600	8.0	3x90	1.03	0.037
2012-11-14.3	56245.3	1.9	DUP	WF	3600-9600	8.0	3x90	1.06	0.073
2012-11-15.2	56246.2	2.9	DUP	WF	3600-9600	8.0	3x90	1.05	0.076
2012-11-16.2	56247.2	3.9	DUP	WF	3600-9600	8.0	3x90	1.06	0.088
2012-11-17.2	56248.2	4.9	DUP	WF	3600-9600	8.0	3x90	1.03	0.091
2012-11-18.2	56249.2	5.9	DUP	WF	3600-9600	8.0	3x90	1.06	0.099
2012-11-19.2	56250.2	6.9	DUP	WF	3500-9600	8.0	100	1.01	0.047
2012-11-20.2	56251.2	7.9	DUP	WF	3500-9600	8.0	100	1.01	0.047
2012-11-21.1	56252.1	8.8	DUP	WF	3500-9600	8.0	3x100	1.03	0.034
2012-11-30.1	56261.1	17.8	BAA	IM	3370-9550	2.7	300	1.07	0.066
2012-12-16.9	56277.9	34.6	NOT	AL	3300-9100	17.0	1200	2.52	0.043
2013-01-04.2	56296.2	52.8	CLA	LD	3700-9400	9.0	2x200	1.19	0.037
2013-01-06.1	56298.1	54.8	DUP	WF	3550-9600	8.0	2x200	1.06	0.024
2013-01-11.1	56303.1	59.8	DUP	WF	3500-9500	8.0	2x200	1.12	0.024
2013-02-18.0	56341.0	97.7	DUP	BC	3300-9500	7.0	300	1.19	0.024
2013-08-08.4	56512.4	269.1	BAA	IM	4270-11200	7.5	2x1200	1.03	...
2014-03-25.0	56741.0	497.7	BAA	IM	4000-10000	3.5	1200	1.61	...
SN 2012gm									
2012-12-05.8 <sup>c</sup>	56266.8	5.1	NOT	AL	3500-9100	17.0	1200	1.04	0025
SN 2012hd									
2012-12-22.1	56283.1	17.3	DUP	WF	3680-9600	8.0	300	1.12	0.055
2013-01-06.1	56298.1	32.2	DUP	WF	3700-9600	8.0	2x400	1.29	0.034

Table 3 continued on next page

**Table 3** (*continued*)

Date [UT]	MJD	Phase [d]	Tel.	Inst.	$\lambda$ range [Å]	Res. [Å]	exp. [s]	airmass	rms
(1)	(2)	(3)	(4)	(5)	(6)	(7)	(8)	(9)	(10)
SN 2012hl									
2012-12-13.9 <sup>c</sup>	56274.9	2.8	NOT	AL	3500-9100	17.0	1800	1.03	0.062
SN 2012hr									
2012-12-21.3	56282.3	-6.6	DUP	WF	3580-9600	8.0	300	1.25	0.020
2012-12-22.3	56283.3	-5.6	DUP	WF	3580-9600	8.0	2x300	1.22	0.008
2013-01-04.3	56296.3	7.4	CLA	LD	3715-9430	7.0	2x150	1.44	0.020
2013-01-06.1	56298.1	9.2	DUP	WF	3580-9600	8.0	2x200	1.17	0.038
2013-01-11.3	56303.3	14.2	DUP	WF	3580-9600	8.0	2x200	1.29	0.028
2013-02-18.2	56341.2	51.9	DUP	BC	3300-9450	8.0	900	1.55	0.051
SN 2012ht									
2012-12-27.2 <sup>c</sup>	56288.2	-7.6	NOT	AL	3300-9120	17.0	1500	1.12	0.058
2013-01-05.4	56297.4	1.6	CLA	LD	3715-9430	7.0	2x100	1.43	0.038
2013-01-06.3	56298.3	2.6	DUP	WF	3570-9600	8.0	2x150	1.49	0.057
2013-02-04.1 <sup>c</sup>	56327.1	31.2	NOT	AL	3400-9130	17.0	1800	1.05	0.032
2013-02-18.2	56341.2	45.3	DUP	BC	3300-9400	8.0	600	1.43	0.028
2013-03-29.1 <sup>c</sup>	56380.1	84.0	NOT	AL	3500-9100	17.0	2400	1.13	0.033
SN 2012id									
2013-01-06.1	56298.1	10.9	DUP	WF	3800-9600	8.0	2x600	1.52	0.017
SN 2012ij									
2013-01-07.4	56299.4	-3.1	DUP	WF	3700-9600	8.0	200	1.46	0.057
2013-01-10.4	56302.4	-0.2	DUP	WF	3600-9600	8.0	3x200	1.46	0.035
2013-02-04.1 <sup>c</sup>	56327.1	24.3	NOT	AL	3500-9050	17.0	1800	1.06	0.027
2013-02-18.3	56341.3	38.3	DUP	BC	3600-9400	8.0	3x400	1.46	0.070
SN 2013E									
2013-01-06.2	56298.2	-10.0	DUP	WF	3570-9600	8.0	3x150	1.50	0.018
2013-01-07.4	56299.4	-8.8	DUP	WF	3570-9600	8.0	200	1.03	0.017
2013-01-10.3	56302.3	-5.9	DUP	WF	3570-9600	8.0	2x150	1.02	0.021
2013-02-18.3	56341.3	32.7	DUP	BC	3300-9500	8.0	400	1.08	0.021
SN 2013H									
2013-01-07.2	56299.2	-10.5	DUP	WF	3570-9600	8.0	2x600	1.59	0.016
2013-01-10.3	56302.3	-7.4	DUP	WF	3570-9600	8.0	2x500	1.46	0.025
2013-02-18.3	56341.3	31.0	DUP	BC	3300-9470	8.0	900	1.73	0.023
SN 2013U									
2013-02-18.3	56341.3	6.0	DUP	BC	3300-9500	8.0	3x600	1.33	0.121
SN 2013Y									
2013-02-11.2 <sup>c</sup>	56334.2	0.6	NOT	AL	3500-9100	17.0	2400	1.05	0.053
SN 2013aa									
2013-02-18.4	56341.4	-2.0	DUP	BC	3300-9480	8.0	3x40	1.04	0.012

Table 3 continued on next page

**Table 3** (*continued*)

Date [UT]	MJD	Phase [d]	Tel.	Inst.	$\lambda$ range [\AA]	Res. [\AA]	exp. [s]	airmass	rms
(1)	(2)	(3)	(4)	(5)	(6)	(7)	(8)	(9)	(10)
2013-04-05.3 <sup>c</sup>	56387.3	43.7	DUP	WF	3700-9300	8.0	300	1.04	...
SN 2013ad									
2013-02-25.9	56348.9	0.8	NOT	AL	3500-9000	17.0	2400	1.16	0.015
SN 2013aj									
2013-03-20.1 <sup>c</sup>	56371.1	9.7	NOT	AL	3300-9050	17.0	1800	1.27	0.011
2013-04-02.	56384.34	22.8	HET	LRS	4200-10600	12.0	1800	1.22	...
2013-04-07.4 <sup>c</sup>	56389.4	27.7	DUP	WF	3700-9300	8.0	400	1.60	...
SN 2013ao									
2013-03-19.1	56371.1	10.0	NOT	AL	3400-9100	17.0	2400	1.55	0.026
2013-04-06.0.	56388.08	26.3	SALT	RSS	4000-9900	1500	4.0	1.29	...
2013-04-24.0	56407.0	44.4	NOT	AL	3900-9000	17.0	2400	1.606	0.079
SN 2013as									
2013-03-21.0 <sup>c</sup>	56372.0	5.8	NOT	AL	3500-9100	17.0	2400	1.60	0.048
SN 2013ba									
2013-04-07.1 <sup>c</sup>	56389.1	-7.0	NOT	AL	3500-9100	17.0	2700	1.02	0.027
SN 2013bz									
2013-05-14.0 <sup>c</sup>	56427.0	17.0	NOT	AL	3500-9100	17.0	1800	1.30	0.069
2013-05-28.0 <sup>c</sup>	56440.0	29.8	NOT	AL	3400-9140	17.0	2400	1.42	0.012
SN 2013cs									
2013-05-17.0 <sup>c</sup>	56430.0	-6.8	NOT	AL	3300-9100	17.0	1800	1.51	0.048
2013-05-19	56431.01	-5.8	SALT	RSS	3500-9500	4.3	600	1.24	...
2013-05-25	56437.01	0.2	SALT	RSS	3500-9500	4.3	600	1.24	...
2013-06-10	56453.93	16.9	SALT	RSS	3500-9500	4.3	600	1.22	...
SN 2013ct									
2013-08-03.2 <sup>c</sup>	56507.2	95.5	NOT	AL	3500-9000	17.0	2400	1.20	...
SN 2013fy									
2013-11-09.1	56605.1	4.9	DUP	WF	3640-9150	8.0	700	1.35	0.042
SN 2013gr									
2013-12-02.0 <sup>c</sup>	56628.0	11.1	BAA	IM	4080-10000	5.0	2x360	1.17	0.035
2013-12-14.0 <sup>c</sup>	56640.0	23.0	CLA	MA	3600-9400	1.0	1200	1.15	0.029
2013-12-31.2	56657.2	40.0	BAA	IM	3600-9750	3.0	600	1.73	0.023
2014-08-14.3	56883.3	264.5	BAA	IM	3800-9222	3.0	1800	1.22	...
SN 2013gy									
2013-12-14.0	56640.0	-8.7	CLA	MA	3100-9500	1.0	450	1.37	0.072
2013-12-25.8	56651.8	3.1	NOT	AL	3250-9100	17.0	2000	1.57	0.023
2013-12-31.2	56657.2	8.4	BAA	IM	3500-9700	3.0	600	1.71	0.057
2014-01-08.0	56665.0	16.2	DUP	WF	3600-9200	8.0	2x400	1.10	0.035

Table 3 continued on next page

**Table 3** (*continued*)

Date [UT]	MJD	Phase [d]	Tel.	Inst.	$\lambda$ range [\AA]	Res. [\AA]	exp. [s]	airmass	rms
(1)	(2)	(3)	(4)	(5)	(6)	(7)	(8)	(9)	(10)
2014-01-14.0	56671.0	22.2	NOT	AL	3500-9100	17.0	2000	1.51	0.041
2014-02-09.9	56697.9	49.1	NOT	AL	3500-9100	17.0	2400	1.25	0.085
2014-08-14.4	56883.4	234.7	BAA	IM	3600-9250	3.0	2000	1.14	...
SN 2013hh									
2013-12-21.2 <sup>c</sup>	56647.2	8.3	NOT	AL	3500-9100	17.0	2400	1.25	0.024
2014-01-14.2 <sup>c</sup>	56671.2	32.0	NOT	AL	3500-9100	17.0	2400	1.03	0.065
SN 2014D									
2014-01-12.1 <sup>c</sup>	56669.1	3.8	NOT	AL	3500-9100	17.0	2400	1.30	0.039
SN 2014I									
2014-01-27.9 <sup>c</sup>	56684.9	1.0	NOT	AL	3500-9100	17.0	1800	1.99	0.119
2014-02-09.9 <sup>c</sup>	56697.9	13.6	NOT	AL	3500-9100	17.0	2400	1.71	0.142
2014-03-12.9 <sup>a,c</sup>	56728.9	43.7	NOT	AL	3500-9100	17.0	2400	1.75	0.252
SN 2014ao									
2014-05-07.0	56784.0	15.9	DUP	WF	3640-9200	8.0	900	1.20	0.039
SN 2014at									
2014-05-07.3	56784.3	9.9	DUP	WF	3640-9200	8.0	3x1000	1.72	0.052
SN 2014dk									
2014-10-01.1 <sup>c</sup>	56931.1	-0.1	NOT	AL	3500-9100	17.0	2100	1.08	0.041
SN 2014dl									
2014-09-27.0	56927.0	-7.8	DUP	WF	3640-9200	8.0	900	2.08	0.009
SN 2014dn									
2014-09-28.3	56928.3	2.9	DUP	WF	3640-9200	8.0	900	1.13	0.020
SN 2014dt									
2015-02-24.2	57077.2	126.7	DUP	WF	3600-9100	8.0	700	1.26	
SN 2014du									
2014-11-14.9 <sup>a,c</sup>	56975.9	7.1	NOT	AL	3600-9000	17.0	2400	1.10	0.112
SN 2014eg									
2014-11-28.1	56989.1	-2.1	DUP	WF	3640-9200	8.0	500	1.12	0.041
SN 2014ek									
2014-11-12.0 <sup>a,c</sup>	56973.0	13.4	NOT	AL	3600-9150	17	1800	1.16	0.130
SN 2015F									
2015-04-24.1	57136.1	29.1	DUP	WF	3640-9200	8.0	300	1.51	0.036
SN 2015H									
2015-02-18.4	57072.4	18.2	DUP	WF	3700-9160	8.0	...	1.56	0.041
2015-02-25.2	57078.2	23.9	DUP	WF	3700-9160	8.0	...	1.05	0.066

Table 3 continued on next page

**Table 3** (*continued*)

Date [UT]	MJD	Phase [d]	Tel.	Inst.	$\lambda$ range [\AA]	Res. [\AA]	exp. [s]	airmass	rms
(1)	(2)	(3)	(4)	(5)	(6)	(7)	(8)	(9)	(10)
SN 2015M									
2015-05-16.1 <sup>a,c</sup>	57158.1	-10.1	NOT	AL	3500-9100	17.0	1800	1.65	0.291
2015-05-23.9 <sup>a,c</sup>	57165.9	-2.5	NOT	AL	3500-9100	17.0	1800	1.00	0.298
2015-06-02.9 <sup>a,c</sup>	57175.9	7.3	NOT	AL	3500-9100	17.0	1800	1.02	0.321
2015-06-06.9 <sup>c</sup>	57179.9	11.2	NOT	AL	3500-9100	17.0	1800	1.00	0.097
2015-06-17.0 <sup>c</sup>	57191.0	22.0	NOT	AL	3500-9100	17.0	1800	1.34	...
SN 2015bo									
2015-02-25.3	57078.3	2.3	DUP	WF	3640-9150	8.0	700	1.47	0.073
2015-03-04.1 <sup>a,c</sup>	57085.1	9.0	NOT	AL	3500-9100	17.0	2400	1.10	0.262
2015-03-11.2 <sup>a,c</sup>	57092.2	15.9	NOT	AL	3500-9120	17.0	1800	1.02	0.305
2015-03-27.1 <sup>c</sup>	57108.1	31.6	NOT	AL	3700-9120	17.0	2400	1.02	0.056
SN 2015bp									
2015-03-27.2 <sup>c</sup>	57108.2	-4.5	NOT	AL	3400-9100	17.0	1500	1.13	0.021
2015-04-13.1 <sup>c</sup>	57125.1	12.4	NOT	AL	3400-9100	17.0	2x1800	1.13	0.093
2015-04-24.3	57136.3	23.6	DUP	WF	3640-9200	8.0	600	1.34	0.019
2015-05-12.0 <sup>a,c</sup>	57154.0	41.2	NOT	AL	3550-9000	17.0	1800	1.14	0.245
2015-07-19.0	57222.0	108.9	DUP	WF	3700-9150	8.0	3x1000	1.18	0.059
2015-08-14.9	57248.9	135.7	NOT	AL	3700-9000	17.0	2400	1.41	0.109

<sup>a</sup>Spectrum corrected to match photometry.<sup>b</sup>Phase estimated using SNID.<sup>c</sup>Spectrum not corrected for telluric absorption.

NOTE—Column 1: UT date of the observation. Column 2: Modified Julian Date. Column 3: phase in days relative to time of maximum light corrected for redshift. Column 4: telescope code. 3P6: ESO 3.6 m Telescope at La Silla; BAA: Las Campanas Magellan I 6.5 m Baade Telescope; CLA: Las Campanas Magellan II 6.5 m Clay Telescope; DUP: Las Campanas 2.5 m du Pont Telescope; GEN: Gemini-N 8 m Telescope; GES: Gemini-S 8 m Telescope; NTT: ESO New Technology Telescope at La Silla; NOT: Nordic Optical Telescope at Roque de los Muchachos, Canary Islands. Column 5: instrument code. AL: Alhambra Faint Object Spectrograph and Camera (ALFOSC); BC: Boller & Chivens spectrograph; EF: ESO Faint Object Spectrograph and Camera (EFOSC-2); EM: ESO Multi-Mode Instrument (EMMI); GM: Gemini Multiple-Object Spectrograph (GMOS); IM: Inamori Kyocera Magellan Areal Camera and Spectrograph (IMACS); LD: Low Dispersion Survey Spectrograph (LDSS); MA: Magellan Echelle spectrograph (MagE); MI: Magellan Inamori Kyocera Echelle spectrograph (MIKE); MS: Las Campanas Modular Spectrograph (MODSPEC); WF: Wide Field Reimaging CCD Camera (WFCCD). Column 6: observed spectral range expressed in Å. Column 7: spectral resolution in Å; Column 8: exposure time in seconds. Column 9: airmass at middle of exposure. Column 10: r.m.s. of the differences between synthetic and observed broadband magnitudes (when available).

**Table 4.** Optical Spectroscopic observations of historical SNe Ia

Date [UT]	MJD	Phase [d]	Tel.	Inst.	$\lambda$ range [\AA]	exp. [s]	airmass
(1)	(2)	(3)	(4)	(5)	(6)	(7)	(8)
SN 1986G							
1986-05-05.1	46555.1	-6.1	C60	RC60	4787-7179	...	...
1986-05-06.1	46556.1	-5.1	C60	RC60	4787-7179	...	...
1986-05-07.0	46557.0	-4.2	C60,BLA	RC60,RC4	3600-7154	...	...
1986-05-08.1	46558.1	-3.2	C60,BLA	RC60,RC4	3600-7162	...	...
1986-05-09.0	46559.0	-2.2	BLA	RC4	3600-5171	...	...
1986-05-10.2	46560.2	-1.0	BLA	RC4	3918-7018	...	...
1986-05-11.3	46561.3	0.1	BLA	RC4	3556-6638	...	...
1986-05-12.2	46562.2	1.0	BLA	RC4	3556-6638	...	...
1986-05-13.1	46563.1	1.9	BLA	RC4	3698-5265	...	...
1986-05-15.4	46565.4	4.2	H88	...	4374-6330	...	...
1986-05-17.0	46567.0	5.8	BLA	RC4	5991-7012	...	...
1986-06-09.5 <sup>a</sup>	46590.5	29.3	YAL	YBC	3800-7218	...	...
1986-06-25.0	46606.0	44.8	YAL	YBC	3800-7218	...	...
1986-06-27.1	46608.1	46.9	DUP	DBC	4600-7200	...	...
1986-06-29.0	46610.0	48.8	YAL	YBC	3800-7218	...	...
1986-07-04.0	46615.0	53.8	YAL	YBC	3800-7218	...	...
1986-07-06.0	46617.0	55.8	DUP	DBC	3300-7100	...	...
SN 1989B							
1989-01-31.2	47557.2	-8.2	K84	GOLD	3531-4506	600	...
1989-01-31.3	47557.3	-8.1	MMT	RED	3200-6400	600	1.91
1989-01-31.5	47557.5	-7.9	SHA	CS3	2980-7906	...	...
1989-02-01.4	47558.4	-6.9	TIL	ZM	4545-7065	840	1.07
1989-02-03.6	47560.6	-4.8	TIL	ZM	3188-7635	300	1.57
1989-02-04.3	47561.3	-4.1	YAL	YBC	3641-4864	360	1.37
1989-02-04.4	47561.4	-4.0	K84	GOLD	3540-7405	...	...
1989-02-04.6	47561.6	-3.8	TIL	ZM	3188-7724	840	1.07
1989-02-05.3	47562.3	-3.1	YAL	YBC	3640-4865	600	1.39
1989-02-06.3	47563.3	-2.1	C60	RC60	6500-10800	600	1.38
1989-02-06.4	47563.4	-2.0	C60	RC60	3001-11167	400	1.49
1989-02-07.4	47564.4	-1.0	K84	GOLD	3540-7405	...	...
1989-02-08.3	47565.3	-0.1	TIL	ZM	4545-7065	840	1.07
1989-02-10.3	47567.3	1.9	YAL	YBC	3450-7000	1800	1.40
1989-02-12.3	47569.3	3.9	YAL	YBC	3450-7110	1800	1.37
1989-02-14.3	47571.3	5.9	YAL	YBC	3450-7025	1800	1.38
1989-02-14.4	47571.4	6.0	TIL	ZM	4545-7065	360	1.07
1989-02-16.3	47573.3	7.9	YAL	YBC	3450-7000	1800	1.42
1989-02-18.3	47575.3	9.9	YAL	YBC	3450-7000	1800	1.41
1989-02-19.3	47576.3	10.9	YAL	YBC	3450-7000	1800	1.38
1989-02-20.3	47577.3	11.9	YAL	YBC	3450-7000	1800	1.38
1989-02-21.2	47578.2	12.9	YAL	YBC	3450-7000	3900	1.37

*Table 4 continued on next page*

**Table 4** (*continued*)

Date [UT]	MJD	Phase [d]	Tel.	Inst.	$\lambda$ range [\AA]	exp. [s]	airmass
(1)	(2)	(3)	(4)	(5)	(6)	(7)	(8)
1989-02-23.2	47580.2	14.8	YAL	YBC	3450-7000	3600	1.38
1989-02-24.2	47581.2	15.8	YAL	YBC	3450-7000	1800	1.39
1989-02-25.2	47582.2	16.8	YAL	YBC	3450-7000	1785	1.38
1989-02-26.2	47583.2	17.9	YAL	YBC	3450-7000	1800	1.38
1989-02-26.4	47583.4	18.0	NIC	CS1	4205-8845	...	...
1989-02-27.2	47584.2	18.9	YAL	YBC	3450-7000	1800	1.38
1989-02-28.2	47585.2	19.8	YAL	YBC	3450-7000	1800	1.38
1989-03-01.2	47586.2	20.8	YAL	YBC	3450-7000	1800	1.38
1989-03-01.4	47586.4	21.0	TIL	ZM	3188-7245	240	1.16
1989-03-02.2	47587.2	21.8	YAL	YBC	3450-7000	1800	1.38
1989-03-02.3	47587.3	21.9	TIL	ZM	4510-6965	720	1.06
1989-03-03.2	47588.2	22.8	YAL	YBC	3450-7000	1800	1.37
1989-03-04.3	47589.3	23.8	YAL	YBC	3450-7000	1800	1.43
1989-03-08.3	47593.3	27.9	TIL	ZM	4511-6965	720	1.06
1989-03-10.2	47595.2	29.8	YAL	YBC	3575-7100	1800	1.39
1989-03-13.3	47598.3	32.8	TIL	ZM	4511-7032	360	1.07
1989-03-16.2	47601.2	35.7	YAL	YBC	3575-7100	1800	1.37
1989-03-28.1	47613.1	47.6	YAL	YBC	3630-7180	1200	1.41
1989-03-29.5	47614.5	49.0	SHA	CS3	3120-9995	...	...
1989-03-30.4	47615.4	49.9	MMT	RED	3878-8973	600	1.26
1989-04-05.4	47621.4	55.9	TIL	ZM	3188-7437	480	2.27
1989-04-11.2	47627.2	61.7	TIL	ZM	4545-7065	720	1.06
1989-04-15.2	47631.2	65.7	NIC	CS1	4405-8305	...	...
1989-04-19.5	47635.5	70.0	BLA	RC4	7898-10636	600	1.38
1989-04-19.6	47635.6	70.0	BLA	RC4	4959-8220	600	1.46
1989-04-20.1	47636.1	70.5	BLA	RC4	2952-6212	900	1.37
1989-05-08.0	47654.0	88.6	C60	RC60	6500-10000	600	1.39
1989-05-08.1	47654.1	88.7	C60	RC60	3200-7700	1200	1.42
1989-05-09.1	47655.1	89.7	BLA	RC4	3023-9960	1200	1.43
1989-05-10.4	47656.4	90.8	MMT	RED	5024-7749	600	1.11
1989-05-30.1	47676.1	110.4	YAL	YBC	3400-7000	3000	1.57
1989-06-03.2	47680.2	114.5	TIL	ZM	4545-7065	720	1.28
1989-06-14.0	47692.0	126.3	C60	RC60	6500-10000	600	1.43
1989-06-14.0	47692.0	126.3	C60	RC60	3500-7500	600	1.74
1989-06-27.0	47704.0	138.3	C60	RC60	3500-7700	1800	1.88
1990-01-04.3	47895.3	329.1	BLA	RC4	3560-6840	1200	1.71
1990-01-20.5	47911.5	345.3	SHA	CS3	3955-7005	...	...
SN 1990N							
1990-06-26.2	48068.2	-14.0	MMT	...	3100-8150	300	1.21
1990-07-03.0	48075.0	-7.2	C60	RC60	3100-7690	300	1.43
1990-07-24.0	48097.0	14.7	BLA	RC4	3300-6500	60	1.73
1990-07-25.0	48098.0	15.7	BLA	RC4	6290-9580	300	1.56
1990-07-27.0	48100.0	17.7	MMT	...	3200-7400	360	1.80
1990-08-11.0	48114.0	31.6	C60	RC60	6045-10400	900	2.97

Table 4 continued on next page

**Table 4** (*continued*)

Date [UT]	MJD	Phase [d]	Tel.	Inst.	$\lambda$ range [\AA]	exp. [s]	airmass
(1)	(2)	(3)	(4)	(5)	(6)	(7)	(8)
1990-08-17.0	48120.0	37.6	C60	RC60	3500-7690	600	2.69
SN 1990O							
1990-06-26.3	48068.3	-7.4	MMT	...	3120-8100	1000	1.05
1990-06-27.3	48069.3	-6.5	MMT	...	3130-7900	1256	1.05
1990-06-28.4	48070.4	-5.4	MMT	...	3130-7900	1000	1.16
1990-07-03.2	48075.2	-0.7	C60	RC60	3500-7500	1800	1.60
1990-07-23.3	48095.3	18.8	MMT	...	3100-7200	840	1.27
1990-07-24.1	48096.1	19.6	C60	RC60	3200-6350	900	1.53
SN 1990T							
1990-07-26.1	48098.1	14.5	BLA	RC4	6050-9200	901	1.16
1990-07-26.2	48098.2	14.6	3P6	...	3600-9600	900	1.13
1990-08-16.1	48119.1	34.7	BLA	RC4	5900-9100	1200	1.14
1990-08-16.2	48119.2	34.7	BLA	RC4	3500-5400	1200	1.12
SN 1990Y							
1990-08-30	48133.5	19	...	...	4000-6700	...	...
SN 1990af							
1990-10-28.1	48192.1	-3.6	BLA	RC4	6000-8800	900	1.24
1990-10-28.1	48192.1	-3.6	BLA	RC4	4280-6050	600	1.36
SN 1991S							
1991-04-20.4	48366.4	18.5	BLA	RC4	3500-6500	1200	1.65
SN 1991T							
1991-04-16.0	48362.0	-12.9	TIL	ZM	4610-7060	1800	1.52
1991-04-20.0	48366.0	-8.9	C60	RC60	3200-7600	180	1.57
1991-04-20.1	48366.1	-8.9	C60	RC60	6300-10000	600	1.35
1991-04-21.4	48367.4	-7.5	BLA	RC4	3247-7531	688	1.39
1991-04-22.2	48368.2	-6.8	C60	RC60	4981-9500	600	1.19
1991-04-25.0	48371.0	-4.0	C60	RC60	3200-7600	300	1.74
1991-04-25.1	48371.1	-3.8	C60	RC60	6300-10000	600	1.20
1991-05-02.1	48378.1	3.1	YAL	YBC	3218-6707	1200	1.19
1991-05-08.0	48384.0	9.0	C60	RC60	3200-7600	300	1.34
1991-05-09.0	48385.0	9.9	C60	RC60	6300-10000	600	1.42
1991-05-13.0	48389.0	13.9	C60	RC60	3200-7600	600	1.24
1991-05-23.0	48398.0	22.8	C60	RC60	3200-7600	300	1.25
1991-06-12.0	48419.0	43.7	BLA	RC4	3300-7460	400	1.20
1991-06-13.0	48420.0	44.7	BLA	RC4	5500-9980	400	1.19
1991-06-16.0	48423.0	47.6	C60	RC60	6250-9000	600	1.19
1991-07-04.0	48441.0	65.5	C60	RC60	3200-7600	1200	1.22
1991-07-11.0	48448.0	72.5	C60	RC60	6220-10000	1800	1.27
1992-02-05.4	48657.4	280.4	BLA	RC4	3200-7400	600	1.20
1992-04-04.1	48716.1	338.7	BLA	RC4	3300-7400	1200	1.38
1992-04-04.1	48716.1	338.8	BLA	RC4	6200-9700	1200	1.23

Table 4 continued on next page

**Table 4** (*continued*)

Date [UT]	MJD	Phase [d]	Tel.	Inst.	$\lambda$ range [\AA]	exp. [s]	airmass
(1)	(2)	(3)	(4)	(5)	(6)	(7)	(8)
SN 1991U							
1991-04-20.2	48366.2	11.5	C60	RC60	6122-9000	1800	1.10
1991-04-20.6	48366.6	11.9	BLA	RC4	3500-6600	600	1.03
SN 1991ag							
1991-06-12.2	48419.2	5.6	BLA	RC4	3300-7400	600	1.28
1991-06-13.3	48420.3	6.7	BLA	RC4	5460-9740	600	1.12
SN 1991bg							
1991-12-13.5	48603.5	0.1	TIL	...	4650-7000	...	...
1991-12-15.4	48605.4	1.9	BLA	RC4	3200-7400	150	2.05
1991-12-27.3	48617.3	13.9	C60	RC60	3100-7700	600	1.75
1991-12-28.3	48618.3	14.9	C60	RC60	5140-9625	600	1.78
1992-12-31.6	48621.6	18.2	MMT	BLUE	3190-7885	...	...
1992-01-07.3	48628.3	24.9	BLA	RC4	3300-7486	600	1.72
1992-01-08.3	48629.3	25.8	BLA	RC4	6300-10500	...	...
1992-01-14.4	48635.4	31.9	MMT	RED	3710-8770	...	...
1992-01-28.3	48649.3	45.7	C60	RC60	3500-7750	1800	1.46
1992-02-05.3	48657.3	53.7	BLA	RC4	3300-7400	300	1.39
1992-04-04.2	48716.2	112.4	BLA	RC4	3700-7300	1200	1.38
SN 1992A							
1992-01-12.2	48633.2	-7.3	BLA	RC4	4770-6530	300	1.70
1992-01-13.1	48634.1	-6.4	BLA	RC4	3300-7580	120	1.03
1992-01-14.1	48635.1	-5.4	YAL	YBC	3550-7080	1800	1.12
1992-01-18.1	48639.1	-1.4	YAL	YBC	3570-7030	1500	1.20
1992-01-22.0	48643.0	2.5	YAL	YBC	3550-7020	1500	1.02
1992-01-25.0	48646.0	5.5	C60	RC60	3400-8120	500	1.02
1992-01-26.0	48647.0	6.4	YAL	YBC	3550-7700	1500	1.02
1992-01-28.0	48649.0	8.4	C60	RC60	3144-7790	300	1.04
1992-01-28.1	48649.1	8.5	C60	RC60	6062-9910	450	1.17
1992-01-30.0	48651.0	10.4	YAL	YBC	3685-7100	1500	1.04
1992-02-04.0	48656.0	15.4	YAL	YBC	3677-7100	1500	1.05
1992-02-05.0	48657.0	16.4	BLA	RC4	3600-7200	180	1.10
1992-02-10.0	48662.0	21.4	C60	RC60	5110-9610	600	1.13
1992-02-11.0	48663.0	22.3	BLA	RC4	3230-7505	300	1.09
1992-02-12.0	48664.0	23.3	YAL	YBC	3700-6900	1500	1.08
1992-02-16.0	48668.0	27.3	YAL	YBC	3700-7000	1500	1.10
1992-02-25.0	48677.0	36.2	YAL	YBC	3700-7000	2700	1.14
1992-03-05.0	48686.0	45.2	BLA	RC4	3000-7730	900	1.32
1992-04-04.0	48716.0	75.0	BLA	RC4	6190-9710	300	1.78
1992-04-04.0	48716.0	75.0	BLA	RC4	3230-7400	300	2.16
1992-10-31.2	48926.2	283.9	BLA	RC4	3210-7300	1800	1.01
SN 1992J							

Table 4 continued on next page

**Table 4** (*continued*)

Date [UT]	MJD	Phase [d]	Tel.	Inst.	$\lambda$ range [\AA]	exp. [s]	airmass
(1)	(2)	(3)	(4)	(5)	(6)	(7)	(8)
1992-03-05.4	48686.4	12.1	3500-7000	BLA	RC4	300	2.36
1992-03-06.1	48687.1	12.8	3500-7300	C60	RC60	3600	1.03
SN 1992K							
1992-03-06.3	48687.3	12.2	C60	RC60	3500-7650	1200	1.04
1992-04-04.0	48716.0	40.7	BLA	RC4	3300-7400	600	1.42
SN 1992P							
1992-04-06.3	48718.3	-0.6	BLA	RC4	5100-6800	300	2.45
1992-04-11.3	48723.3	4.2	C60	RC60	4000-7500	1200	1.51
SN 1992ae							
1992-07-04.3	48807.3	3.5	1P5	EBC	3300-9000	3600	1.20
SN 1992ag							
1992-07-03.0	48806.0	0.0	C60	RC60	3300-7500	1200	1.11
1992-07-29.1	48832.1	25.3	BLA	RC4	3300-7300	1200	1.65
SN 1992al							
1992-07-29.3	48832.3	-5.6	BLA	RC4	3300-7400	600	1.18
1992-08-07.2	48841.2	3.1	C60	RC60	3300-7600	300	1.08
SN 1992aq							
1992-08-02.3	48836.3	2.4	BLA	RC4	3300-6700	600	1.03
SN 1992au							
1992-10-01.2	48896.2	59.3	BLA	RC4	3200-7000	1800	1.07
SN 1992bc							
1992-10-06.1	48901.1	-10.7	BLA	RC4	3200-7200	300	1.62
1992-10-27.1	48922.1	9.9	C60	RC60	3100-7500	1800	1.16
1992-11-23.2	48949.2	36.4	BLA	RC4	3300-7300	600	1.08
SN 1992bg							
1992-10-27.2	48922.2	7.3	C60	RC60	3300-7400	1800	1.59
SN 1992bh							
1992-10-27.2	48922.2	2.5	C60	RC60	3300-7350	1800	1.31
SN 1992bk							
1992-11-21.1	48947.1	7.6	BLA	RC4	3300-7000	600	1.12
1992-11-22.2	48948.2	8.6	BLA	RC4	3300-7000	500	1.09
SN 1992bl							
1992-11-22.1	48948.1	0.9	BLA	RC4	3300-7100	600	1.14
SN 1992bo							
1992-12-31.0	48987.0	0.8	C60	RC60	3500-7300	600	1.08

Table 4 continued on next page

**Table 4** (*continued*)

Date [UT]	MJD	Phase [d]	Tel.	Inst.	$\lambda$ range [\AA]	exp. [s]	airmass
(1)	(2)	(3)	(4)	(5)	(6)	(7)	(8)
SN 1992bp							
1992-12-31.2	48987.2	6.8	C60	RC60	3600-6900	1800	1.22
SN 1992br							
1992-12-31.1	48987.1	0.1	C60	RC60	3500-6800	1800	1.25
SN 1992bs							
1992-12-31.2	48987.2	3.3	C60	RC60	3600-7000	1800	1.43
SN 1993B							
1993-01-28.3	49015.3	12.4	BLA	RC4	3500-6500	900	1.00
SN 1993H							
1993-03-21.2	49067.2	-1.3	BLA	RC4	5690-8900	480	1.06
1993-03-23.1	49069.1	0.6	C60	RC60	3300-7500	1800	1.40
1993-03-25.3	49071.3	2.7	BLA	RC4	3620-6840	900	1.01
1993-04-01.2	49078.2	9.7	C60?	...	3500-7500	1200	1.00
SN 1993O							
1993-05-21.1	49128.1	-5.7	C60	RC60	3200-7150	1800	1.03
1993-05-27.1	49134.1	0.0	BLA	RC4	3200-7150	900	1.01
SN 1993af							
1993-11-27.2	49318.2	185 <sup>b</sup>	NTT	EM	3880-9020	1200	1.01
SN 1993ag							
1993-11-26.3	49318.3	2.2	NTT	EM	3800-8600	1800	1.51
SN 1993ah							
1993-11-27.0	49318.0	15.9	NTT	EM	3800-8800	1200	1.04
SN 1994D							
1993-03-16.	49426.5	-6	...	...	3860-10000	...	...
1994-03-23.	49433.5	1	...	...	3100-9700	...	...
1994-04-04.	49445.5	13	...	...	3500-9800	...	...
1994-04-06.	49447.5	15	...	...	3640-7400	...	...
1994-04-12.2	49454.2	21.6	YAL	YBC	3770-6980	1200	1.27
SN 1999aw							
1999-03-16.1	51253.1	-0.6	NOT	AL	4302-7994	...	...
1999-03-17.3	51254.3	0.6	BLA	RC4	3504-8460	...	...
1999-03-20.2	51257.2	3.3	DUP	WF	3600-9270	600	1.09
1999-04-23.0	51291.0	35.9	DUP	WF	3790-9300	600	1.09
1999-05-19.1	51317.1	61.1	NTT	EM	4685-10098	600	1.28
SN 1999cs							
1999-04-29.1	51297.1	6	NTT	EM	3030-9500 <sup>c</sup>	900	1.01
1999-05-03.0	51301.0	10	NTT	EM	3040-9500	600	1.07

*Table 4* continued on next page

**Table 4** (*continued*)

Date [UT] (1)	MJD (2)	Phase [d] (3)	Tel. (4)	Inst. (5)	$\lambda$ range [\AA] (6)	exp. [s] (7)	airmass (8)
SN 1999ei							
1999-10-16.2	51467.2	15.2	DUP	WF	3600-9240	600	1.00
SN 1999ek							
1999-10-25.4	51476.4	-5.6	C60	RC60	3070-9858	1200	1.52
1999-10-26.3	51477.3	-4.7	C60	RC60	3830-9850	1800	1.47
1999-10-30.3	51481.3	-0.7	C60	RC60	3646-9875	1200	1.46
1999-11-01.3	51483.3	1.2	C60	RC60	3650-9875	1200	1.47
SN 2000bh							
2000-04-08.1	51643.1	6.5	NTT	EM	3300-9800	300	1.01
2000-05-01.1	51666.1	29.5	NTT	EM	3300-9800	300	1.20
SN 2000ca							
2000-05-01.0	51666.0	0.1	NTT	EM	3300-9800	300	1.52
2000-05-07.0	51672.0	6.2	NTT	EM	3300-9800	300	1.10
2000-05-30.0	51695.0	29.1	NTT	EM	3300-9800	450	1.15
SN 2001ba							
2001-05-01.0	52030.0	-3.8	DUP	WF	3400-8800	4x600	1.01
2001-05-17.0	52046.0	11.7	DUP	WF	3400-8800	4x600	1.00
2001-05-26.0	52055.0	20.5	DUP	WF	3700-8900	4x600	1.01
SN 2001bt							
2001-05-26.4	52055.4	-8.6	DUP	WF	3750-9050	600	1.19
SN 2001cn							
2001-06-14.3	52074.3	2.2	C60	RC60	3840-7200	600	1.26
2001-06-22.3	52082.3	10.1	C60	RC60	3730-7090	600	1.31

<sup>a</sup>This spectrum is the sum of spectra taken on 1986-06-08 and 1986-06-11.

<sup>b</sup>Phase estimated using SNID.

<sup>c</sup> This spectrum has a gap between 4870 and 5100 Å.

NOTE—Column 1: UT date of observation. Column 2: Modified Julian Date. Column 3: Phase in days relative to maximum light corrected for redshift. Column 4: telescope code. BLA: CTIO 4.0-m Blanco Telescope; C60: Cerro Tololo Inter-American Observatory (CTIO) 1.5 m Telescope; DUP: Las Campanas 2.5 m du Pont Telescope; H88: U. Hawaii 2.2-m Telescope; K84: Kitt Peak National Observatory (KPNO) 2.1-m Telescope; MMT: Multiple Mirror Telescope (MMT) at the Fred Lawrence Whipple Observatory; NIC: Lick Observatory 1.0-m Nickel Telescope; NOT: Nordic Optical Telescope at Roque de los Muchachos, Canary Islands; NTT: ESO New Technology Telescope at La Silla; SHA: Lick Observatory 3.0-m Shane Telescope; TIL: 1.5-m Tillinghast Telescope at the Fred Lawrence Whipple Observatory; YAL: CTIO 1.0-m Yale Telescope; 1P5: ESO 1.5-m Telescope at La Silla; 3P6: ESO 3.6 m Telescope at La Silla. Column 5: instrument code. AL: Alhambra Faint Object Spectrograph and Camera (ALFOSC); DBC: Las Campanas 2.5 m Boller & Chivens spectrograph; EBC: ESO 1.5 m Boller & Chivens spectrograph; EF: ESO Faint Object Spectrograph and Camera (EFOSC-2); EM: ESO Multi-Mode Instrument (EMMI); GOLD: Gold Camera; RC4: CTIO 4.0-m R-C Spectrograph; RC60: CTIO 1.5-m R-C Spectrograph; RED: Red Channel; WF: Wide Field Reimaging CCD Camera (WFCCD); YBC: Yale 1.0-m Boller & Chivens spectrograph; ZM: Z-Machine; CS1: Lick 1.0-m Cassegrain Spectrograph; CS3: Lick 3.0-m Cassegrain Spectrograph. Column 6: Observed spectral range in Å. Column 7: Exposure time in seconds. Column 8: Airmass at middle of the observation. Spectra already available via WISEREP are not included in this table, although they are considered in the analysis of SN properties at maximum light that follows.

**Table 5.** Pseudo equivalent widths at maximum light [Å]

SN	pW1	pW2	pW3	pW4	pW5	pW6	pW7	pW8	project
	Ca II H&K	Si II 4130	Mg II	Fe II	S II W	Si II 5972	Si II 6355	Ca II IR	
<b>CN</b>									
2007ol	106(1)	22(1)	80(1)	82(1)	56(1)	16(1)	78(1)	...	CSP I
2008bz	86(2)	22(2)	70(1)	106(2)	88(1)	17(1)	99(1)	105(3)	CSP I
2008fr	107(2)	11(1)	71(2)	109(1)	80(1)	17(1)	82(2)	72(5)	CSP I
2009I	140(3)	9(1)	82(3)	111(2)	72(1)	10(1)	70(1)	89(3)	CSP I
2009cz	120(1)	9(1)	92(1)	131(1)	67(1)	12(1)	81(1)	104(4)	CSP I
2009le	60(2)	11(1)	104(2)	124(1)	62(1)	9(1)	86(1)	114(2)	CSP I
ASASSN-14hr	135(2)	32(1)	101(2)	138(1)	67(2)	30(1)	104(2)	107(4)	CSP II
ASASSN-14hu	150(2)	11(1)	97(2)	115(1)	76(1)	7(1)	83(1)	...	CSP II
ASASSN-14kq	139(1)	11(1)	100(1)	115(1)	73(1)	11(1)	77(1)	127(3)	CSP II
ASASSN-14lp	116(3)	10(1)	93(4)	140(3)	69(1)	13(1)	70(1)	117(4)	CSP II
ASASSN-15al	121(2)	8(1)	87(3)	106(2)	74(2)	7(1)	73(2)	118(7)	CSP II
ASASSN-15be	151(2)	8(1)	100(3)	120(2)	85(2)	9(1)	86(2)	160(7)	CSP II
ASASSN-15bm	165(1)	16(1)	95(2)	140(2)	65(1)	12(1)	80(2)	120(4)	CSP II
ASASSN-15cb	125(1)	5(1)	97(1)	137(2)	58(2)	12(2)	80(3)	...	CSP II
ASASSN-15cd	116(2)	13(1)	93(2)	112(2)	71(2)	8(1)	103(2)	...	CSP II
ASASSN-15da	92(3)	20(1)	67(3)	105(2)	80(2)	17(1)	86(2)	...	CSP II
ASASSN-15db	131(1)	13(1)	74(1)	107(1)	71(1)	15(1)	85(1)	106(4)	CSP II
ASASSN-15dd	108(2)	23(1)	75(2)	111(1)	82(1)	18(1)	99(1)	143(3)	CSP II
ASASSN-15go	132(2)	8(1)	98(2)	107(1)	74(1)	<3	83(1)	92(4)	CSP II
ASASSN-15gr	115(3)	17(1)	102(3)	119(2)	85(2)	13(1)	93(2)	172(7)	CSP II
ASASSN-15hf	92(2)	19(1)	93(2)	139(1)	64(1)	18(1)	87(1)	85(2)	CSP II
CSS130315:114144-171348	149(1)	6(1)	93(1)	106(1)	88(1)	4(1)	79(1)	113(6)	CSP II
CSS131031:095508+064831	137(3)	10(1)	95(4)	113(4)	94(4)	17(3)	85(5)	...	CSP II
CSS140501-170414+174839	55(3)	9(1)	88(4)	89(3)	48(3)	16(3)	74(3)	...	CSP II
CSS140914-010107-101840	126(2)	14(1)	67(2)	102(1)	84(1)	17(1)	102(2)	213(6)	CSP II
iPTF13duj	123(2)	10(1)	98(2)	170(1)	78(1)	4(1)	101(1)	125(4)	CSP II
iPTF14gnl	108(2)	7(1)	76(1)	114(2)	77(2)	<4	72(2)	...	CSP II
KISS13j	151(2)	20(1)	95(2)	168(2)	78(1)	23(1)	106(2)	286(5)	CSP II
LSQ11bk	...	...	76(2)	104(1)	75(1)	<3	101(3)	103(4)	CSP II
LSQ11ot	120(3)	13(1)	86(3)	109(2)	63(1)	11(1)	79(1)	120(3)	CSP II
LSQ12blp	113(2)	10(1)	87(3)	153(2)	95(2)	11(1)	98(2)	...	CSP II
LSQ12ca	140(2)	12(1)	78(3)	115(2)	90(2)	11(1)	76(2)	...	CSP II
LSQ12cdl	131(3)	13(1)	97(4)	119(3)	87(4)	<6	88(4)	...	CSP II
LSQ12fxd	117(2)	12(1)	99(2)	114(1)	67(1)	13(1)	71(1)	120(3)	CSP II
LSQ12gxj	90(2)	6(1)	78(2)	100(1)	70(1)	9(1)	70(2)	90(3)	CSP II
LSQ12gyc	133(3)	10(1)	94(3)	108(3)	72(4)	9(3)	85(4)	...	CSP II
LSQ12hno	125(3)	16(1)	92(3)	116(2)	72(2)	12(1)	81(2)	...	CSP II
LSQ14asu	135(3)	31(1)	99(3)	116(2)	59(1)	27(1)	88(2)	...	CSP II
LSQ14auy	157(4)	15(2)	86(5)	137(6)	93(6)	10(6)	72(8)	...	CSP II
LSQ14gov	111(3)	9(1)	103(3)	108(3)	88(2)	12(2)	82(3)	...	CSP II
LSQ14xi	129(5)	13(2)	93(5)	138(5)	53(5)	<10	76(6)	...	CSP II
LSQ15aja	115(1)	12(1)	101(1)	107(2)	75(2)	5(1)	70(2)	...	CSP II
LSQ15alq	94(3)	24(1)	87(3)	143(2)	78(2)	22(1)	98(3)	...	CSP II
OGLE-2013-SN-118	113(2)	7(1)	92(1)	115(1)	79(2)	9(2)	80(3)	99(4)	CSP II
OGLE-2013-SN-123	75(1)	16(1)	79(1)	123(2)	43(2)	14(2)	78(2)	...	CSP II
PS1-14xw	125(2)	8(1)	85(2)	119(1)	62(1)	8(1)	78(1)	121(3)	CSP II
PTF11qnr	107(2)	21(1)	71(2)	120(1)	77(1)	22(1)	96(1)	125(3)	CSP II
2012aq	125(2)	16(1)	81(3)	100(2)	76(1)	21(1)	93(2)	...	CSP II
2012bl	104(2)	<2	84(2)	113(1)	75(1)	<2	94(1)	126(4)	CSP II

Table 5 continued on next page

**Table 5** (*continued*)

SN	pW1	pW2	pW3	pW4	pW5	pW6	pW7	pW8	project
	Ca II H&K	Si II 4130	Mg II	Fe II	S II W	Si II 5972	Si II 6355	Ca II IR	
2013aa	94(2)	16(1)	93(2)	121(1)	61(1)	8(1)	88(2)	103(3)	CSP II
2013fz	104(2)	8(1)	94(2)	131(1)	76(1)	5(1)	83(1)	139(4)	CSP II
2013gy	118(2)	17(1)	82(2)	134(1)	80(1)	21(1)	104(1)	202(3)	CSP II
2014D	183(3)	19(1)	79(3)	127(2)	83(1)	23(1)	102(1)	225(4)	CSP II
2014I	100(2)	16(1)	86(3)	124(1)	70(1)	23(1)	86(2)	160(4)	CSP II
2014ao	121(2)	22(1)	83(2)	125(1)	62(1)	14(1)	97(1)	124(2)	CSP II
2014at	88(2)	18(1)	97(2)	112(1)	70(1)	19(1)	80(1)	...	CSP II
2014dk	163(1)	8(1)	93(1)	114(1)	80(1)	8(1)	73(1)	93(5)	CSP II
2015F	80(2)	26(1)	104(2)	150(1)	76(1)	20(1)	101(1)	170(2)	CSP II
1990O	123(3)	...	107(3)	130(3)	76(6)	8(5)	89(6)	...	historical
1990af	...	...	...	102(2)	67(2)	25(2)	79(3)	...	historical
1992P	...	...	...	...	81(1)	15(2)	85(1)	...	historical
1992al	107(1)	14(1)	69(1)	113(1)	70(1)	11(1)	95(1)	...	historical
1992bh	138(1)	15(1)	89(1)	127(2)	74(1)	8(1)	85(2)	...	historical
1992bs	...	...	...	...	45(3)	19(3)	72(4)	...	historical
1993O	123(1)	21(1)	92(1)	141(1)	92(1)	16(1)	103(1)	...	historical
1994D	98(1)	19(1)	74(1)	107(1)	76(1)	17(1)	92(1)	72(1)	historical
1999ee	110(1)	7(1)	100(1)	147(1)	67(1)	6(1)	84(1)	142(1)	historical
2000ca	103(1)	6(1)	84(1)	116(1)	79(1)	4(1)	80(1)	...	historical
<b>CL</b>									
2008O	155(1)	49(1)	132(1)	244(1)	87(1)	48(1)	175(1)	296(3)	CSP I
ASASSN-15aj	98(1)	23(1)	92(1)	143(1)	74(1)	33(1)	114(1)	154(3)	CSP II
iPTF13ebh	96(1)	33(1)	106(1)	137(1)	75(1)	43(1)	127(1)	220(2)	CSP II
iPTF14w	119(1)	29(1)	143(1)	153(4)	68(2)	42(1)	135(2)	246(7)	CSP II
KISS15m	229(1)	...	268(1)	160(2)	28(2)	53(2)	130(3)	367(8)	CSP II
LSQ12aor	114(1)	19(1)	97(1)	119(5)	79(3)	31(2)	122(3)	...	CSP II
LSQ14act	115(2)	27(2)	103(3)	132(7)	94(4)	40(3)	122(5)	219(13)	CSP II
LSQ14ip	115(3)	18(2)	155(3)	225(7)	62(4)	56(3)	161(4)	244(9)	CSP II
LSQ14fms	136(1)	36(1)	154(1)	238(5)	88(3)	40(2)	140(3)	...	CSP II
LSQ14gfb	124(3)	...	226(4)	183(7)	73(4)	64(3)	138(4)	233(10)	CSP II
PS1-14ra	121(1)	31(1)	97(1)	145(1)	78(1)	31(1)	126(1)	205(3)	CSP II
2011hk	96(1)	...	242(1)	180(4)	38(2)	53(2)	121(3)	319(6)	CSP II
2011iv	72(1)	16(1)	117(1)	136(1)	76(1)	32(1)	82(1)	73(1)	CSP II
2011jh	...	27(1)	102(1)	165(1)	79(2)	35(1)	135(7)	216(7)	CSP II
2012ij	113(1)	26(1)	123(1)	127(1)	75(1)	41(1)	122(1)	303(1)	CSP II
2013bc	104(1)	...	269(1)	161(1)	55(1)	44(1)	98(1)	282(2)	CSP II
2014dn	148(1)	...	270(1)	229(5)	45(2)	60(1)	138(2)	340(6)	CSP II
2015bo	116(1)	...	242(1)	225(5)	65(2)	56(1)	147(2)	334(7)	CSP II
2015bp	94(1)	19(1)	116(1)	143(4)	66(2)	39(1)	115(2)	195(5)	CSP II
1986G	114(1)	...	230(1)	195(1)	78(1)	40(1)	117(1)	...	historical
1991bg	121(1)	...	289(1)	142(1)	29(1)	44(1)	100(1)	247(1)	historical
1992aq	97(3)	16(2)	94(3)	127(5)	80(5)	31(5)	96(7)	...	historical
1993H	115(1)	18(1)	78(1)	118(1)	62(1)	34(1)	117(1)	235(1)	historical
<b>BL</b>									
2008fl	...	...	82(2)	166(1)	78(1)	29(1)	120(1)	112(2)	CSP I
2008go	120(1)	18(1)	98(1)	155(1)	93(1)	<4	148(1)	177(3)	CSP I
2008hj	...	...	90(1)	147(1)	77(1)	15(1)	107(1)	174(3)	CSP I
ASASSN-14jc	158(1)	30(1)	110(1)	215(1)	80(1)	19(1)	133(1)	240(3)	CSP II
ASASSN-14my	113(1)	16(1)	96(3)	156(4)	71(3)	20(2)	107(3)	166(10)	CSP II
ASASSN-15ba	137(1)	19(1)	91(3)	138(3)	86(3)	14(1)	113(2)	158(6)	CSP II
ASASSN-15fr	103(1)	22(1)	79(1)	107(1)	84(1)	20(1)	112(1)	121(6)	CSP II

Table 5 continued on next page

**Table 5** (*continued*)

SN	pW1	pW2	pW3	pW4	pW5	pW6	pW7	pW8	project
	Ca II H&K	Si II 4130	Mg II	Fe II	S II W	Si II 5972	Si II 6355	Ca II IR	
LSQ12agq	164(1)	17(1)	85(3)	139(3)	102(2)	19(1)	147(1)	202(7)	CSP II
LSQ12btn	111(1)	21(1)	105(3)	180(3)	77(3)	22(2)	139(3)	211(9)	CSP II
LSQ13dcy	181(2)	20(1)	113(4)	198(5)	88(4)	20(3)	143(5)	...	CSP II
LSQ14azy	141(3)	13(1)	71(4)	122(4)	88(3)	12(2)	107(2)	154(8)	CSP II
OGLE-2014-SN-021	183(2)	16(2)	124(5)	151(6)	98(6)	24(4)	123(6)	...	CSP II
PSN J13471211-2422171	98(1)	32(1)	116(1)	165(5)	74(2)	27(1)	112(3)	135(12)	CSP II
SMTJ03253351-5344190	189(1)	15(1)	107(3)	130(4)	73(3)	12(2)	115(3)	...	CSP II
2012E	92(1)	29(1)	87(1)	120(1)	78(1)	20(1)	111(1)	166(1)	CSP II
2012ah	145(1)	26(1)	66(3)	124(3)	92(3)	21(2)	121(2)	204(8)	CSP II
2012hd	155(1)	24(1)	100(2)	185(2)	84(2)	27(1)	115(2)	289(4)	CSP II
2012hl	149(2)	15(1)	108(2)	192(1)	82(1)	12(2)	135(2)	250(2)	CSP II
2012hr	147(2)	21(1)	99(1)	116(1)	81(1)	17(1)	134(1)	279(2)	CSP II
2012ht	111(2)	19(1)	84(5)	116(5)	83(4)	22(2)	112(3)	230(8)	CSP II
2013aj	131(1)	30(1)	95(1)	123(1)	83(1)	25(1)	112(1)	214(2)	CSP II
2013cs	119(1)	12(1)	86(1)	166(1)	88(1)	9(1)	144(1)	147(1)	CSP II
2013hn	94(1)	18(1)	74(3)	102(2)	95(2)	19(1)	117(2)	159(5)	CSP II
2014Z	110(1)	18(1)	87(3)	132(3)	82(3)	13(1)	123(2)	198(9)	CSP II
1981B	120(1)	24(1)	110(1)	160(1)	86(1)	14(1)	126(1)	175(2)	historical
1989B	132(1)	20(1)	97(1)	139(1)	82(1)	21(1)	120(2)	...	historical
1992A	100(1)	27(1)	91(1)	143(1)	96(1)	25(1)	118(1)	...	historical
1992bl	85(1)	21(1)	88(1)	127(1)	83(1)	22(1)	107(1)	...	historical
1992bo	110(1)	29(1)	83(1)	118(1)	74(1)	27(1)	113(2)	...	historical
1993ag	...		83(1)	202(1)	93(2)	30(2)	151(3)	...	historical
1999ek	116(2)	17(1)	122(2)	129(2)	80(2)	21(2)	111(2)	145(4)	historical
2001ba	107(1)	18(1)	108(1)	132(1)	77(1)	17(1)	106(1)	155(2)	historical
2001cn	...	27(1)	94(1)	161(2)	90(1)	23(1)	124(2)	...	historical
<b>SS</b>									
2007if	...	...	...	...	...	<6	28(3)	...	CSP I
2008cf	83(1)	6(1)	76(1)	93(1)	66(1)	<3	55(1)	41(6)	CSP I
2009P	86(1)	4(1)	90(1)	104(1)	52(1)	7(1)	58(1)	93(5)	CSP I
2009dc	54(1)	10(1)	58(1)	82(1)	49(1)	9(1)	53(1)	...	CSP I
2009ds	...	...	106(1)	101(1)	53(1)	9(1)	62(1)	80(5)	CSP I
ASASSN-14hp	95(1)	9(1)	116(2)	120(2)	56(2)	<4	63(2)	...	CSP II
ASASSN-14kd	48(1)	6(1)	75(1)	77(1)	52(1)	4(1)	36(1)	...	CSP II
ASASSN-14lt	115(1)	11(1)	78(1)	97(1)	43(1)	10(1)	52(1)	...	CSP II
ASASSN-14me	106(1)	6(1)	87(1)	94(1)	57(1)	<2	63(1)	...	CSP II
ASASSN-15as	138(1)	9(1)	88(1)	106(1)	77(1)	4(1)	68(1)	160(7)	CSP II
LSQ12gdj	30(1)	...	82(1)	74(1)	62(1)	6(1)	38(1)	...	CSP II
LSQ12gpw	45(1)	8(1)	48(1)	73(1)	42(1)	14(1)	53(1)	70(5)	CSP II
LSQ12hnr	98(1)	3(1)	86(2)	97(3)	63(4)	<6	43(3)	...	CSP II
LSQ12hvj	118(2)	18(1)	94(2)	89(3)	54(3)	<8	47(4)	...	CSP II
LSQ12hzj	105(1)	13(1)	76(1)	106(1)	56(1)	13(1)	57(1)	...	CSP II
LSQ15aae	97(1)	8(1)	99(1)	142(2)	44(2)	<6	64(3)	...	CSP II
LSQ15agh	98(1)	13(1)	114(1)	123(1)	56(1)	<4	57(1)	...	CSP II
MASTERJ093953.18+165516.4	66(1)	6(1)	86(2)	100(2)	65(2)	<4	44(2)	...	CSP II
OGLE-2014-SN-107	56(1)	...	80(2)	103(2)	58(3)	7(2)	41(3)	...	CSP II
PS15sv	88(1)	6(1)	107(1)	84(1)	47(2)	<4	50(2)	...	CSP II
2012G	122(1)	12(1)	69(2)	106(2)	63(2)	11(2)	63(2)	79(9)	CSP II
2012fr	136(1)	8(1)	95(1)	116(1)	76(1)	4(1)	66(1)	126(3)	CSP II
2013ad	75(1)	<3	92(1)	91(1)	70(2)	<6	61(2)	...	CSP II
2013ao	19(1)	11(1)	79(1)	107(2)	63(2)	11(2)	50(2)	...	CSP II
2013hh	100(1)	12(1)	89(1)	125(2)	51(1)	<5	50(2)	100(3)	CSP II

Table 5 continued on next page

**Table 5** (*continued*)

SN	pW1	pW2	pW3	pW4	pW5	pW6	pW7	pW8	project
	Ca II H&K	Si II 4130	Mg II	Fe II	S II W	Si II 5972	Si II 6355	Ca II IR	
2014eg	20(1)	<3	98(1)	104(2)	57(2)	<3	38(1)	...	CSP II
2015M	17(1)	10(1)	75(1)	96(1)	51(1)	<3	51(1)	...	CSP II
1990N	...	10(1)	89(1)	134(1)	52(1)	11(1)	69(1)	...	historical
1991T	...	...	87(1)	109(1)	...	...	28(1)	...	historical
1992ae	76(2)	14(1)	50(2)	73(3)	50(3)	17(3)	62(3)	...	historical
1992ag	96(1)	15(1)	76(1)	79(2)	49(1)	3(1)	63(2)	...	historical

NOTE—All pW values and their errors (in parentheses) are expressed in Å.

**Table 6.** Expansion velocities at maximum light and Si II 6355 velocity decline [km s<sup>-1</sup>]

SN	Ca II H&K	Si II 4130	S II 5449	S II 5622	Si II 5972	Si II 6355	Ca II IR	$\Delta v_{20}(\text{Si})$	project
<b>CN</b>									
2007ol	17110(212)	11217(98)	9822(258)	9365(222)	11546(244)	11577(195)	...	1559(331)	CSP I
2008bz	15632(266)	10534(27)	8883(58)	8992(47)	10704(72)	11303(39)	9710(257)	1253(151)	CSP I
2008fr	12296(141)	10175(95)	9940(436)	9208(117)	10709(198)	11098(118)	12239(335)	...	CSP I
2009I	12000(187)	9764(84)	9296(136)	9696(94)	9959(147)	10768(79)	12169(192)	675(165)	CSP I
2009cz	18359(65)	8448(60)	8270(136)	8086(99)	9560(192)	9697(78)	17545(248)	...	CSP I
2009le	12570(247)	12259(51)	10495(145)	10948(65)	11071(181)	12654(66)	12273(396)	...	CSP I
ASASSN-14hr	17242(140)	10650(70)	8783(125)	8527(137)	11083(182)	11747(306)	11905(251)	...	CSP II
ASASSN-14hu	13054(191)	10634(27)	9797(63)	10047(35)	...	11511(36)	...	1143(89)	CSP II
ASASSN-14kq	12573(214)	9165(82)	8626(192)	9067(82)	10000(223)	10584(112)	10482(271)	...	CSP II
ASASSN-14lp	11605(103)	11356(259)	10526(127)	10790(266)	12499(246)	11982(303)	16772(656)	693(303)	CSP II
ASASSN-15al	13350(151)	11031(143)	10135(267)	10131(154)	...	12011(157)	13540(277)	795(157)	CSP II
ASASSN-15be	13992(454)	11071(83)	9996(262)	10362(177)	11379(323)	11882(108)	8838(472)	...	CSP II
ASASSN-15bm	19490(105)	9299(105)	9014(62)	9314(115)	10176(197)	11314(141)	12064(425)	...	CSP II
ASASSN-15cb	14819(191)	...	7023(231)	7490(262)	...	9902(288)	...	...	CSP II
ASASSN-15cd	11222(174)	9415(97)	8772(221)	8791(203)	10028(441)	11035(171)	...	...	CSP II
ASASSN-15da	14331(174)	10316(119)	9383(253)	9867(185)	11241(253)	12189(200)	...	...	CSP II
ASASSN-15db	14548(80)	9342(97)	8974(164)	8862(121)	9795(295)	10509(112)	10898(344)	...	CSP II
ASASSN-15dd	15739(88)	9668(38)	8415(119)	8533(55)	10930(68)	11190(49)	11724(211)	...	CSP II
ASASSN-15go	19215(104)	11899(53)	10006(85)	11281(66)	...	13032(59)	14477(128)	...	CSP II
ASASSN-15gr	11809(158)	9397(105)	9248(188)	9371(193)	10579(546)	11017(142)	11305(444)	...	CSP II
ASASSN-15hf	12292(120)	10353(34)	9160(68)	9045(34)	10434(63)	11168(35)	11595(193)	...	CSP II
CSS130315:114144-171348	14064(334)	11492(121)	10396(279)	10774(144)	11455(334)	12611(133)	13544(329)	...	CSP II
CSS131031:095508+064831	11090(250)	9747(240)	9501(437)	9527(308)	8685(642)	11055(12)	...	1261(12)	CSP II
CSS140501-170414+174839	11515(236)	11943(249)	9548(352)	10649(281)	10923(604)	12298(147)	...	...	CSP II
CSS140914-010107-101840	12947(93)	9223(60)	8670(90)	8801(115)	10657(234)	10669(102)	11524(152)	...	CSP II
iPTF13duj	18175(164)	12880(92)	...	11416(200)	14747(316)	14166(80)	15492(204)	...	CSP II
iPTF14gnl	10648(267)	9884(247)	9136(266)	8919(220)	...	10399(210)	...	...	CSP II
KISS13j	15848(207)	9546(105)	8286(283)	8072(143)	10352(178)	10960(152)	13864(183)	...	CSP II
LSQ11bk	...	...	10552(142)	10355(84)	...	12756(56)	12430(390)	1593(117)	CSP II
LSQ11ot	10615(195)	9495(85)	9416(109)	8728(171)	10095(206)	10693(143)	10400(336)	...	CSP II
LSQ12blp	13157(127)	10745(113)	9786(187)	9443(132)	11563(250)	11925(122)	...	...	CSP II
LSQ12ca	11163(111)	9662(90)	9694(147)	9267(104)	10395(161)	10704(122)	...	...	CSP II
LSQ12cdl	13544(337)	10018(397)	8317(277)	9178(643)	...	10878(343)	...	...	CSP II
LSQ12fdx	11526(84)	10190(285)	10235(263)	9443(45)	10676(108)	11155(135)	8345(78)	851(135)	CSP II
LSQ12gxj	13576(93)	11704(75)	10168(115)	10367(95)	12423(271)	11738(113)	12993(139)	...	CSP II
LSQ12gyc	14000(343)	10927(151)	10409(313)	10634(271)	10738(660)	11942(240)	...	...	CSP II
LSQ12hno	9457(134)	8640(127)	8080(209)	8013(142)	9087(254)	9428(141)	...	...	CSP II
LSQ14asu	14065(353)	9639(112)	7177(169)	6276(99)	9448(234)	9389(151)	...	...	CSP II
LSQ14auy	12934(348)	9402(411)	8243(621)	9210(444)	9856(1068)	10296(580)	...	...	CSP II
LSQ14gov	10688(166)	10540(150)	9064(192)	9604(292)	11200(427)	10935(205)	...	...	CSP II
LSQ14xi	10927(387)	9369(472)	8872(590)	9230(457)	...	10770(558)	...	...	CSP II
LSQ15aja	11683(95)	8887(112)	8411(209)	8550(131)	9899(233)	9962(175)	...	...	CSP II
LSQ15alq	10711(118)	9971(143)	9095(256)	8864(143)	10965(151)	11009(289)	...	...	CSP II
OGLE-2013-SN-118	12067(104)	10072(220)	9678(149)	9955(67)	9470(580)	11642(167)	12058(190)	...	CSP II
OGLE-2013-SN-123	12083(198)	9270(254)	8468(447)	8749(241)	10467(379)	10760(230)	...	...	CSP II
PS1-14xw	11452(219)	11389(84)	9603(63)	10381(50)	11424(110)	11581(56)	12802(261)	...	CSP II
PTF11qnr	12530(214)	10528(79)	9491(165)	9779(88)	10648(102)	11356(86)	10270(253)	...	CSP II
2012aq	15103(490)	10773(125)	9411(208)	9768(129)	11954(240)	12090(145)	...	...	CSP II
2012bl	18604(192)	...	9042(221)	12866(168)	...	14698(82)	15752(299)	815(72)	CSP II

Table 6 continued on next page

**Table 6** (*continued*)

SN	Ca II H&K	Si II 4130	S II 5449	S II 5622	Si II 5972	Si II 6355	Ca II IR	$\Delta v_{20}$ (Si)	project
2013aa	11964(223)	9504(35)	8930(39)	8732(27)	10464(61)	10505(44)	11814(366)	...	CSP II
2013fz	12336(412)	9848(34)	8895(120)	9542(78)	11066(162)	10842(65)	11290(566)	...	CSP II
2013gy	14177(143)	8641(99)	7893(48)	7992(44)	9903(130)	10790(107)	11769(177)	2000(107)	CSP II
2014D	15817(400)	9705(142)	9162(164)	8876(164)	10250(155)	10822(117)	17524(296)	...	CSP II
2014I	13855(160)	9657(69)	8703(164)	9071(83)	10217(125)	11150(132)	10876(169)	...	CSP II
2014ao	11619(625)	11178(151)	10113(211)	9447(270)	11450(443)	11540(265)	11995(141)	968(265)	CSP II
2014at	10204(113)	9162(27)	8827(31)	8855(50)	10329(104)	10536(64)	...	...	CSP II
2014dk	19916(252)	8142(82)	7401(141)	7381(115)	8660(222)	9085(87)	19586(358)	...	CSP II
2015F	10795(111)	8988(40)	7777(57)	8071(33)	10050(32)	10069(44)	11144(120)	...	CSP II
1990O	17268(612)	...	9559(165)	9902(129)	...	11695(84)	...	821(184)	historical
1990af	...	...	9229(198)	9971(121)	10963(151)	11613(465)	...	...	historical
1992P	...	...	8699(142)	9050(148)	...	10971(64)	...	...	historical
1992al	11905(146)	9111(127)	8445(181)	8162(99)	9568(224)	10443(89)	...	...	historical
1992bh	16112(128)	10462(172)	8615(266)	8937(296)	10959(630)	11967(167)	...	...	historical
1992bs	...	...	9006(583)	9382(550)	9972(648)	10421(332)	...	...	historical
1993O	11762(47)	9371(37)	8421(62)	8534(38)	10108(125)	10819(49)	...	...	historical
1994D	11047(26)	8546(11)	8387(51)	9269(22)	10619(38)	10900(26)	8574(95)	1165(47)	historical
1999ee	19451(41)	9057(15)	8622(28)	8860(33)	8549(62)	10245(44)	19035(130)	927(86)	historical
2000ca	12385(87)	10785(98)	9382(210)	9733(110)	...	11509(74)	...	...	historical
<b>CL</b>									
2008O	17852(89)	9128(90)	7722(85)	7714(60)	10015(67)	13270(84)	13354(124)	...	CSP I
ASASSN-15aj	12020(150)	8806(90)	8112(192)	7938(77)	9498(98)	10555(83)	11159(196)	1359(83)	CSP II
iPTF13ebh	14130(124)	9134(23)	7241(192)	7685(36)	9993(67)	10798(63)	8361(115)	1757(63)	CSP II
iPTF14w	16806(126)	9593(117)	8127(220)	8864(89)	10740(94)	11753(77)	13980(165)	...	CSP II
KISS15m	13270(159)	...	...	6500(147)	9827(99)	10659(88)	13749(161)	...	CSP II
LSQ12aor	13795(472)	9467(118)	8164(258)	8619(156)	10484(170)	11103(167)	...	...	CSP II
LSQ14act	11464(254)	9348(322)	8094(820)	8612(500)	10758(292)	11277(235)	12353(393)	...	CSP II
LSQ14ip	17623(323)	10304(421)	8499(743)	9236(364)	11069(256)	12442(177)	13738(260)	...	CSP II
LSQ14fms	16925(88)	10264(113)	8772(210)	9045(176)	10749(224)	13182(178)	...	...	CSP II
LSQ14gfb	15159(328)	...	8129(305)	7489(377)	10257(265)	10537(323)	...	...	CSP II
PS1-14ra	10648(102)	9464(52)	8552(107)	8793(88)	11174(78)	11611(78)	11801(309)	1604(142)	CSP II
2011hk	13059(257)	...	7045(97)	6882(187)	10087(119)	10897(166)	14128(171)	2410(64)	CSP II
2011iv	11375(663)	...	...	...	10212(239)	10017(50)	...	4310(162)	CSP II
2011jh	12890(165)	10585(160)	9096(202)	9268(63)	12063(51)	12381(144)	13030(440)	2321(232)	CSP II
2012ij	14087(64)	8986(60)	7232(79)	7605(38)	10182(36)	10799(29)	12917(88)	994(35)	CSP II
2013bc	11199(221)	...	7068(197)	7097(82)	9492(72)	9824(73)	11939(80)	...	CSP II
2014dn	14791(112)	...	6983(73)	6053(66)	9851(67)	11115(83)	12958(95)	...	CSP II
2015bo	14935(144)	...	7460(113)	6709(103)	10088(67)	11553(83)	12975(193)	3123(145)	CSP II
2015bp	12130(94)	9290(96)	8054(264)	8123(31)	9927(60)	10721(25)	12537(72)	1208(24)	CSP II
1986G	15167(105)	...	6285(540)	7277(207)	9746(189)	10486(156)	...	...	historical
1991bg	13452(87)	...	6064(28)	6811(21)	9303(24)	9891(34)	9312(72)	1820(150)	historical
1992aq	15132(704)	9653(487)	8644(577)	9256(412)	10016(675)	11143(392)	...	...	historical
1993H	15210(163)	10005(128)	7684(300)	8291(138)	10154(68)	11192(34)	12729(66)	2319(125)	historical
<b>BL</b>									
2008fl	...	...	7724(70)	8015(48)	9801(59)	11098(55)	11037(273)	1374(100)	CSP I
2008go	15872(72)	11996(264)	10618(80)	10399(88)	...	13614(84)	13858(113)	...	CSP I
2008hj	...	...	9646(185)	10033(114)	11739(350)	12184(154)	12845(270)	1935(308)	CSP I
ASASSN-14jc	17984(372)	9539(127)	8176(164)	8234(77)	10065(182)	12132(74)	13588(140)	...	CSP II
ASASSN-14my	13523(160)	10304(75)	8910(114)	8896(67)	9672(104)	10912(83)	10623(156)	1058(83)	CSP II
ASASSN-15ba	15282(124)	9561(34)	9533(80)	9275(35)	11303(68)	12327(40)	14017(189)	...	CSP II
ASASSN-15fr	14508(110)	10401(113)	9221(187)	9419(264)	10779(245)	11772(93)	10870(203)	...	CSP II
LSQ12agq	17257(355)	11770(67)	9679(96)	9366(65)	10538(162)	12662(77)	14363(465)	...	CSP II

Table 6 continued on next page

**Table 6** (*continued*)

SN	Ca II H&K	Si II 4130	S II 5449	S II 5622	Si II 5972	Si II 6355	Ca II IR	$\Delta v_{20}$ (Si)	project
LSQ12btn	20953(374)	9733(137)	8439(139)	9638(142)	10600(199)	12402(116)	12737(516)	...	CSP II
LSQ13dcy	20668(318)	10995(384)	9369(463)	8624(450)	9495(747)	13844(504)	...	...	CSP II
LSQ14azy	15361(168)	11906(249)	9951(307)	10135(214)	11370(479)	12024(162)	12334(430)	...	CSP II
OGLE-2014-SN-021	19592(252)	9861(1057)	9171(570)	9222(633)	10782(792)	11487(408)	...	2484(440)	CSP II
PSN J13471211-2422171	19320(114)	11891(98)	9967(216)	10518(100)	11377(146)	13604(94)	14031(308)	...	CSP II
SMTJ03253351-5344190	20936(122)	9397(165)	7812(272)	8386(176)	9445(382)	10138(230)	...	...	CSP II
2012E	12541(32)	10581(15)	9334(11)	9425(16)	11877(31)	11361(20)	12731(135)	...	CSP II
2012ah	15538(442)	9795(92)	8546(146)	8526(74)	10178(153)	11579(91)	13351(602)	...	CSP II
2012hd	16602(65)	8274(40)	8351(20)	7980(20)	9915(30)	10431(20)	13481(144)	1432(51)	CSP II
2012hl	16929(109)	9976(198)	8954(225)	9921(241)	11496(242)	13146(134)	15697(223)	...	CSP II
2012hr	17526(80)	9384(216)	8799(123)	8577(55)	11028(175)	12160(96)	14633(284)	2552(96)	CSP II
2012ht	14475(57)	9576(34)	8829(137)	8384(116)	10571(186)	11291(189)	13082(228)	...	CSP II
2013aj	12660(48)	9322(15)	8957(132)	8367(25)	10367(99)	10604(39)	11631(146)	1110(165)	CSP II
2013cs	14856(40)	11296(15)	9885(17)	9854(17)	12692(26)	12980(20)	14117(51)	2520(40)	CSP II
2013hn	11783(119)	10461(23)	10178(138)	10075(30)	11748(119)	12664(37)	12617(117)	...	CSP II
2014Z	14628(135)	10019(75)	8908(160)	8709(94)	10857(203)	12038(100)	13196(360)	...	CSP II
1981B	15520(12)	10437(8)	9612(14)	9779(13)	11041(27)	12095(17)	13764(66)	1556(45)	historical
1989B	16120(146)	9571(142)	8296(259)	8164(117)	10066(142)	10814(106)	...	1525(205)	historical
1992A	14587(83)	10235(70)	8796(189)	9387(94)	11541(109)	12419(78)	...	2021(123)	historical
1992bl	13513(129)	10675(99)	9244(148)	9736(73)	11338(132)	11710(65)	...	...	historical
1992bo	13757(124)	9873(69)	8133(203)	8668(110)	10359(92)	11226(84)	...	...	historical
1993ag	...	...	...	8882(198)	11312(500)	12995(210)	...	...	historical
1999ek	13659(135)	9491(217)	9145(250)	8806(236)	9375(186)	10995(132)	10881(322)	...	historical
2001ba	16540(118)	9009(34)	8391(63)	8371(61)	10281(137)	10999(61)	10311(313)	1756(117)	historical
2001cn	...	9618(262)	8793(215)	9421(132)	11288(246)	12117(104)	...	...	historical
<b>SS</b>									
2007if	...	...	...	...	...	9218(125)	...	4343(177)	CSP I
2008cf	10463(195)	9893(46)	8437(160)	8991(105)	...	10191(85)	10967(188)	1142(327)	CSP I
2009P	14308(172)	12193(44)	...	12360(113)	14334(252)	13748(87)	11108(145)	380(103)	CSP I
2009dc	14448(80)	6002(91)	5630(124)	5469(110)	...	7797(59)	...	1916(104)	CSP I
2009ds	...	...	11753(338)	10990(106)	12900(112)	12676(103)	...	376(145)	CSP I
ASASSN-14hp	10441(165)	9442(150)	8735(226)	8912(247)	...	10435(240)	...	...	CSP II
ASASSN-14kd	11300(123)	11322(99)	9095(84)	10561(84)	12557(309)	11357(52)	...	...	CSP II
ASASSN-14lt	10375(175)	9113(187)	9517(176)	8793(137)	10234(284)	10063(137)	...	...	CSP II
ASASSN-14me	10793(110)	9499(96)	8488(102)	9234(100)	...	10459(79)	...	752(160)	CSP II
ASASSN-15as	12012(450)	10363(48)	9384(164)	9823(88)	11569(130)	11296(70)	12065(305)	...	CSP II
LSQ12gdj	10412(63)	...	8649(119)	10157(88)	7989(304)	10694(95)	...	...	CSP II
LSQ12gpw	7121(163)	5862(207)	6191(348)	6399(240)	10332(338)	9225(152)	10324(213)	...	CSP II
LSQ12hnr	17756(275)	10276(285)	8481(402)	8841(346)	...	12890(370)	...	...	CSP II
LSQ12hvj	19445(106)	9594(180)	9336(239)	8779(429)	...	10094(318)	...	...	CSP II
LSQ12hzj	8615(71)	8423(45)	8320(79)	7942(49)	8783(191)	9524(58)	...	...	CSP II
LSQ15aae	11423(728)	8104(157)	7820(164)	7957(236)	...	10127(346)	...	...	CSP II
LSQ15agh	9351(110)	9450(82)	7718(311)	8867(203)	...	10166(161)	...	...	CSP II
MASTERJ093953.18+165516.4	10370(329)	10530(172)	8855(359)	9842(246)	...	10761(214)	...	...	CSP II
OGLE-2014-SN-107	...	...	...	...	...	10836(494)	...	...	CSP II
PS15sv	9669(90)	8918(164)	8283(153)	8551(209)	...	9984(146)	...	...	CSP II
2012G	11245(196)	9095(115)	9671(176)	9919(162)	10701(508)	10993(163)	...	...	CSP II
2012fr	11914(171)	11871(151)	11450(102)	10872(112)	12035(133)	12276(90)	9125(80)	545(90)	CSP II
2013ad	10228(135)	...	8910(256)	9495(21)	...	10325(147)	...	...	CSP II
2013ao	11231(136)	11187(135)	12450(515)	10972(272)	11419(600)	12324(183)	9544(768)	732(183)	CSP II
2013hh	16720(161)	9045(187)	7333(130)	8502(99)	...	9056(204)	10700(210)	...	CSP II
2014eg	10670(102)	...	9085(182)	10860(216)	...	11131(171)	...	...	CSP II

Table 6 continued on next page

**Table 6** (*continued*)

SN	Ca II H&K	Si II 4130	S II 5449	S II 5622	Si II 5972	Si II 6355	Ca II IR	$\Delta v_{20}$ (Si)	project
2015M	10750(110)	12151(60)	9030(238)	10524(182)	...	12604(59)	...	2687(18)	CSP II
1990N	...	10222(34)	9780(86)	9057(45)	10864(190)	10914(76)	...	1286(120)	historical
1991T	...	...	...	...	...	9922(44)	...	372 (57)	historical
1992ae	12766(276)	11128(227)	8083(406)	8490(290)	11427(407)	10082(307)	...	...	historical
1992ag	16679(112)	11634(174)	10231(239)	9968(248)	11016(354)	11644(157)	...	...	historical

NOTE—Velocities and their error estimates (in parentheses) are expressed in km s<sup>-1</sup>.

**Table 7.** Temporal evolution of the Si II  $\lambda 6355$  expansion velocities in the CSP I & II sample. Phase: Rest frame phase of bin center; Exp.vel.: average expansion velocity; Sigma: standard deviation; N: number of data in bin.

Phase	Exp. vel.	Sigma	N	Phase	Exp. vel.	Sigma	N	Phase	Exp. vel.	Sigma	N
-9.5	12449	869	9	1.5	10950	451	29	13.5	10261	600	5
-7.5	11861	886	16	3.5	10706	494	20	15.5	10319	665	6
-5.5	11437	802	17	5.5	10805	468	6	19.0	9937	693	5
-3.5	11532	903	19	7.5	10453	649	11	21.0	9116	832	4
-1.5	11066	696	26	9.5	10190	653	12	24.0	9812	543	6
0	10861	619	71	11.5	10290	514	8				